



PHD

**Cloning of citrate synthase from the halophilic archaeon *Haloferax volcanii***

James, Keith D.

*Award date:*  
1994

*Awarding institution:*  
University of Bath

[Link to publication](#)

**Alternative formats**

If you require this document in an alternative format, please contact:  
[openaccess@bath.ac.uk](mailto:openaccess@bath.ac.uk)

Copyright of this thesis rests with the author. Access is subject to the above licence, if given. If no licence is specified above, original content in this thesis is licensed under the terms of the Creative Commons Attribution-NonCommercial 4.0 International (CC BY-NC-ND 4.0) Licence (<https://creativecommons.org/licenses/by-nc-nd/4.0/>). Any third-party copyright material present remains the property of its respective owner(s) and is licensed under its existing terms.

**Take down policy**

If you consider content within Bath's Research Portal to be in breach of UK law, please contact: [openaccess@bath.ac.uk](mailto:openaccess@bath.ac.uk) with the details. Your claim will be investigated and, where appropriate, the item will be removed from public view as soon as possible.

# **Cloning of Citrate Synthase from the Halophilic Archaeon *Haloferax volcanii***

submitted by Keith D. James

for the degree of PhD

of the University of Bath

1994

## **Copyright**

Attention is drawn to the fact that copyright of this thesis rests with its author. This copy of the thesis has been supplied on the condition that anyone who consults it is understood to recognise that its copyright rests with its author and no information derived from it may be published without the prior written consent of the author.

This thesis may be made available for consultation within the University Library and may be photocopied or lent to other libraries for the purposes of consultation.

A handwritten signature in black ink, reading "Keith James", with a horizontal line underneath the name.

UMI Number: U552707

All rights reserved

INFORMATION TO ALL USERS

The quality of this reproduction is dependent upon the quality of the copy submitted.

In the unlikely event that the author did not send a complete manuscript and there are missing pages, these will be noted. Also, if material had to be removed, a note will indicate the deletion.



UMI U552707

Published by ProQuest LLC 2013. Copyright in the Dissertation held by the Author.  
Microform Edition © ProQuest LLC.

All rights reserved. This work is protected against  
unauthorized copying under Title 17, United States Code.



ProQuest LLC  
789 East Eisenhower Parkway  
P.O. Box 1346  
Ann Arbor, MI 48106-1346

UNIVERSITY OF BATH LIBRARY		
26	29 SEP 1994	
PHD		

5084623



## Abstract

The effect of monovalent salt on the activity and stability of citrate synthase from the moderately halophilic Archaeon *Haloferax volcanii* was investigated by assay of enzyme activity over a range of Na<sup>+</sup> and K<sup>+</sup> concentrations and by thermal inactivation experiments over a range of K<sup>+</sup> concentrations.

Based on a 38 residue N-terminal amino acid sequence obtained from *Hf. volcanii* citrate synthase, oligonucleotides were designed and used to probe restriction digests of *Hf. volcanii* genomic DNA. A 2.9 kb genomic fragment was identified by hybridisation to one of these probes. This fragment did not contain the citrate synthase gene; however, a 939 bp open reading frame within this fragment showed significant (33–47%) identity with several bacterial genes involved in the metabolism of sugar-nucleotides. The structural features of this open reading frame are discussed and possible functions in glycolipid and glycoprotein biosynthesis suggested.

To aid the cloning of the citrate synthase, further amino acid sequence data was obtained from the protein. Citrate synthase was purified by an improved affinity chromatography method, using biospecific elution. Cyanogen bromide cleavage of the purified enzyme yielded a 6 kD fragment. Amino acid sequence internal to the enzyme was obtained from this fragment.

PCR primers were designed to the N-terminal and internal amino acid sequences and used to amplify a 960 bp product from genomic DNA. This product is of the size predicted from the relative positions of the amino acid sequences used to design the PCR primers. Due to time constraints the product remains to be cloned and sequenced.

# Table of Contents

Title	i
Abstract	ii
Table of Contents	iii
List of Figures	viii
Abbreviations	xii
Acknowledgements	xiv
<b>Chapter One : Introduction</b>	<b>1</b>
1.1 The diversity of Archaeal phenotypes	1
1.2 Archaeal phylogeny	2
1.2.1 The root of the universal tree	4
1.2.2 How valid is the Archaeal tree	4
1.2.3 Objections to the Archaeal tree	5
1.2.4 A conflict of assumptions, not of data	7
1.3 <i>Haloferax volcanii</i>	8
1.4 The citric acid cycle	8
1.5 Citrate synthase	10
1.5.1 The available data	10
1.5.2 The citrate synthase mechanism	14
1.5.3 Citrate synthase as a model enzyme	15
1.6 The structure of halophilic enzymes	21
1.7 Biotechnology of halophilic systems	24
1.8 Aims of this project	26
<b>Chapter Two : Materials and Methods</b>	<b>27</b>
2.0 Materials	27
2.0.1 Bacterial strains and plasmids	29
2.1 General methods	30
2.1.1 Manipulation of <i>Hf.volcanii</i>	30
2.1.1.1 Culture of <i>Hf.volcanii</i>	30
2.1.1.2 Preparation of cell extract from <i>Hf.volcanii</i>	30
2.2 Protein techniques	31
2.2.1 Chromatographic techniques	31
2.2.1.1 FPLC Superdex 200 gel filtration	31
2.2.1.2 Matrex Gel Red A column	31

2.2.2 TCA precipitation of proteins	32
2.2.3 Protein concentration methods	32
2.2.4 Estimation of protein concentrations	32
2.2.5 SDS polyacrylamide gel electrophoresis	33
2.2.6 Western blotting	34
2.2.7 Citrate synthase assays	35
2.2.8 Acetylation of coenzyme A	35
<b>2.3 DNA methods</b>	<b>36</b>
2.3.1 Quantitation of DNA	36
2.3.2 DNA preparation methods	36
2.3.2.1 Preparation of genomic DNA from <i>Hf. volcanii</i>	36
2.3.2.2 Plasmid DNA 'Maxiprep' method I	37
2.3.2.3 Caesium chloride equilibrium density gradient centrifugation	37
2.3.2.4 Plasmid DNA 'Maxiprep' method II	38
2.3.2.5 Plasmid DNA 'Minipreps'	39
2.3.2.6 Plasmid DNA 'Magic Minipreps'	39
2.3.3 Restriction digests of DNA	39
2.3.4 Agarose gel electrophoresis of DNA	40
2.3.5 Recovery of DNA from agarose gels	40
2.3.6 Purification of DNA fragments	41
2.3.7 Precipitation of DNA	41
2.3.8 Ligation procedures	41
2.3.9 DNA blotting techniques	42
2.3.9.1 Southern blotting	42
2.3.9.2 Dot blotting	42
2.3.9.3 Colony hybridisation	43
2.3.10 Deprotection and purification of synthetic oligonucleotides	43
2.3.11 End-labelling of oligonucleotides	44
2.3.12 Hybridisation of labelled oligonucleotide probes to DNA blots	44
2.3.13 Preparation of competent <i>E.coli</i> JM103 and HB101	45
2.3.14 Transformation of competent <i>E.coli</i> with plasmid DNA	45
2.3.15 PCR techniques	46
2.3.15.1 PCR amplification of genomic DNA	46
2.3.15.2 Asymmetric PCR	46
2.3.16 Sequencing plasmid DNA	47

<b>Chapter Three : Characterisation of activity and stability of <i>Hf.volcanii</i> citrate synthase</b>	<b>49</b>
3.1 Introduction	49
3.2 Salt dependence of citrate synthase activity	50
3.3 Stability of citrate synthase	50
3.4 Thermal inactivation of citrate synthase	50
3.5 Discussion	61
 <b>Chapter Four : Creation of size-restricted genomic libraries and screening for the citrate synthase gene</b>	 <b>65</b>
4.1 Introduction	65
4.2 Oligonucleotide design	66
4.3 Southern blot analysis	66
4.4 Creation of a size-restricted genomic library	69
4.5 Screening for positive clones	69
4.6 Results	70
4.6.1 Screening Southern blots with a non-degenerate 44 base oligonucleotide probe	70
4.6.2 Restriction and hybridisation analysis of positive clones	74
4.6.3 Sub-cloning fragments from 2.9 kb positive clone	76
4.6.4 Restriction analysis of sub-cloned <i>HindIII</i> fragments	82
4.6.5 Sequence analysis of 2.9 kb <i>PstI</i> / <i>EcoRI</i> clone and <i>HindIII</i> sub-clones	82
4.7 Screening with a pair of degenerate 17 base oligonucleotide probes	86
4.7.1 Preliminary dot-blot results	89
4.7.2 Southern blot results	89
4.8 Screening Southern blots with a non-degenerate 29 base oligonucleotide probe	97
4.8.1 Preliminary dot-blot results	97
4.8.2 Southern blot results	99
4.9 Discussion	102
 <b>Chapter Five : Affinity purification of citrate synthase and determination of internal peptide sequence</b>	 <b>108</b>
5.1 Introduction	108
5.2 Outline of the purification scheme	110
5.3 Cyanogen bromide cleavage	111

5.4 N-terminal sequencing	111
5.5 Results	112
5.5.1 Purification	112
5.5.2 N-terminal sequencing	116
5.6 Discussion	116
 <b>Chapter Six : Amplification of the citrate synthase gene of <i>Haloferax volcanii</i> from genomic DNA by Polymerase Chain Reaction</b>	 <b>120</b>
6.1 Introduction	120
6.2 PCR amplification of an 830 bp sequence from genomic DNA using N-terminal and consensus amino acid sequences for primer design	120
6.2.1 Primer design	121
6.2.2 PCR amplification with N-terminal and consensus primers	128
6.2.3 Asymmetric PCR amplification of 830 bp fragment	131
6.2.4 Sequencing of asymmetric PCR products	133
6.3 PCR amplification of a 960 bp sequence from genomic DNA using N-terminal and C-terminal amino acid sequences for primer design	133
6.3.1 Primer design	135
6.3.2 PCR amplification with N-terminal and C-terminal primers	135
6.4 Discussion	138
 <b>Chapter Seven : Analysis of 939 bp open reading frame within the 2.9 kb <i>Pst</i>I / <i>Eco</i>RI clone</b>	 <b>142</b>
7.1 Introduction	142
7.2 Sequence analysis	142
7.3 Database search results	147
7.4 Analysis of the open reading frame	148
7.4.1 Structure and possible regulatory features	148
7.4.2 Multiple sequence alignment	149
7.5 Discussion	149
 <b>Chapter Eight : Conclusions and suggested further work</b>	 <b>155</b>
 <b>Appendix</b>	 <b>160</b>
Outline of purification scheme	64

SDS-polyacrylamide gel electrophoresis and Western blotting	160
N-terminal sequencing	161
<b>References</b>	<b>167</b>

## List of Figures

1.1	Universal phylogenetic tree according to Woese <i>et al.</i>	3
1.2	Universal phylogenetic tree according to Lake	6
1.3	The citric acid cycle	9
1.4	Structural diagrams of pig heart citrate synthase	13
1.5a	Enolisation and condensation steps	17
1.5b	Hydrolysis step mechanism	18
1.5c	Hydrolysis via anhydride formation	19
1.5d	Carbanion formation and condensation steps	20
3.1	Dependence of citrate synthase activity on salt concentration	51
3.2	Thermal inactivation of citrate synthase at 60°C	53
3.3	Thermal inactivation of citrate synthase at 62°C	54
3.4	Thermal inactivation of citrate synthase at 64°C	55
3.5	Thermal inactivation of citrate synthase at 66°C	56
3.6a	Arrhenius plot of thermal inactivation of citrate synthase	58
3.6b	Arrhenius plot of thermal inactivation of citrate synthases	59
3.7	Effect of KCl concentration on thermal inactivation of citrate synthase at 64°C	60
3.8	Effect of KCl concentration on the half-life of citrate synthase at 64°C	64
4.1	Codon preference in <i>Hf.volcanii</i>	67
4.2	Sequence of 44 base oligonucleotide probe	71
4.3a	Electrophoresis of genomic DNA restriction digests on 0.6% agarose gel	72
4.3b	Autoradiograph of Southern blot probed with non- degenerate 44 base oligonucleotide	73
4.4	Autoradiograph of colony blot probed with non- degenerate 44 base oligonucleotide	75
4.5a	Electrophoresis of restriction digests of 2.9 kb <i>Pst</i> I / <i>Eco</i> RI clone on 1% agarose gel	77
4.5b	Autoradiograph of Southern blot probed with non- degenerate 44 base oligonucleotide	78

4.6a	Electrophoresis of restriction digests of 2.9 kb <i>Pst</i> I / <i>Eco</i> RI clone on 1% agarose gel	79
4.6b	Autoradiograph of Southern blot probed with non- degenerate 44 base oligonucleotide	80
4.7	Summary of initial restriction site information obtained from 2.9 kb <i>Pst</i> I / <i>Eco</i> RI clone in pUC18	81
4.8	Electrophoresis of restriction digests of 2.9 kb <i>Pst</i> I / <i>Eco</i> RI clone and <i>Hind</i> III subclones on 1% agarose gel	83
4.9	Electrophoresis of restriction digests of 2.9 kb <i>Pst</i> I / <i>Eco</i> RI clone and <i>Hind</i> III subclones on 2% agarose gel	84
4.10	Regions of 2.9 kb <i>Pst</i> I / <i>Eco</i> RI clone and <i>Hind</i> III subclones sequenced	85
4.11	Restriction map of 2.9 kb <i>Pst</i> I / <i>Eco</i> RI clone	87
4.12	Sequence of 17 base oligonucleotide probes	88
4.13a	Electrophoresis of genomic DNA restriction digests on 0.6% agarose gel	90
4.13b	Autoradiograph of Southern blot probed with degenerate 17 base oligonucleotide A	91
4.14a	Electrophoresis of genomic DNA restriction digests on 0.6% agarose gel	93
4.14b	Autoradiograph of Southern blot probed with degenerate 17 base oligonucleotide A	94
4.15a	Electrophoresis of genomic DNA restriction digests on 0.6% agarose gel	95
4.15b	Autoradiograph of Southern blot probed with degenerate 17 base oligonucleotide A	96
4.16	Sequence of 29 base oligonucleotide probe	98
4.17a	Electrophoresis of genomic DNA restriction digests on 0.6% agarose gel	100
4.17b	Autoradiograph of Southern blot probed with non- degenerate 29 base oligonucleotide	101
4.18	Possible probe binding sites within 2.9 kb <i>Pst</i> I / <i>Eco</i> RI clone	104
5.1	Partial structure of Matrex Gel Red A	109
5.2	Matrex gel Red A chromatography of citrate synthase	113



5.3	FPLC Superdex-200 gel filtration of citrate synthase	114
5.4	SDS-PAGE of citrate synthase	115
5.5	Multiple sequence alignment of citrate synthases showing the <i>Hf.volcanii</i> internal sequence	119
6.1	Multiple sequence alignment citrate synthases	122
6.2	Regions conserved in all know citrate synthase sequences	126
6.3	Predicted DNA sequences corresponding to conserved regions in citrate synthase amino acid sequences	127
6.4	PCR amplification of genomic DNA using 29 base N-terminal and 26 base consensus primers, annealing at 55°C	129
6.5	PCR amplification of genomic DNA using 29 base N-terminal and 26 base consensus primers, annealing at 55°C	130
6.6	PCR amplification of 830 bp band using 29 base N-terminal and 26 base consensus primers	132
6.7	Sequences of each end of the 830 bp PCR fragment	134
6.8	Sequence of anti-sense PCR primer designed from amino acid sequence	136
6.9	PCR amplification of 960 bp band using N-terminal and C-terminal primers	137
6.10	PCR amplification of 960 bp band using N-terminal and C-terminal primers, annealing at 60°C	139
6.11	PCR amplification of 960 bp band using N-terminal and C-terminal primers, annealing at 60°C	140
7.1	Position of the open reading frame within the 2.9 kb <i>Pst</i> I / <i>Eco</i> RI clone	143
7.2	Sequence of the open reading frame and corresponding amino acid sequence	144
7.3	Alignment of the <i>Hf.volcanii</i> ORF with the four sequences of highest identity from database search	150

<b>9.1</b>	<b>SDS-PAGE of purified citrate synthase</b>	<b>162</b>
<b>9.2</b>	<b>Multiple sequence alignment of citrate synthases showing the <i>Hf.volcanii</i> N-terminal sequence</b>	<b>166</b>

## Abbreviations

A <sub>280</sub>	absorbance at 280 nm
BSA	bovine serum albumin
CoA	coenzyme A
CS	citrate synthase (EC 4.1.3.7)
dATP	deoxyadenosine 5'-triphosphate
dCTP	deoxycytidine 5'-triphosphate
DEAE	diethylaminoethyl
dGTP	deoxyguanosine 5'-triphosphate
DNA	deoxyribonucleic acid
DTNB	5,5'-dithiobis-(2-nitrobenzoic acid)
DTT	dithiothreitol
dTTP	deoxythymidine 5'-triphosphate
EDTA	(disodium) ethylenediamine tetraacetate
IPTG	isopropyl- $\beta$ -D-thiogalactoside
kb	kilobase pairs
kD	kilodaltons
LMP Agarose	low melting point agarose
MDH	malate dehydrogenase (EC 3.1.1.1.37)
M <sub>r</sub>	relative molecular mass
ORF	open reading frame
RNAse	ribonuclease A (EC 3.1.27.5)
SDS	sodium dodecyl sulphate
SDS-PAGE	SDS-polyacrylamide gel electrophoresis
TAE	tris-acetate EDTA
TBE	tris-borate EDTA
TCA	trichloroacetic acid

TEMED	N,N,N',N'-tetramethylethylene diamine
T <sub>m</sub>	Melting temperature
Tris	tris-(hydroxymethyl)-methyllamine
X-Gal	5-bromo-4-chloro-3-indolyl-β-D-galctoside

## **Acknowledgements**

I would like to thank Dr. David Hough and Dr. Mike Danson for advice, patience and many helpful discussions. Thanks to Janice Young of Zeneca for cyanogen bromide cleavage and N-terminal sequencing and Dr. David Byrom of ICI for his advice.

Finally, thanks to all the people of the "end" and "middle" labs for their help and for generally making my stay here enjoyable.

I would like to acknowledge that the initial purification was carried out by Dr. Maria Bonete of the University of Alicante and that the citrate synthase multiple sequence alignment was carried out by Michelle McCormack.

Financial support for this work was provided by the SERC and by ICI, through a CASE award.

## Introduction

### 1.1 The diversity of Archaeal phenotypes

A striking feature of the group of organisms that we know as the archaeobacteria, or Archaea, is their range of extreme requirements and tolerances for growth. Although in general their phenotypes can be thought of as either methanogenic, thermophilic or halophilic, within these broad categories are found autotrophic, heterotrophic, anaerobic, aerobic, acidophilic and alkaliphilic representatives.

The methanogens are obligate anaerobes, some of which are thermophilic or halophilic, that metabolise carbon dioxide to methane. Thermophiles may have growth optima anywhere between 55 and 110°C, some also requiring highly acidic conditions. A large proportion of them reduce sulphate or elemental sulphur to hydrogen sulphide to obtain energy. The halophilic Archaea require salt concentrations of greater than 1 M NaCl for growth and include representatives that also require highly alkaline conditions; their internal salt environments are isotonic with the exterior, but KCl replaces NaCl.

In terms of cellular and sub-cellular morphology there is little to distinguish the Archaea from the eubacteria, a fact which originally led to their taxonomic grouping with the latter as prokaryotes. Their physiological peculiarities, such as ether-linked lipids and unusual cell wall structure were

ascribed to convergent evolution and their extremophilic natures to adaptations to their environments. Molecular analysis has since revealed that the Archaea must be considered as phylogenetically distinct from both the eubacteria and the eukaryotes.

## **1.2 Archaeal Phylogeny**

The way in which we view the evolutionary history of life was revolutionised by the first thorough analyses of 16s rRNA sequence data and subsequent inference of previously unknown phylogenetic relationships (Woese & Fox, 1977, Woese *et al.*, 1978). The prokaryote/eukaryote dichotomy was replaced, after some controversy, by the division of life into eukaryotes, eubacteria and archaeobacteria that is now generally accepted. It has recently been proposed that these groups be given the status of "domains" (Eukarya, Bacteria and Archaea respectively), the archaeobacteria being renamed the Archaea to emphasise their distinction from the eubacteria (Woese *et al.*, 1990).

The Archaea are sub-divided into two main branches: the Crenarchaeota, comprising mainly acidophilic and sulphur-dependent thermophiles and the Euryarchaeota, which include the extreme halophiles, the methanogens, sulphate-reducers and some thermophiles (Figure 1.1).

### **1.2.1 The root of the universal tree**

The position of the root shown on the 16S rRNA tree (Woese *et al.*, 1990) has been determined from the data of Gogarten *et al.* (1989) and Iwabe *et al.* (1989) who used pairs of paralogous genes (that were assumed to have arisen by duplication events in the last common ancestor of all life) to locate the root between the Bacteria and Archaea. The root has simply been drawn on the rRNA tree at the equivalent position.

Studies on glutamate dehydrogenase genes (Benachenhou *et al.*, 1993, Forterre *et al.*, 1993) have revealed that they are also suitable for rooting the universal tree by a similar method to that used by Iwabe *et al.*, where one of a pair of ancestrally duplicated genes is used as an outgroup to root the tree of the other. Using several different phylogenetic inference methods these workers did not find it possible to root the tree unambiguously. Forterre *et al.* (1993) have also suggested that the way in which Iwabe *et al.* performed their calculations was not statistically sound. Regardless of the method of analysis, the currently accepted rooting is based on only two gene pairs and therefore needs further testing before it can be regarded as certain.

### **1.2.2 How valid is the Archaeal tree ?**

Since the original proposal for the existence of three branches of life, which was based on partial rRNA sequences, the data have been augmented by complete sequencing of many 16S rRNAs, increasing the resolution of the tree. Phylogenetic trees deduced from 23S rRNA (Leffers *et al.*, 1987), ribosomal proteins (Auer *et al.*, 1990), DNA dependent RNA polymerases



(Zillig *et al.*, 1989a,b), protein elongation factors and ATPases (Iwabe *et al.*, 1989) support the three domain scenario. Acceptance of this relationship has by no means been unanimous; a number of objections have been raised, either to the topology of the 16S rRNA tree (specifically to the monophyletic nature of the Archaea) or to the validity of any tree based on a single molecular feature such as 16S rRNA sequence.

### **1.2.3 Objections to the Archaeal tree**

In the past Lake has argued that the algorithms which support the archaeal tree are subject to errors caused by unequal rate effects, where rapidly changing sequences are artefactually grouped together (Lake, 1988, 1989). He put forward the evolutionary parsimony algorithm as a more suitable alternative on the basis that it is insensitive to unequal rate effects. The branching pattern obtained is different from the archaeal tree: the sulphur-dependent thermoacidophiles group with the eukaryotes while the halophiles and methanogens group with the eubacteria, thus the Archaea appear polyphyletic (Figure 1.2). Although this view has had some support, it has been refuted by the proponents of the archaeal topology (Olsen & Woese, 1989, 1993) on the basis of the regions of sequence chosen for the analysis and the way in which they were aligned.

Zillig *et al.* (1989a,b) do not contest the existence of the Archaea, but have interpreted sequence data from DNA-dependent RNA

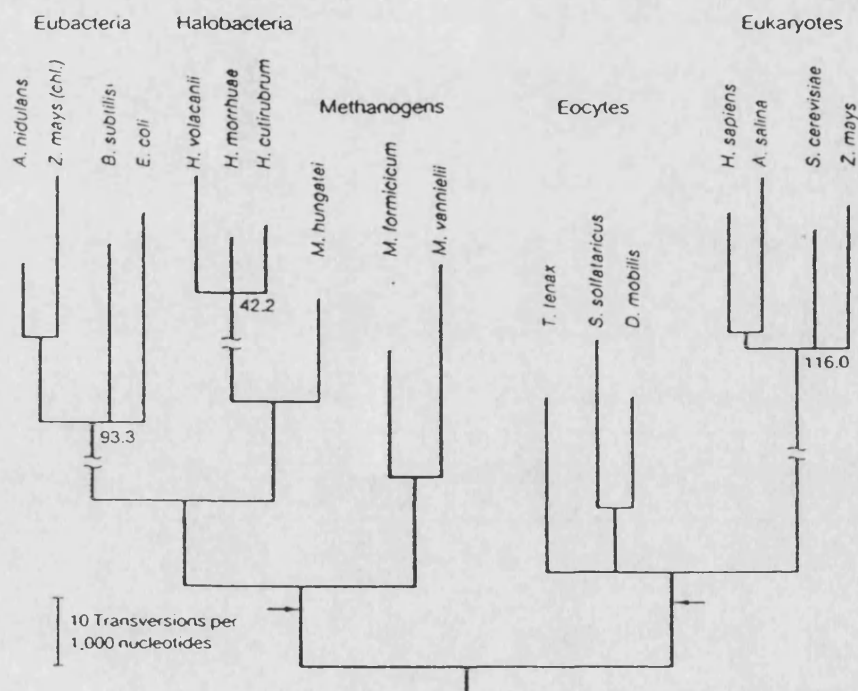


**Figure 1.2 Universal phylogenetic tree according to Lake**

polymerases as showing that the eukaryotes have arisen from a fusion of an ancestral eubacterium and Archaeon.

More fundamental objections are raised by Margulis and Guerrero (1991) and by Mayr (1990), who dispute the importance of the molecular data and who see the structural and genetic differences between "prokaryotes" and eukaryotes as paramount. For these reasons Margulis and Guerrero would prefer a five kingdom system to be adopted and Mayr a system based on two domains. Their proposals are discussed more fully in Mayr (1991), Woese *et al.* (1991) and Wheelis *et al.* (1992).

#### **1.2.4 A conflict of assumptions, not of data**

The arguments surrounding the validity of the various trees stem mainly from differences of opinion on the aims of classification (to show evolutionary relationships, or to act as an information retrieval system) and on the mathematical treatment of the available data. There are several stages at which critical choices must be made: truly homologous sequences must be chosen and aligned with minimal gaps, regions of the alignment suitable for analysis must be identified and finally the phylogenetic inference method(s) selected. There may be a number of equally valid options at each stage. (For a review see Beanland & Howe, 1992.) From the available data the division of life into three domains appears safe, although the current rooting of the tree must be taken with some caution.

### 1.3 *Haloferax volcanii*

*Haloferax volcanii* is a moderately halophilic Archaeon originally isolated from the Dead Sea (Mullakhanbhai & Larsen, 1975). At 30°C it requires a minimum of 1 M NaCl for growth, the optimum being 1.7 M NaCl. *Hf. volcanii* has a high tolerance for magnesium, as would be expected for an organism isolated from the Dead Sea, which contains 1.1 - 1.5 M Mg<sup>2+</sup>. It is capable of growing on a simple, defined minimal medium, allowing the isolation of auxotrophic strains (Mevarech & Werczberger, 1985).

The *Hf. volcanii* genome consists of a circular 2.9 Mbp chromosome and four plasmids of 690, 442, 89 and 6.4 kbp. Detailed physical mapping of the *Hf. volcanii* genome has yielded a set of overlapping cosmid clones that cover 96% of the total sequence (Charlebois *et al.*, 1990, 1991). The *Hf. volcanii* genome contains fewer mobile insertion sequences than those of other halophilic Archaea, (*Halobacterium halobium*, for example) making it relatively stable.

The development of transformation techniques (Charlebois *et al.*, 1987) and *E. coli* / *Hf. volcanii* plasmid shuttle vectors (Lam & Doolittle, 1989, Holmes *et al.*, 1991) has established *Hf. volcanii* in the field of halophile molecular biology.

### 1.4 The citric acid cycle

The citric acid cycle is the site of the terminal reactions of aerobic catabolism in eukaryotes and eubacteria, acting as a source of reducing equivalents for ATP synthesis (Figure 1.3). The cycle also provides a pool of biosynthetic precursors for anabolic processes.

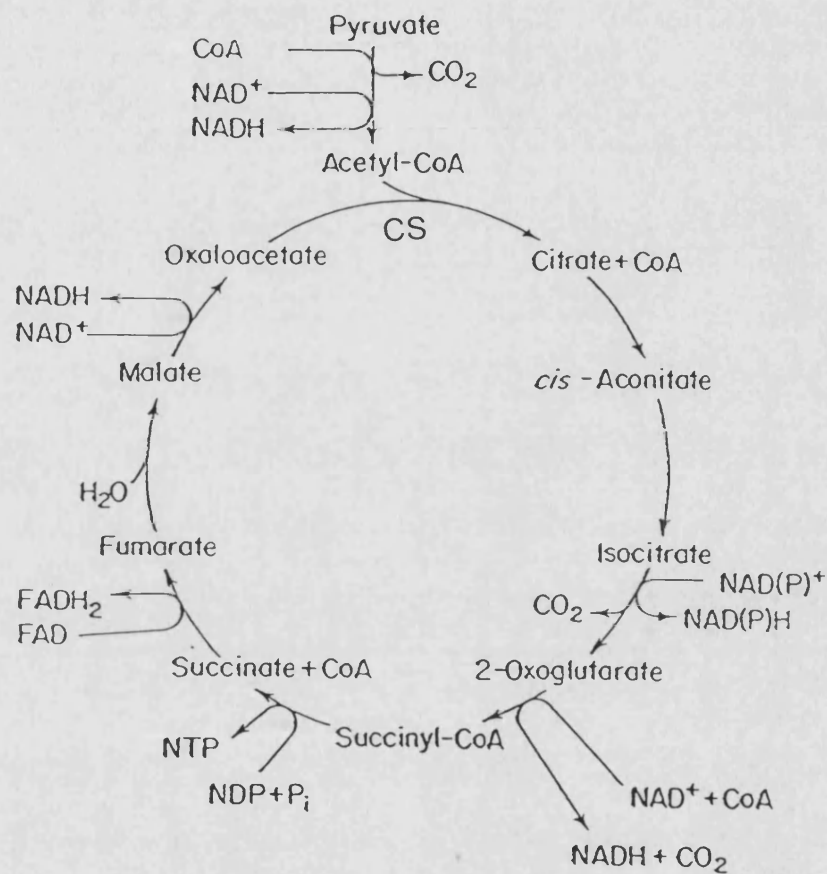


**Figure 1.3 The citric acid cycle**

The position of citrate synthase is indicated (CS).

There has been no thorough study on the presence of the oxidative cycle in Archaea. All of the cycle's enzymes have been reported in *Halobacterium halobium* (Aitken & Brown, 1969) and some in aerobically grown *Thermoplasma acidophilum* (Danson, 1988). Key enzymes (citrate synthase and succinate thiokinase) have been reported in a number of halophiles (Danson *et al.*, 1985). It is likely that a complete cycle is operative in these organisms.

An oxidative cycle may operate in sulphur-dependent Archaea growing heterotrophically and aerobically (*Sulfolobus* species, for example) as some of the required enzymes activities have been observed [see Danson, (1988) for review]. Those sulphur-dependent Archaea that grow autotrophically also possess the majority of the citric acid cycle enzymes, however they appear to be involved in CO<sub>2</sub> fixation via a reductive pathway (Schäfer *et al.*, 1986)

## **1.5 Citrate synthase**

### **1.5.1 The available data**

Citrate synthase (EC 4.1.3.7) acts as a major control point in the citric acid cycle, catalysing the condensation of oxaloacetate and acetyl coenzyme A to form citrate and coenzyme A. The enzymes of the Gram negative bacteria are hexameric and are allosterically inhibited by NADH, while those of Gram positive bacteria, eukaryotes and Archaea are dimeric and are insensitive to NADH, but are isosterically inhibited by ATP. In all cases the subunit relative molecular mass is 45-50 kD.

As a consequence of its metabolic importance, citrate synthase has been extensively studied. The gene sequences of number of citrate

synthases have been determined from a wide variety of sources, shown in Table 1.1

pig kidney	(Evans <i>et al.</i> , 1988)
<i>Saccharomyces cerevisiae</i> mitochondria	(Rosenkrantz <i>et al.</i> , 1986)
<i>Saccharomyces cerevisiae</i> glyoxysome	(Rosenkrantz <i>et al.</i> , 1986)
<i>Arabidopsis thaliana</i>	(Unger <i>et al.</i> , 1989)
<i>Escherichia coli</i>	(Ner <i>et al.</i> , 1983)
<i>Acinetobacter anitratum</i>	(Donald <i>et al.</i> , 1987)
<i>Acetobacter aceti</i>	(Fukaya <i>et al.</i> , 1990)
<i>Pseudomonas aeruginosa</i>	(Donald <i>et al.</i> , 1989)
<i>Bacillus coagulans</i>	(Schendel <i>et al.</i> , 1992)
<i>Rickettsia prowazekii</i>	(Wood <i>et al.</i> , 1987)
<i>Coxiella burnetii</i>	(Heinzen <i>et al.</i> , 1991)
<i>Tetrahymena thermophila</i>	(Numata <i>et al.</i> , 1991)
<i>Mycobacterium smegmatis</i>	(David <i>et al.</i> , 1991)
<i>Thermoplasma acidophilum</i>	(Sutherland <i>et al.</i> , 1990)

**Table 1.1 Citrate synthase gene sequences currently available**

Crystal structures are available for both the pig and chicken heart enzymes (Remington *et al.*, 1982, Liao *et al.*, 1991). Preliminary crystallographic data have recently been obtained for the citrate synthase of the Archaeon *Tp.acidophilum* (Russell *et al.*, 1993).

The crystallographic data show that the enzyme is composed almost entirely of  $\alpha$ -helices. Each subunit consists of a large and small domain, with the active site located in a cleft between them. Each subunit contributes residues to the active site of the other. Multiple sequence alignments (Henneke *et al.*, 1990) have shown that the majority of the twelve active site residues are conserved between all eubacterial and eukaryotic citrate synthases.

Two forms of the enzyme have been observed: the "open" form in which the active site is accessible to the solvent and the "closed" form where the solvent has no access to the active site, providing acetyl coenzyme A is bound. The open form has a binding site for oxaloacetate in the active site, but none for acetyl coenzyme A. When oxaloacetate binds, the large and small domains rotate relative to each other and the enzyme assumes the closed form, which can then bind acetyl coenzyme A. The open form mediates substrate entry and product release, while the closed form carries out catalysis (Remington, 1992). Figure 1.4 shows a diagram the secondary structure of a pig heart citrate synthase monomer and space-filled representations of its dimer in both open and closed forms.



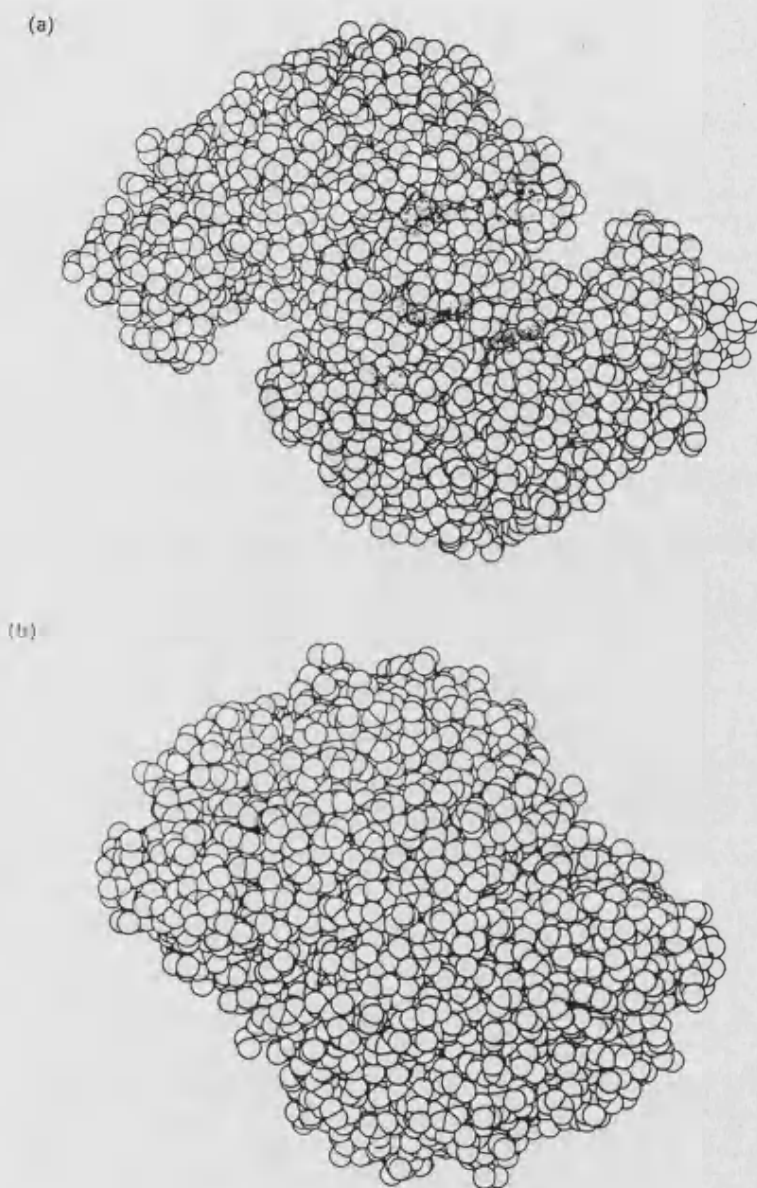


**Figure 1.4 Structural diagrams of pig heart citrate synthase**

"Open" (a) and "closed" (b) forms of the pig heart citrate synthase dimer, from Remington (1992). The two obvious clefts in the open form indicate the position of the active sites.

### 1.5.2 The citrate synthase mechanism

In order to bring about the condensation of acetyl coenzyme A and oxaloacetate, citrate synthase must first deprotonate the methyl carbon of the acetate moiety, using only the weak acids and bases of its amino acid side chains. Simultaneously, oxaloacetate must be activated, making it a suitable target for nucleophilic attack.

The catalytic mechanism has been extensively studied in pig heart citrate synthase (Karpusas *et al.*, 1990, Alter *et al.*, 1990). From studies of the binding of acetyl coenzyme A and the proposed transition state analogue carboxymethyl coenzyme A, residues His274 and Asp375 have been identified as acting in concert on acetyl coenzyme A (Karpusas *et al.*, 1990, Karpusas *et al.*, 1991). These residues are thought to promote formation of a neutral enol by general acid-base catalysis. Almost any mutation of the catalytic residues results in a substantial increase of the enzyme's stability to thermal inactivation (Wang *et al.*, 1991). This was taken to indicate that in the native enzyme these residues are held in unfavourable positions such that their  $pK_a$  values are radically changed from their solution values, enabling them to deprotonate the methyl carbon.

Bound oxaloacetate is surrounded by three arginines and two histidines, polarizing the carbonyl bond and making it prone to nucleophilic attack (Karpusas *et al.*, 1990). The stereospecificity of the reaction is explained by the binding of oxaloacetate, as only one side of the molecule is open to attack, the other being obscured by the enzyme.

The subsequent condensation step is proposed to occur as the planar

enol attacks the C3 of oxaloacetate and the proton originally donated by His274 is recycled by passing back to that residue. Figure 1.5a summarises these steps.

The resulting citryl coenzyme A intermediate is then hydrolysed by a mechanism that has not been fully characterised. Remington (1992) has suggested that hydrolysis by an activated water molecule may occur (Figure 1.5b), while Alter *et al.* (1990) suggest that an anhydride is formed with Asp375 prior to a similar hydrolysis by an activated water molecule. After the condensation step Asp375 is protonated, enabling it to donate the proton to the thioester sulphur atom and thereby activate it, since sulphonium ions are good leaving groups (Figure 1.5c).

Mutation of the active site aspartate of the *Escherichia coli* citrate synthase (Man *et al.*, 1991) has shown that this residue is involved in the hydrolysis step. When changed to glutamate the forward reaction rate is greatly reduced, although the hydrolysis of citryl-coenzyme A is unaffected. This has led them to propose a reaction scheme which does not involve the aspartate residue until the hydrolysis step, assuming that a carbanion is formed, instead of a neutral enol (Figure 1.5d). They propose that the developing carbanion is stabilised by the partial positive charge on the carbonyl of oxaloacetate. The *E.coli* enzyme may therefore operate by a slightly different mechanism to the eukaryotic enzyme.

### **1.5.3 Citrate synthase as a model enzyme**

The extensive database of structural and mechanistic information available for citrate synthase make it an ideal candidate for comparative

molecular enzymology. It is a widely occurring enzyme which has a conserved function in all organisms where it occurs and as such is suitable for phylogenetic analysis.

Citrate synthase has been reported in the three major groups of Archaea (Danson *et al.*, 1985), presenting an opportunity to compare the structures of thermophilic and halophilic enzymes with those already determined for a variety of mesophiles.

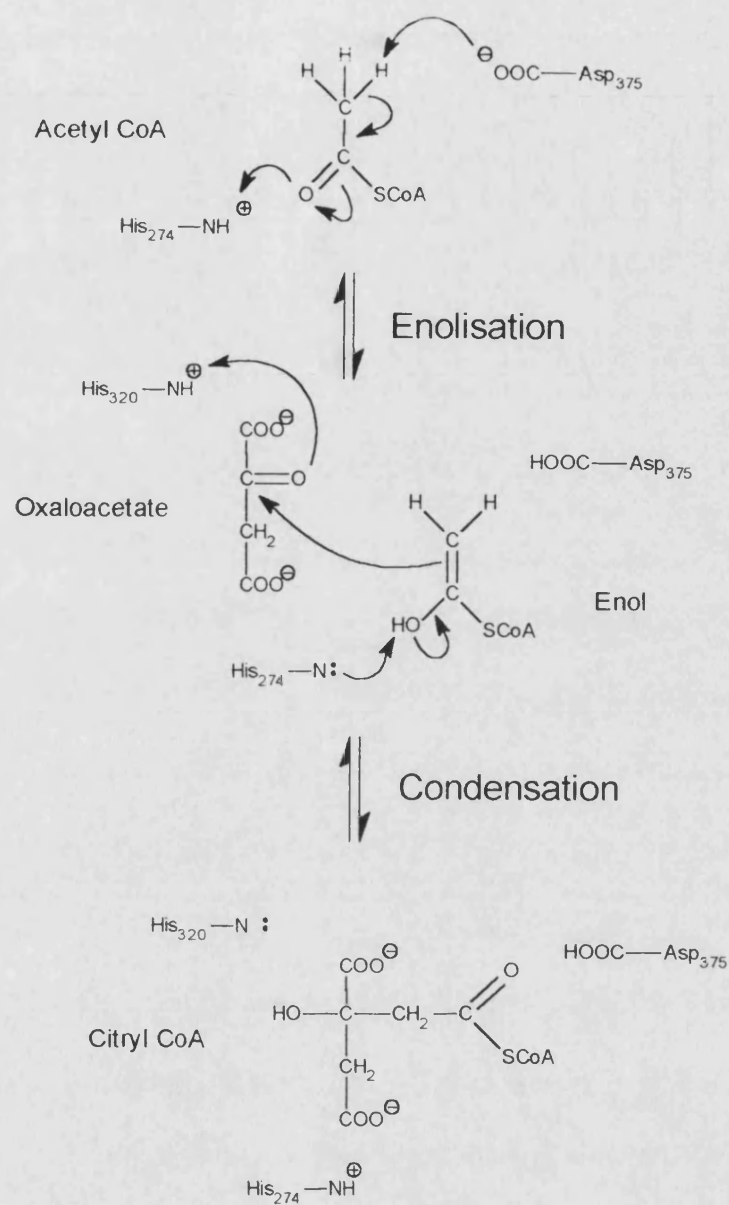


**Figure 1.5a Enolisation and condensation steps**

This proposed mechanism is based on data from the pig heart enzyme.

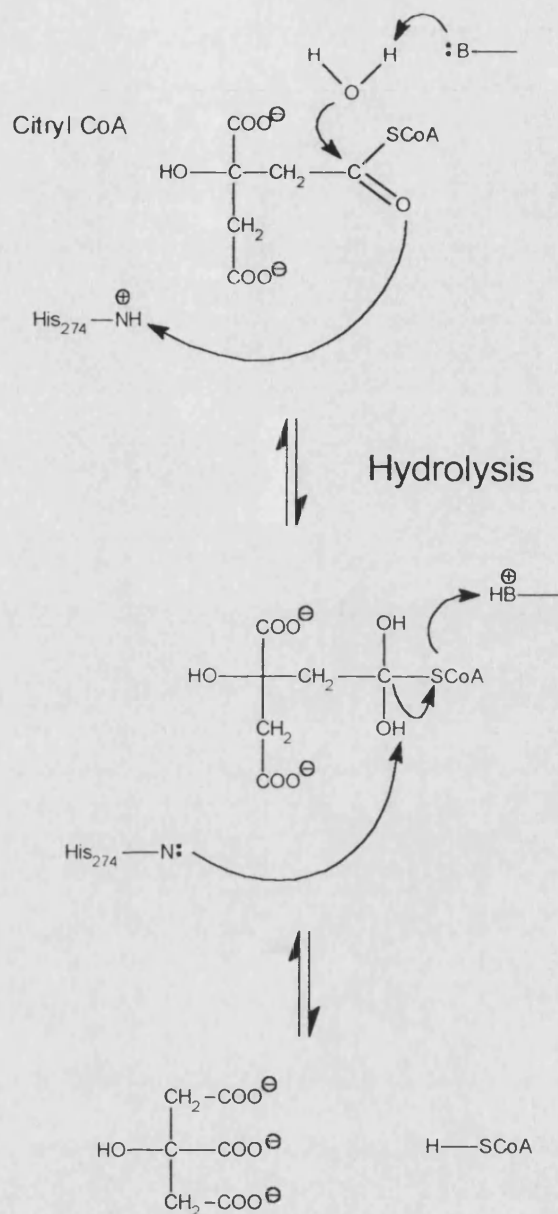


**Figure 1.5b Hydrolysis step mechanism**

This proposed mechanism is based on data from the pig heart enzyme. B- represents an unknown base on the enzyme surface.

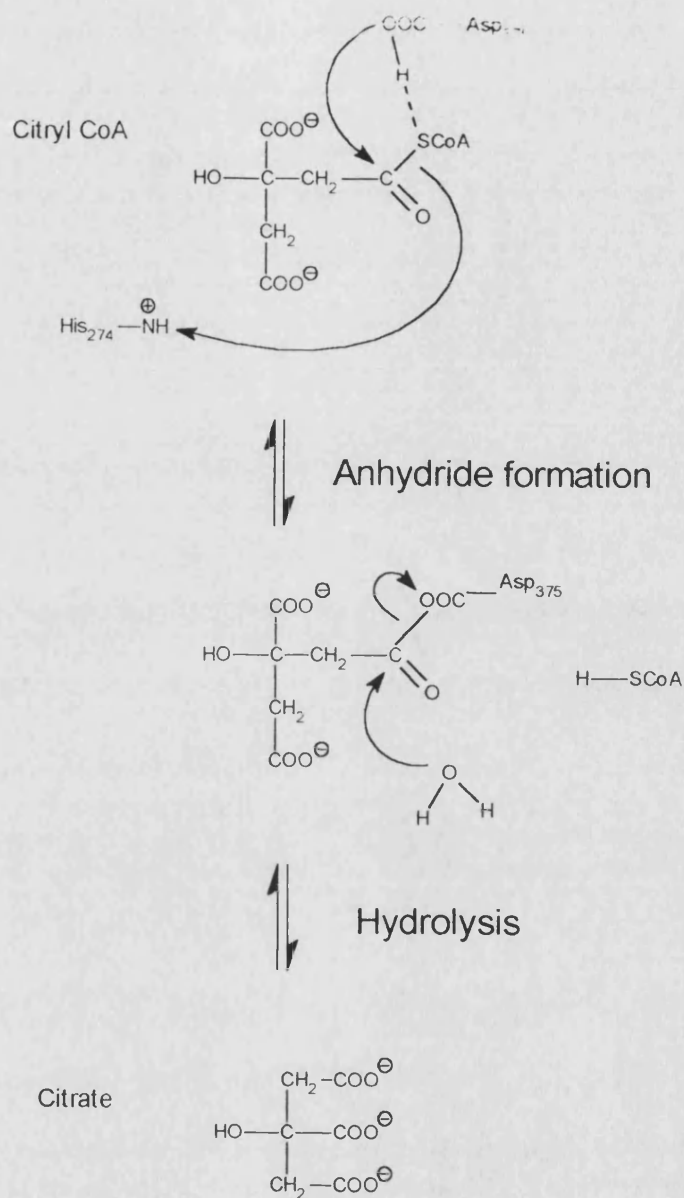


**Figure 1.5c Hydrolysis via anhydride formation**

This proposed mechanism is based on data from the pig heart enzyme.

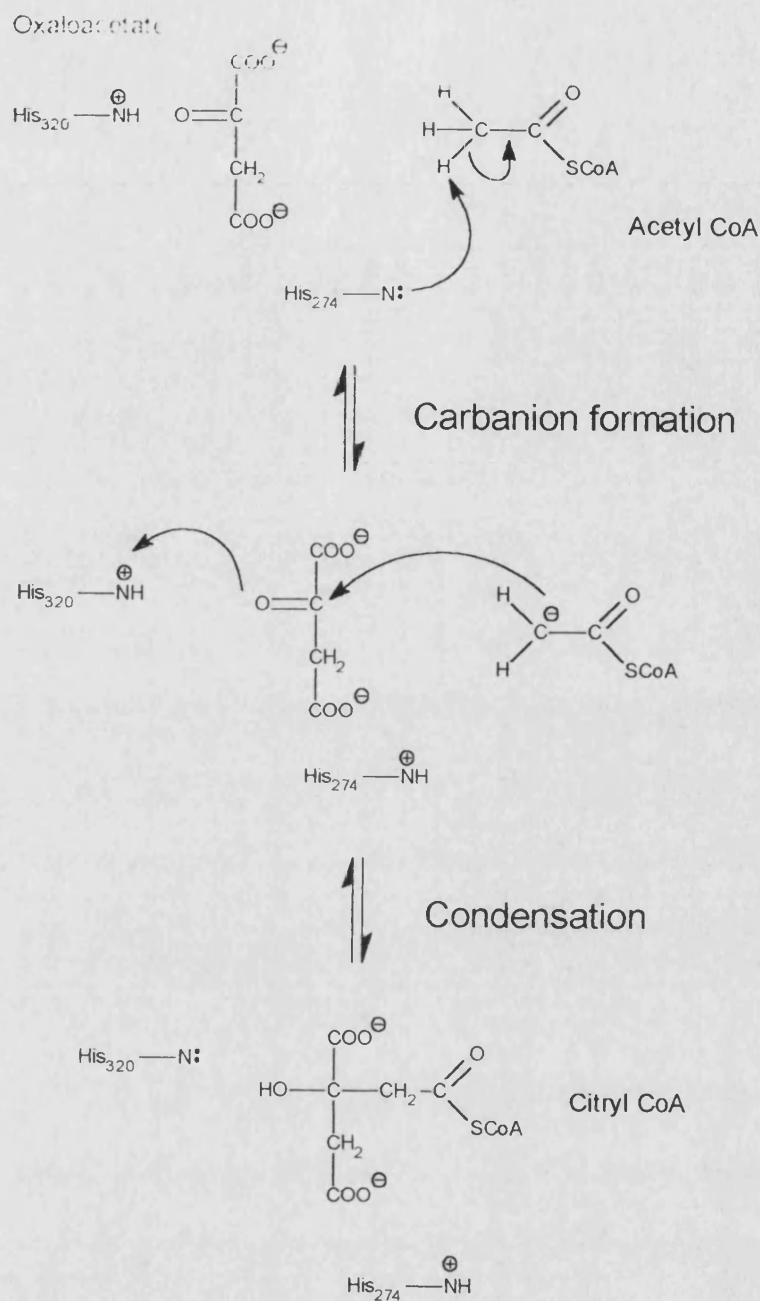


**Figure 1.5d Carbanion formation and condensation steps**

This proposed mechanism is based on data from the *E.coli* enzyme.



## 1.6 The structure of halophilic enzymes

The structural features of halophilic enzymes that are responsible for their extreme salt requirements are not well defined. In the absence of any X-ray crystallographic data, techniques such as light, X-ray and neutron scattering and analytical centrifugation have been used to probe enzyme structures in solution.

It is evident from the primary amino acid compositions of halophilic enzymes that they are generally acidic compared to their mesophilic counterparts and contain a higher proportion of borderline hydrophobic residues (Lanyi, 1974). Current data suggest that the acidic residues are clustered in surface loops surrounding a core similar to a mesophilic protein. Lanyi concluded that at low salt concentrations ( $< 0.5$  M) the predominant reason for salt dependence is the shielding of the many negative charges on the protein, while at higher concentrations hydrophobic interactions become more important.

Studies on the malate dehydrogenase (hMDH) of *Haloarcula marismortui* led to the proposal of a model for the stabilization of halophilic proteins under high salt conditions (Zaccai & Cendrin, 1989, Zaccai & Eisenberg, 1990, Eisenberg *et al.*, 1992). It is argued that the acidic groups on the surface of the protein form a quaternary structure that coordinates hydrated salt ions at a higher concentration than in the bulk solvent. The surface carboxyl groups are assumed to act cooperatively as there are otherwise too few to account for the amount of hydrated salt ions bound (approximately 500  $\text{Na}^+$  ions, 500  $\text{Cl}^-$  ions and 4000 water molecules per hMDH dimer). This salt binding corresponds to 0.35 g NaCl and 0.85 g water

per gram of protein, an exceptionally high value when one considers that non-halophilic proteins bind 0.2-0.4 g of water and negligible amounts of salt. When dissociated into monomers by lowering the salt concentration, hMDH lost its unusual salt and water binding capacity, behaving more like a non-halophilic protein. This was taken as evidence to support the involvement of quaternary structure in salt binding.

The stabilization model has since been revised following the cloning, sequencing and expression in *E.coli* of the hMDH gene (Cendrin *et al.*, 1993). The original model assumed the enzyme to be dimeric and of subunit relative molecular mass 87 kD, as determined by light and neutron scattering and analytical centrifugation (Zaccai & Cendrin, 1989). The relative molecular mass deduced from the sequence data is however 32.6 kD. The accuracy of data obtained from analytical centrifugation and light scattering has been improved and the neutron and X-ray data re-analysed, leading to the conclusion that hMDH is in fact a tetramer of about 140 kD relative molecular mass (Bonnete *et al.*, 1993).

The calculations of the amounts of salt and water bound are significantly affected by these new data; the tetramer appears to bind approximately 0.4 g water and 0.1 g NaCl or KCl per gram of protein. This is about the same amount of water and about ten-fold the amount of salt as a non-halophilic protein. The water binding ability of hMDH does not change significantly upon dissociation of the tetramer in low salt conditions (1 M NaCl); the monomers appear to remain partially folded with the same solvent binding characteristics as the tetramer.

Studies on the elongation factor Tu of *H.marismortui* (hEF-Tu) provide evidence to support this stabilization model (Baldacci *et al.*, 1990). The

translated gene sequence of hEF-Tu was compared with those of *E.coli* and *Methanococcus vanielii* (a methanogenic Archaeon), revealing the expected excess of acidic residues in the hEF-Tu sequence. The predicted antigenicity of hEF-Tu was determined by the method of Parker *et al.* (1986) and compared with the predictions for *E.coli* and *M.vanielii*. The data suggest that nearly all the acidic residues in hEF-Tu are located on the protein surface. By locating the equivalent residues on the X-ray structure of the *E.coli* EF-Tu it appears that the acidic residues in hEF-Tu occur in patches on the exterior of the protein.

Further evidence for the presence of surface charge clusters as a common feature of halophilic proteins has been presented by Bohm and Jaenicke (1994), who constructed a homology model of the *Hf.volcanii* dihydrofolate reductase (hDHFR) based on the crystal structure of the *E.coli* enzyme. These workers considered halophilicity in terms of the enzyme's instability at low salt concentrations, rather than its ability to function at high salt concentrations.

They observed that hDHFR retained activity under acid conditions, in the absence of monovalent salt. This was explained by suggesting that the driving force behind the inactivation in low salt was the charge repulsion between the negative surface residues no longer shielded from each other by salt ions. Under acid conditions these residues are protonated and electrostatically neutral, preventing disruption of the protein structure.

The hDHFR model identified five surface clusters of 2-3 amino acids each (aspartate and glutamate) that may be relevant to the protein's halophilic properties. One of these clusters occurs at the C-terminal end of an  $\alpha$ -helix, an unusual feature as this is the negative end of the helix dipole

(the dipole moment of an  $\alpha$ -helix is approximately 0.5 - 0.75 of a negative charge at the C-terminal end, and a similar positive charge at the N-terminal end). Bohm and Jaenicke termed this a "halophilic helix motif", as in general positive charges are preferred at the C-termini of helices (Richardson & Richardson, 1988).

## **1.7 Biotechnology of halophilic systems**

The characteristics of the halophilic Archaea have not yet been widely exploited in biotechnological processes. Present areas of interest include applications of isolated halobacterial purple membrane and the production of biopolymers by *Haloferax mediterranei*.

The photosensitive, proton-pumping membranes of some halobacteria have been isolated in a highly stable and active form which has potential uses in photoelectric cells and photosensitive films (Rodriguez-Valera, 1991).

Under certain growth conditions *Hf.mediterranei* can be made to accumulate the high molecular weight polymer, poly- $\beta$ -hydroxybutyrate in intracellular granules. This material is used in the manufacture of biodegradable plastics (Rodriguez-Valera *et al.*, 1989).

The unusual water-retaining properties of halophilic enzymes have yet to be applied in any industrial fermentations. These enzymes may find future applications as biocatalysts in non-aqueous media, particularly hydrophilic solvents which are thought to denature enzymes by stripping essential water molecules from them (Klibanov, 1989). Under these very low water conditions enzymes become rigid and as a consequence exhibit novel substrate specificities and increased thermostability (Klibanov, 1989, Gupta,

1992). An extracellular protease from *Halobacterium halobium* has been shown to be stable and active in the polar organic solvents DMSO and ethyleneglycol; furthermore, its activity changes from amide hydrolysis to an esterase activity, enabling it to catalyse peptide syntheses (Ryu & Dordick, 1993).

Halophilic enzymes may also find applications in aqueous environments maintained at high solute concentrations, such as in industrial processes where operation at a high substrate or product concentration would be advantageous.

In the long term it may be possible to engineer features that confer halophilicity into enzymes with useful catalytic activities, if such general features can be identified.

### **1.8 Aims of this project**

Using citrate synthase as a model, our group hopes to identify features that confer on archaeal enzymes their stability to extremes of temperature and salinity. This is to be achieved by comparison of high resolution three dimensional structures, coupled with mutational studies to test the deductions.

We aim to clone, sequence and express at high level citrate synthase from a variety of Archaea whose growth optima span the temperature range of 30 to 110°C and salinity range up to saturation. Once sufficient pure protein is available, crystallisation and rational mutagenesis studies will follow.

The protein sequence data inferred from the citrate synthase gene sequences will be used to construct phylogenetic trees, with the aim of

further clarifying the phylogeny of the Archaea and their evolutionary relationship to other organisms.

The halophilic Archaeal citrate synthases we intend to study are those from the moderate halophile, *Haloferax volcanii* and the extreme halophile, *Halobacterium halobium*. As part of our overall scheme, this project aims to clone, sequence and express at high level the gene for citrate synthase of *Hf.volcanii*, either in a mesophilic host, or in a *Hf.volcanii* citrate synthase-deficient mutant. Sequence data obtained will be subject to phylogenetic analysis, while expressed protein will be used to begin crystallisation studies.

## Materials and Methods

### 2.0 Materials

Chromatography: DEAE-Sepharose CL-6B was supplied by Pharmacia Biotech Ltd., Milton Keynes, UK, Hydroxylapatite Bio Gel HT by Bio-Rad Laboratories Ltd. Herts., UK and Matrex gel Red A by Amicon Corporation, MA, USA.

Citrate synthase assays: Coenzyme A (CoA) was supplied by Calbiochem-Novobiochem, Nottingham, UK, 5,5'-dithiobis-(2-nitrobenzoic acid) (DTNB) and oxaloacetic acid by Sigma Chemical Co. Ltd., Poole, UK.

Electrophoresis: Acrylamide Sequagel and Protogel were supplied by National Diagnostics Ltd., NJ, USA, and N,N,N',N'-tetramethylethylene diamine (TEMED) by Sigma. Protein molecular weight standards were supplied by Bio-Rad Laboratories Ltd. Agarose (standard and low melting point (LMP)) and ethidium bromide solution were supplied by Sigma.

Blotting: Genescreen transfer membrane was supplied by DuPont NEN Research Products, Stevenage, UK, Hybond N membrane by Amersham International, Aylesbury, UK and Immobilon P transfer membrane by Millipore Ltd., Watford, UK. Whatman 3MM chromatography paper was supplied by Whatman Scientific Ltd., Maidstone, UK.

Bacterial culture: Yeast extract, tryptone, casamino acids and Bacto-agar were supplied by Difco Laboratories, MI, USA. Ampicillin (sodium salt) was supplied by Sigma.

Molecular biology: Restriction enzymes were supplied by Pharmacia and by Gibco BRL Life Technologies Ltd., Uxbridge, UK. Alkaline phosphatase was supplied by Pharmacia, Klenow DNA polymerase and Taq DNA polymerase by Gibco BRL or by Northumbria Biologicals Ltd (NBL), Cramlington, UK. Lambda DNA, Lambda DNA *Hind*III and *Pst*I digests, 5-bromo-4-chloro-3-indolyl- $\beta$ -D-galactoside (X-Gal) and isopropyl- $\beta$ -D-thiogalactoside (IPTG) were supplied by NBL. NENsorb 20 columns were supplied by DuPont NEN and GeneClean II kits by Bio 101, La Jolla, CA, USA. Magic Miniprep kits were obtained from Promega Corporation, WI, USA. Low molecular DNA markers were supplied by Bio-Rad Laboratories Ltd. Sequenase kits were supplied by United States Biochemical Corp., Ohio, USA. Dithiothreitol was supplied by ICN Biomedicals Ltd., High Wycombe, UK. Redistilled phenol was supplied by Rathburn Chemicals Ltd., Walkersburn, UK.

Radiochemicals: Adenosine-5'-triphosphate, tetra (trimethylammonium) salt, [ $\gamma$   $^{32}$ P] 3000Ci/mmol was supplied by DuPont NEN and deoxyadenosine-5'-( $\alpha$ -thio)-triphosphate, [ $\alpha$   $^{35}$ S] 1000Ci/mmol by ICN Biomedicals Ltd.

Oligonucleotides were synthesised on an Applied Biosystems 381A DNA synthesiser or were ordered through Pharmacia's custom oligonucleotide synthesis service.

Polyallomer Quick-seal ultracentrifuge tubes were supplied by Beckman Instruments Inc., USA and X-ray film by Fuji Photo Film Co., Japan.



All other reagents (SLR, AnalaR and Aristar grades) were supplied by BDH Ltd., Poole, UK and Fisons, Loughborough, UK.

DNA and amino acid sequence analysis was carried out using the GCG Sequence Analysis Software Package Version 6.0 (Devereux *et al.*, 1984).

### 2.0.1 Bacterial strains, culture conditions and plasmids

*Haloferax volcanii* (DSM 3757<sup>T</sup>) was obtained as a freeze-dried culture from Deutsche Sammlung von Mikroorganismen und Zellkulturen, Germany. *Hf.volcanii* was grown in liquid batch culture in DSM medium 372 (200 g NaCl, 20 g MgSO<sub>4</sub>·7 H<sub>2</sub>O, 2g KCl, 36 mg FeCl<sub>2</sub>·4 H<sub>2</sub>O, 0.36 mg MnCl<sub>2</sub>·4H<sub>2</sub>O, 3 g trisodium citrate, 1 g sodium glutamate, 5 g yeast extract and 5 g casamino acids per litre, pH 7.2.) at 37°C, shaken at 180 rpm. Frozen stocks were maintained at -70°C in the same medium containing 15% glycerol.

*Escherichia coli* K12 HB101 F<sup>-</sup> pro<sup>-</sup> leu<sup>-</sup> thi<sup>-</sup> Sm<sup>r</sup> endoI<sup>-</sup> recA<sup>-</sup> rK<sup>-</sup> mK<sup>-</sup> and *E.coli* K12 JM105 thi rpsL endA sbcB15 hspR4 Δ(lac-proAB)(F' traD36 proAB lacI<sup>q</sup> Z M15) was grown in 2xYT medium (16 g tryptone, 10 g yeast extract and 5 g NaCl per litre) at 37°C, shaken at 200 rpm. When required the medium was solidified by addition of 1.5% agar. Frozen stocks were maintained at -20°C and -70°C in the same medium containing 30% glycerol.

Ampicillin resistance plasmids were maintained or selected for in solid and liquid media by addition of ampicillin to a concentration of 100 µg ml<sup>-1</sup>.

## **2.1 General methods**

### **2.1.1 Manipulation of *Hf.volcanii***

#### **2.1.1.1 Culture of *Hf.volcanii***

A freeze-dried culture was used to inoculate 50 ml of DSM medium 372 (Section 2.0.1) and grown for 5 days. Subsequent 1 litre cultures were inoculated with 5 ml of growing cells. After inoculation, 1 litre cultures were grown for 5-7 days. Cells were harvested by centrifugation at 8000g for 10 minutes in a Sorvall GSA rotor. Typical yield was 7-8 g litre<sup>-1</sup> (cell pellet wet weight). The cell pellets were stored in sterile tubes at -20°C until required.

Plates were prepared by addition of 1.5% (w/v) agar to DSM medium 372. Colonies generally appeared 5 - 10 days after plating out cells. Plates were stored at 4°C for up to 4 weeks, or until the medium started to become dry and crystalline. When growing liquid cultures from plates a single colony was used to inoculate 20 ml of DSM medium 372.

#### **2.1.1.2 Preparation of cell extract from *Hf.volcanii***

Cell pellets were resuspended (approximately 0.2 g ml<sup>-1</sup>) in 20 mM Tris-(hydroxymethyl)-methylamine (Tris) -HCl (pH 8.0), 2 mM (disodium) ethylenediaminetetraacetate (EDTA) containing the required concentration of KCl or glycerol. The suspension was sonicated on ice in an MSE 150 Watt Ultrasonic Disintegrator Mk2 using a 9.5 mm probe. Four to six 20-second bursts were used, with 30 seconds cooling time between each. Cell debris

was removed by centrifugation at 10,000g for 20 minutes in a Sorvall SS-34 rotor.

## **2.2 Protein techniques**

### **2.2.1 Chromatographic techniques**

#### **2.2.1.1 FPLC Superdex 200 gel filtration**

The column was run in 20 mM Tris-HCl (pH 8.0), 2 mM EDTA, 2 M KCl at 1 ml min<sup>-1</sup>. The enzyme was loaded using a 2 ml loop and 1 ml fractions were collected after the void volume (30 ml).

#### **2.2.1.2 Matrex Gel Red A column**

Columns of 10 ml bed volume were prepared in 10 ml disposable syringes plugged with siliconised glass wool. These columns were found to run freely under gravity at 1-2 ml min<sup>-1</sup>. A column was first equilibrated with 20 mM Tris-HCl (pH 8.0), 2 mM EDTA, 0.1M KCl. Cell extract (10 ml) in the same buffer was passed through a 0.45 µm filter and loaded onto the column. The column was washed with 150 ml equilibration buffer to remove unbound proteins. Citrate synthase was eluted with 20 ml of 0.2 mM coenzyme A, 1 mM oxaloacetate in the same buffer, collecting in 2 ml fractions.

After each use the column was cleaned with 30 ml of 5 M urea, 0.5 M NaOH and washed with 200 ml Milli Q water before re-equilibrating.

### 2.2.5 SDS polyacrylamide gel electrophoresis

Pre-mixed Protogel 30% acrylamide, 0.8% N N' -methylene bisacrylamide was used. Acrylamide solution, gel buffer concentrate and water were mixed according to the table below and polymerised by the addition of ammonium persulphate and TEMED to a final concentration of 0.07% (w/v) and 0.075% (v/v) respectively.

Stacking gel buffer concentrate was 0.49 M Tris-HCl (pH 6.8), 0.4% (w/v) SDS. Resolving gel buffer concentrate was 1.50 M Tris-HCl (pH 8.9), 0.4% (w/v) SDS. These were mixed according to the table below:

		Resolving gel		Stack gel
	8%	10%	12.5%	
Acrylamide solution/ml	13	16	2	1.8
Gel buffer concentrate/ml	12	12	12	4.8
distilled water/ml	23	20	16	7.2

Samples were diluted two-fold in 0.125 M Tris-HCl (pH 6.8), 0.04% (w/v) SDS, 20% (w/v) sucrose, 10% (v/v)  $\beta$ -mercaptoethanol, 0.04% (w/v) bromophenol blue and boiled for 2 minutes prior to loading on the gel.

Gels were run in 0.052 M Tris, 0.001% (w/v) SDS, 0.4% (w/v) glycine. Small (60 x 100 x 1 mm) gels were run on an Atto Corp. Mini-Atto system at 10 mA (stacking gel) and 20 mA (resolving gel). Large (160 x 160 x 2 mm)

gels were run on a Bio-Rad Protean II xi system at 20 mA (stacking gel) and 30 mA (resolving gel). All were run at constant current.

The protein standards used were from Biorad (low molecular weight range): Phosphorylase b ( $M_r$  97,400), Bovine serum albumin ( $M_r$  66,200), Ovalbumin ( $M_r$  45,000), Carbonic anhydrase ( $M_r$  31,000), Soybean trypsin inhibitor ( $M_r$  21,500) and Lysozyme ( $M_r$  14,400).

Gels were stained in 45% (v/v) methanol, 10% (v/v) acetic acid, 0.25% (w/v) Coomassie Blue R for 30-60 minutes and destained in 5% (v/v) methanol, 7.5% (v/v) acetic acid.

### **2.2.6 Western blotting**

A large polyacrylamide gel was run as described above, although the gel was not stained. A 100 x 100 mm region containing the protein bands was cut from the gel and a blotting sandwich prepared with this region alone. The blotting sandwich was set up in the following order:

Five 100 x 100 mm sheets of Whatman 3MM paper soaked in blotting buffer (50 mM Tris, 50 mM glycine, 20% (v/v) methanol), the gel section, two 100 x 100 mm sheets of Immobilon P (Polyvinylidene difluoride) membrane (pre-wetted in 100% methanol and then soaked in blotting buffer for 10 minutes) and a further five 100 x 100 mm sheets of Whatman 3MM paper also soaked in blotting buffer.

The sandwich was placed in a blotting tank containing 3.5 litres of blotting buffer pre-cooled to 4°C and electrophoretically blotted at 4°C for 15 hours at 200 mA constant current.

The gel was then removed and stained with Coomassie Blue R as described above. The membranes were stained for 15 minutes in 50%

methanol, 10% (v/v) acetic acid, 0.025% (w/v) Coomassie Blue R and destained for 20-30 minutes in several changes of 50% (v/v) methanol, 10% (v/v) acetic acid. The membranes were then washed 3 times in Milli Q water for 20 minutes, sealed in bags while still wet and stored at -20°C.

### **2.2.7 Citrate synthase assays**

Citrate synthase activity was measured spectrophotomerically by the method of Srere *et al.* (1963). Free coenzyme A reacts with 5,5'-dithio bis-2-nitrobenzoate (DTNB), releasing thionitrobenzoate which has an absorbtion maximum at 412 nm and a molar extinction coefficient of  $13,600 \text{ l mol}^{-1}\text{cm}^{-1}$ .

Assays were carried out at 30°C in a Perkin Elmer Lambda 3B spectrophotometer. Initial rates were calculated using the PECSS software supplied with the instrument. 1 unit of enzyme activity is defined as the amount which produces  $1 \mu\text{mol}$  of product  $\text{min}^{-1}$ .

Unless otherwise specified, assays were carried out in 1 ml of 20 mM Tris-HCl (pH 8.0), 2 mM EDTA, 2 M KCl containing 0.2 mM oxaloacetate, 0.4 mM acetyl coenzyme A and 0.1 mM DTNB.

### **2.2.8 Acetylation of coenzyme A**

Coenzyme A was acetylated by dissolving 10 mg CoA in 1 ml of Milli Q water, cooling on ice and adding 0.2 ml of 1 M  $\text{KHCO}_3$ , followed by 0.1 ml of 1 M acetic anhydride freshly diluted with Milli Q water. This gives a seven-fold molar excess of acetic anhydride over CoA. After incubation on ice for 10 minutes, acetylation was checked by addition of a 20  $\mu\text{l}$  sample to assay buffer containing DTNB.

## **2.3 DNA methods**

### **2.3.1 Quantitation of DNA**

DNA concentrations were determined spectrophotometrically by measurement of absorbance at 260 and 280 nm. An absorbance of 1 at 260 nm corresponds to approximately 37 µg (single-stranded) or 50 µg (double-stranded) DNA. An  $A_{260}/A_{280}$  ratio of greater than 1.8 was taken to indicate purity (Maniatis *et al.*, 1982).

### **2.3.2 DNA preparation methods**

#### **2.3.2.1 Preparation of genomic DNA from *Hf.volcanii***

Genomic DNA was prepared by a modification of the method of Holmes & Dyll-Smith (1991).

15 ml of culture was transferred to a sterile 50 ml tube and spun at 3,000 rpm for 10 minutes in a benchtop centrifuge to pellet the cells.

The pellet was resuspended in 6 ml of TE pH 8.0 containing 0.5% SDS, 100 µg ml<sup>-1</sup> proteinase K and incubated at 37°C for 1 hour.

1 ml of 5.0 M NaCl was added and mixed thoroughly, followed by 0.8 ml of 8% (w/v) hexadecyltrimethyl ammonium bromide (CTAB), 0.6 M NaCl. The mixture was incubated at 65°C for 10 minutes.

The supernatant was removed to a clean, sterile tube and extracted with an equal volume of chloroform/isoamyl alcohol for 10 minutes.

The phases were separated by spinning at 2000 rpm for 5 minutes and the supernatant transferred to a clean, sterile tube. 0.6 Volumes of

isopropanol were added to the supernatant. The precipitated DNA was transferred to 70% (v/v) ethanol by spooling onto a sterile glass rod.

The DNA was washed with 70% (v/v) ethanol, allowed to air-dry and dissolved in 2 ml of TE pH 8.0.

#### **2.3.2.2 Plasmid DNA 'Maxiprep' method I**

Log phase *E.coli* culture (1 ml) was used to inoculate 500 ml 2xYT, containing ampicillin ( $100\text{ }\mu\text{g ml}^{-1}$ ) which was then grown overnight. The cells were spun down for 10 minutes at 8,000g in a Sorvall GSA rotor. The pellet was resuspended in 2 ml of 25 mM Tris-HCl (pH 8.0), 50 mM glucose, 10 mM EDTA and transferred to a 30 ml Corex tube.

NaOH (4 ml of 0.2 M) containing 1% (w/v) SDS was added, mixed by inversion and incubated on ice for 5 minutes. Ice-cold potassium acetate (3 ml of 3 M, pH 4.8) was added, mixed by inversion and incubated on ice for 10 minutes.

Cell debris was removed by spinning in a Sorvall SS-34 rotor at 8,000g for 20 minutes at 4°C. The supernatant was made up to 10 ml with distilled water and the DNA purified by caesium chloride density gradient centrifugation.

#### **2.3.2.3 Caesium chloride equilibrium density gradient centrifugation**

To the 10 ml of DNA solution prepared by the 'Maxiprep' method I, 10.17 g caesium chloride was added. This was sealed in a 13 x 51 mm Beckman Quick-Seal ultracentrifuge tube and spun at 55,000 rpm for 24 hours at 4°C in a Beckman Ti70 rotor.



The plasmid DNA was recovered under UV illumination using a syringe and 19G needle and extracted three times with an equal volume of water-saturated butanol to remove the ethidium bromide. The DNA was then precipitated with ethanol, washed in 70% (v/v) ethanol, dried and dissolved in 0.5 ml of TE (pH 8.0).

#### **2.3.2.4 Plasmid DNA 'Maxiprep' method II**

Cells were grown overnight in 100 ml 2xYT, containing ampicillin (100  $\mu\text{g ml}^{-1}$ ) after inoculation with 1 ml of log phase *E.coli* culture.

The cells were spun in a benchtop centrifuge at 3,000 rpm for 10 minutes and the pellet resuspended in 4 ml of 25 mM Tris-HCl (pH 8.0), 50 mM glucose, 10 mM EDTA. NaOH (8 ml of 0.2 M) containing 1% (w/v) SDS was added, mixed by inversion and incubated on ice for 10 minutes. Ice-cold potassium acetate (6 ml of 3 M, pH 4.8) was added, mixed by inversion and incubated on ice for 15-30 minutes. Cell debris was removed by spinning at 3,000 rpm for 15 minutes in a benchtop centrifuge.

The supernatant was added to 18 ml of propan-2-ol and incubated on ice for 30 minutes. The precipitated nucleic acid was pelleted in a benchtop centrifuge at 3,000 rpm for 20 minutes. The pellet was dissolved in 1 ml of TE (pH 8.0), 1 ml of 6 M LiCl was added and incubated on ice for 15 minutes. The precipitate was removed by spinning in a microcentrifuge for 10 minutes. The supernatant was added to 4 ml of absolute ethanol and the nucleic acids precipitated at  $-20^{\circ}\text{C}$  for 30 minutes.

The precipitate was pelleted in a microcentrifuge for 10 minutes, washed with 70% (v/v) ethanol, dried and dissolved in 0.4 ml of TE (pH 8.0). To the solution, 4  $\mu\text{l}$  of 10  $\text{mg ml}^{-1}$  RNase A was added and the mixture

incubated at 37°C for 30 minutes. To inactivate the RNase 20 µl of 10% (w/v) SDS was added, the solution was heated to 75°C for 10 minutes, 0.42 ml of 6 M LiCl was added and mixture incubated at room temperature for 15 minutes. The precipitate was pelleted in a microcentrifuge for 10 minutes and the supernatant added to 2 ml ethanol containing 40 µl of 3M sodium acetate (pH 5.2); DNA was precipitated at -20°C for 30 minutes.

The DNA was pelleted in a microcentrifuge for 10 minutes, washed with 70% (v/v) ethanol, dried and dissolved in 0.4 ml of distilled water. The DNA solution was extracted once with phenol / chloroform and twice with chloroform and ethanol precipitated. The precipitate was pelleted in a microcentrifuge for 10 minutes, washed with 70% (v/v) ethanol, dried and dissolved in 0.1 ml of distilled water.

This procedure yields 400-800 µg plasmid DNA suitable for restriction digests or sequencing, without CsCl density gradient centrifugation.

#### **2.3.2.5 Plasmid DNA 'Minipreps'**

Small-scale isolation of plasmid DNA was carried out by the alkaline lysis method of Maniatis *et al.* (1982).

#### **2.3.2.6 Plasmid DNA 'Magic Minipreps'**

Plasmid DNA was isolated using the Magic Minipreps kit, following the manufacturer's instructions.

### **2.3.3 Restriction digests of DNA**

DNA was digested with the appropriate enzyme under the buffer conditions specified by the manufacturer. When the DNA was digested with

two enzymes requiring different buffer concentrations, the first enzyme was heat inactivated under the conditions recommended by the supplier and further 10x buffer was added to the reaction mixture prior to addition of the second enzyme.

#### **2.3.4 Agarose gel electrophoresis of DNA**

Agarose gels containing 0.6-1.0% (w/v) agarose were made with 1x Tris-acetate-EDTA (TAE) buffer containing  $0.5 \mu\text{g ml}^{-1}$  ethidium bromide. Loading buffer (6x concentration) was 40% (w/v) sucrose, 0.25% (w/v) bromophenol blue, 0.25% (w/v) xylene cyanol. Gels were run at  $6 \text{ Vcm}^{-1}$  (Plasmid DNA and plasmid digests) or  $2 \text{ Vcm}^{-1}$  (genomic DNA digests) in 1x TAE buffer. When the DNA bands were to be cut from the gel and purified, ultra-pure low-melting point agarose was used.

#### **2.3.5 Recovery of DNA from agarose gels**

DNA was recovered from low-melting point agarose gels by a modification of the freeze-squeeze method of Tautz & Renz (1983). The gel slice was placed in a 0.5 ml Eppendorf tube which had been pierced at the base and the hole stopped with siliconised glass wool. The tube was frozen in liquid nitrogen for 30 seconds, placed into a 1.5 ml Eppendorf tube and spun in a micro centrifuge for 5 minutes. The eluent containing the DNA was collected.

### **2.3.6 Purification of DNA fragments**

Phenol was equilibrated with Tris-HCl (pH 8.0), phenol / chloroform / isoamyl alcohol and chloroform / isoamyl alcohol extractions were performed as described by Maniatis *et al.*(1989).

DNA was purified using NENsorb cartridges according to the manufacturer's instructions, eluting with 30% (v/v) ethanol. Aristar grade methanol was used to wet the columns. Alternatively, the Geneclean II kit was used to purify DNA fragments, according to the manufacturer's instructions.

Spun columns of Sepharose CL-6B, Sephadex G-25 and Sephadex G-50 were prepared in 0.5 ml Eppendorf tubes which had been pierced at the base and the hole stopped with siliconised glass wool. 400 µl of 50% slurry was packed by spinning inside a 1.5 ml Eppendorf tube. Four column volumes of TE (pH 8.0) were passed through by spinning under the same conditions and the DNA sample was loaded onto the dry column and re-spun into a fresh tube.

### **2.3.7 Precipitation of DNA**

DNA precipitations were carried out using ethanol and sodium acetate as described by Maniatis *et al.*(1982).

### **2.3.8 Ligation procedures**

Ligation of cohesive ends was carried out using 0.1 Units of Gibco BRL T4 DNA ligase in the buffer supplied by the manufacturer. The ratio of insert to vector was approximately 5 to 1, estimated by ethidium bromide

staining on agarose gel. Ligation was carried out overnight at 15°C in a total volume of 20 µl.

The Gibco T4 ligase buffer is suitable for blunt-end ligations, which were therefore carried out under the same conditions except that the ratio of insert to vector was increased to approximately 10 or 20 : 1.

### **2.3.9 DNA blotting techniques**

#### **2.3.9.1 Southern blotting**

Restriction digests of plasmid DNA were carried out as described. Digests were run on 1% (w/v) agarose gels in 1x TAE buffer at 2 - 6 Vcm<sup>-1</sup>, dependent upon the size of the DNA fragments. The size markers used were 2 µg of  $\lambda$  HindIII digested DNA.

Blotting onto Genescreen membrane was carried out by the capillary method (Southern, 1975). The DNA was first denatured by incubation in 0.2 M NaOH, 0.6 M NaCl for 30 minutes at room temperature. The gel was then washed three times in 10x SSC (1.5 M NaCl, 0.15 M sodium citrate) for 20 minutes at room temperature. The Genescreen membrane was soaked in 10x SSC for 10 minutes and the blotting stack was set up using a reservoir containing 10x SSC. Blotting was carried out for 18 hours. The membrane was removed and air dried. The DNA was baked onto the membrane at 80°C for 3 hours.

#### **2.3.9.2 Dot blotting**

The DNA sample was dissolved in water and spotted onto dry Genescreen membrane using a fine-tipped pipette. Generally 1 µg of DNA was applied in a single dot. The dot was allowed to dry and then the blot was

treated with 1.5 M NaCl, 0.5 M NaOH and 1.5 M NaCl, 0.5 M Tris-HCl (pH 7.2), 1 mM EDTA as described in 2.3.9.3 below. The blot was placed on a filter-paper pad soaked in 2x SSC for 2 minutes, air-dried and baked at 80°C for 2 hours.

### **2.3.9.3 Colony hybridisation**

Gridded Hybond-N nylon membranes were placed on the surface of 2xYT plates containing ampicillin ( $100 \mu\text{g ml}^{-1}$ ). Bacteria were streaked onto the membranes and grown overnight at 37°C. The membranes were placed on a pad of filter paper soaked in 1.5 M NaCl, 0.5 M NaOH for 7 minutes. They were then transferred to a fresh pad soaked in 1.5 M NaCl, 0.5 M Tris-HCl (pH 7.2), 1 mM EDTA for 3 minutes. This last step was repeated once and the membranes then washed in 2x SSC before being allowed to air-dry. The DNA was baked onto the membranes at 80°C for 2 hours.

### **2.3.10 Deprotection and purification of synthetic oligonucleotides**

Columns from the DNA synthesiser were opened and the resin removed to a 2 ml screw-cap tube containing 1ml concentrated ammonia. The resin was resuspended and incubated at 55°C for 18 hours to cleave the DNA from the column and remove protecting groups.

The solution was cooled on ice, centrifuged to pellet the resin and the supernatant containing the DNA removed. The solution was dried under vacuum, dissolved in 0.5 ml distilled water, centrifuged to remove any remaining resin and precipitated with ethanol. The pellet was redissolved as

before and precipitated a second time before finally dissolving in 0.5 ml of sterile Milli Q water.

### **2.3.11 End-labelling of oligonucleotides**

Oligonucleotides were end-labelled with [ $\gamma$ - $^{32}\text{P}$ ] ATP by incubating 20 pmoles oligonucleotide with 100  $\mu\text{Ci}$  [ $\gamma$ - $^{32}\text{P}$ ] ATP (33 pmoles) and 10 units of T4 polynucleotide kinase in 1x kinase buffer (20 mM Tris-HCl (pH 7.6), 5 mM  $\text{MgCl}_2$ , 5 mM dithiothreitol, 50  $\mu\text{g ml}^{-1}$  bovine serum albumin (BSA)) at 37°C for 30 minutes. Total reaction volume was 40  $\mu\text{l}$ .

Incorporation of radiolabel was checked and unincorporated label removed by passing the solution through a Sephadex G-25 spun column (for 17-20mers) or a G-50 spun column (for larger oligonucleotides), as described under DNA purification methods.

### **2.3.12 Hybridisation of labelled oligonucleotide probes to DNA blots**

The dried membrane was sealed in a bag containing 50 ml pre-hybridisation solution (5.2x SSC, 5x Denhardt's solution [0.1% (w/v) Ficoll, 0.1% (w/v) polyvinylpyrrolidone, 0.1% (w/v) BSA], 0.1% (w/v) , 0.6% (w/v) SDS, 20  $\mu\text{g ml}^{-1}$  salmon sperm DNA). The salmon sperm DNA was boiled for 5 minutes and then cooled on ice for 5 minutes prior to addition. The membrane was incubated overnight at the desired temperature. To this, 20 pmoles of labelled oligonucleotide probe were added and the membrane incubated for a further 12-18 hours.

The membrane was washed twice with 50 ml of 2x SSC, 0.1% (w/v) SDS at the same temperature, sealed in a plastic bag and autoradiographed

using pre-flashed X-ray film and intensifying screens at -70°C. Two pieces of film were used, the first developed after 2 days, the second after 4-30 days depending on the intensity of the bands observed on the first.

### **2.3.13 Preparation of competent *E.coli* JM103 and HB101**

Competent *E.coli* were prepared by the calcium chloride method. Growth medium (50 ml of 2xYT in a 250 ml flask) was inoculated with 1 ml of an overnight bacterial culture and grown at 37°C for 2 hours with vigorous shaking. The culture was chilled on ice for 10 minutes and spun at 2,500 rpm in a benchtop centrifuge for 5 minutes.

The supernatant was discarded and the cell pellet resuspended in 50 ml of ice-cold, sterile 50 mM CaCl<sub>2</sub>. The cell suspension was kept on ice for 30 minutes and the centrifugation repeated. The cells were resuspended in 5 ml of ice-cold 50 mM CaCl<sub>2</sub> and kept on ice for 60 minutes before use.

### **2.3.14 Transformation of competent *E.coli* JM103 and HB101 with plasmid DNA**

Competent cells (200 µl) were added to 5 µl of a ligation mixture and incubated on ice for 30 minutes in polypropylene tubes. The cells were heat-shocked at 42°C for 90 seconds and replaced on ice for 60 seconds. The culture was made up to 1 ml by addition of 800 µl of 2xYT and the cells incubated at 37°C for 1 hour without shaking. X-Gal (50 µl of 20 mg ml<sup>-1</sup>, in DMF) and IPTG (50 µl of 24 mg<sup>-1</sup> ml<sup>-1</sup>) were added and 200-350 µl of the mixture plated on 2xYT agar containing ampicillin (100 µg ml<sup>-1</sup>). Plates were incubated at 37°C overnight.



### **2.3.15 PCR techniques**

#### **2.3.15.1 PCR amplification of genomic DNA**

Amplification was carried out using NBL and Gibco BRL Taq polymerases in 100  $\mu$ l of 20mM Tris-HCl (pH 8.3), 25 mM KCl, 0.5-5 mM  $MgCl_2$ , 0.1 mg  $ml^{-1}$  BSA overlaid with 50  $\mu$ l of mineral oil. Reactions were carried out in a Perkin Elmer Cetus DNA Thermal Cycler using Perkin Elmer GeneAmp reaction tubes.

Reaction mixtures contained 80 ng of target DNA, 50  $\mu$ M dATP, deoxycytidine triphosphate (dCTP), deoxyguanosine triphosphate (dGTP) and deoxythymidine triphosphate (dTTP), primers at a concentration of 0.4  $\mu$ M each and 2.5 U of Taq polymerase. The mixture was heated to 94°C for 4 minutes, maintained at 94°C while the polymerase was added and then 30 reaction cycles were carried out using the following profile:

- 94°C for 1 minute
- 37°C-65°C for 1.5 minutes
- 72°C for 2 minutes.

A final 10 minute extension was run after the last cycle was complete. A 10  $\mu$ l aliquot from each reaction was run on a 1% (w/v) agarose gel.

#### **2.3.15.2 Asymmetric PCR**

The technique of asymmetric PCR described by McCabe (1990) was used to generate single-stranded DNA by reamplification of a gel-purified PCR product.

Reactions were carried out in 100  $\mu$ l of 20 mM Tris-HCl (pH 8.3), 25 mM KCl, 1.5 mM MgCl<sub>2</sub>, 0.1 mg ml<sup>-1</sup> BSA, overlaid with 50  $\mu$ l of mineral oil. The ratio of primers was 50 pmoles to 1 pmole. The primer to be extended into the single-stranded product was present in the greater amount.

The template was prepared by running 10  $\mu$ l of a previous PCR reaction on a 1% (w/v) agarose gel, excising the band to be reamplified, recovering the DNA by freeze-squeeze followed by ethanol precipitation or using GeneClean and finally dissolving the dried pellet in 20  $\mu$ l distilled water. Of this, 0.5  $\mu$ l was used for each reamplification reaction.

The reactions were carried out as described above, the mineral oil was removed by extraction with chloroform and an equal volume of 4 M ammonium acetate was added to the aqueous phase. DNA was precipitated by adding isopropanol to a final concentration of 50% (v/v) and leaving the solution for 10 minutes at room temperature. The precipitate was pelleted by spinning for 10 minutes in a microcentrifuge, washed with ice cold 70% (v/v) ethanol and dried.

The pellet was dissolved in 7  $\mu$ l of distilled water and sequenced using 1 pmole of the PCR primer that was at the lower concentration in the amplification reaction. The sequencing procedure was identical to that for plasmid DNA, except that the denaturing step was omitted.

### **2.3.16 Sequencing plasmid DNA**

Sequencing of double-stranded template DNA (pUC18) was carried out by the dideoxy chain termination method, using Sequenase kits and  $\alpha$ -<sup>35</sup>S-dATP (1000Ci/mmol), according to the manufacturer's instructions. For each set of 4 reactions 3-5  $\mu$ g of template DNA were used. Between 1 and

20 pmoles of primer were used per set of reactions. When sequencing close to the primer 1  $\mu$ l of Sequenase  $Mn^{2+}$  buffer was added to the reaction mixture.

Sequencing reactions were run in Tris-borate-EDTA (TBE) buffer on 0.4 mm thick 8% polyacrylamide gels made using Sequagel reagent kits. Gels were left 2-3 hours after pouring before use and were pre-run for 1 hour. Using a Bio-Rad Sequi-Gen II 50 x 21cm sequencing cell, gels were run at 40-50 Watts constant power and at a constant temperature of 50°C. Gels were fixed in 10% (v/v) acetic acid, 10% (v/v) methanol for 15 minutes before drying under vacuum.

Dried gels were autoradiographed overnight, or longer if necessary.

## **Characterisation of activity and stability of *Hf.volcanii* citrate synthase**

### **3.1 Introduction**

The effect of monovalent salt concentration on the activity and stability of *Hf.volcanii* citrate synthase was studied under different conditions as a basis for the design of improved purification procedures. The effect of KCl concentration on stability was investigated by thermal inactivation experiments. These serve as the first steps in the thorough characterisation of the enzyme that will be necessary if it is to be used as a model for the study of halophilicity.

The studies described below were carried out on cell extracts prepared as described in Section 2.1.1.2. When citrate synthase assays were carried out on unfractionated extracts, background activities of coenzyme A hydrolysis were measured by assays omitting oxaloacetate. In cases where this rate was not zero, the background value was subtracted from the measured rate to give the citrate synthase activity.

The apparent  $K_m$  values of the *Hf.volcanii* citrate synthase for oxaloacetate and coenzyme A have been determined as 38  $\mu\text{M}$  and 75  $\mu\text{M}$  respectively in 2M NaCl (Danson *et al.*, 1985). This was taken as a guide to the enzyme's kinetic characteristics in 2M KCl: assays were therefore carried out in 200  $\mu\text{M}$  oxaloacetate and 400  $\mu\text{M}$  coenzyme A.

### **3.2 Salt dependence of citrate synthase activity**

Cell extracts were prepared in 20 mM Tris-HCl (pH 8.0), 2 mM EDTA, containing either 0.5 M NaCl or KCl. Samples of 10  $\mu$ l were assayed at increasing final concentrations of NaCl or KCl as shown in Figure 3.1. Each assay was carried out in triplicate.

### **3.3 Stability of citrate synthase**

Cell extracts were prepared in 20 mM Tris-HCl (pH 8.0), 2 mM EDTA, containing either 0.5 M NaCl or KCl. Samples of 90  $\mu$ l were diluted into 3 ml 20 mM Tris-HCl (pH 8.0), 2 mM EDTA, containing NaCl or KCl, to give final concentrations of 0, 0.05, 0.1, 0.5, 1, 2, 3 and 4 M salt. The enzyme solution was incubated at 25°C and 30  $\mu$ l samples were assayed for citrate synthase activity in buffer containing 2 M NaCl or KCl after 0, 24, 48 and 120 hours.

It was found that at NaCl or KCl concentrations below 0.1 M, total inactivation occurred within 24 hours. At higher concentrations of either salt no activity was lost during the 120 hour course of the incubation (data not shown).

### **3.4 Thermal inactivation of citrate synthase**

Cell-free extracts were prepared in 20 mM Tris-HCl (pH 8.0), 2 mM EDTA containing 2 M KCl. A glass tube containing 2.85 ml of the same buffer was heated in a water bath and 150  $\mu$ l of cell extract added. The solutions were mixed briefly with a 1 ml automatic pipette. Inactivations were carried out at 60, 62, 64, and 66°C. At higher temperatures the mixing

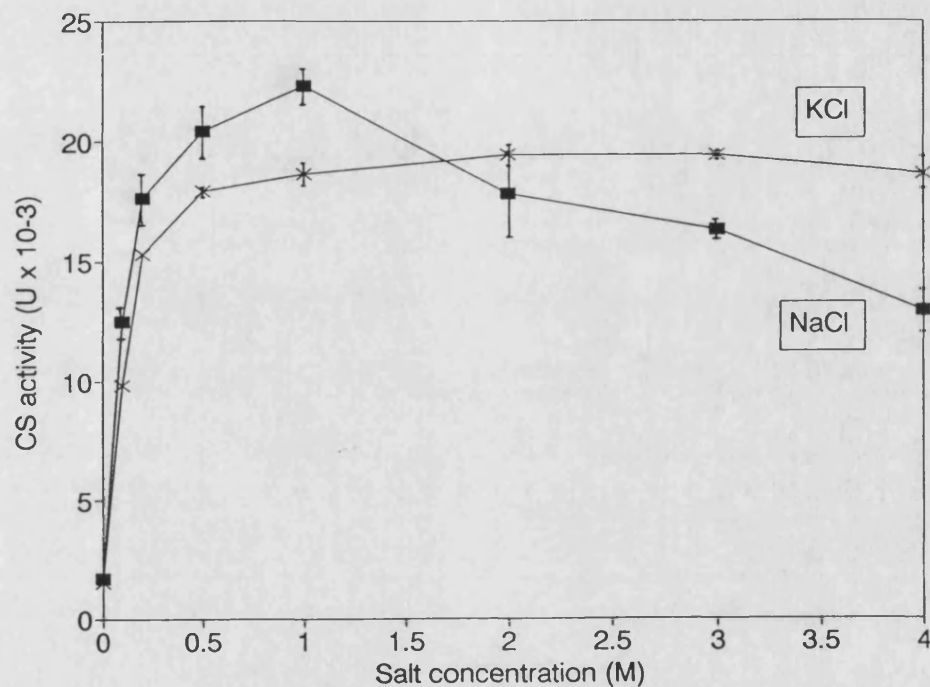


**Figure 3.1 Dependence of citrate synthase activity on salt concentration**

Initial rates are plotted against the concentration of NaCl or KCl in the assay. Each point is the mean value of triplicate assays; the error bars indicate 1 standard deviation.

process was found to produce transient cooling of the system, resulting in non-linear rates of inactivation. The effect became more marked with increasing inactivation temperatures.

Temperatures were measured using a thermocouple in a separate, identical tube and were maintained to within 0.2°C of the target temperature throughout the timecourse.

Aliquots of approximately 150 µl were removed at intervals, cooled rapidly by pipetting into ice-cold glass tubes and 50 µl of this sample were then assayed immediately. As it was not possible to measure hot liquids accurately with the air-displacement pipettes used, the rapid cooling of the aliquots by pipetting into an ice-cold glass tube was essential before removing the 50 µl for assay. A value for 100% activity was obtained by diluting 150 µl of cell-free extract into 2.85 ml of the same buffer at 4°C and assaying 50 µl aliquots. The rates of inactivation were determined by plotting the natural logarithm of the percentage initial activity as a function of time. The apparent first order rate constants are given by the slopes of these plots, which are shown in Figures 3.2-3.5.

According to transition-state theory, the relationship between the rate constant of a reaction and the absolute temperature can be expressed as:

$$k = k_B T / h \cdot e^{-\Delta G^\circ / RT}$$

Where  $k$  is the rate constant of the reaction,  $k_B$  is Boltzmann's constant,  $h$  is Planck's constant,  $R$  is the gas constant,  $T$  is the absolute temperature in degrees Kelvin and  $\Delta G^\circ$  is the free energy change in going from the ground state of the reactant(s) to the transition state (Creighton, 1993).

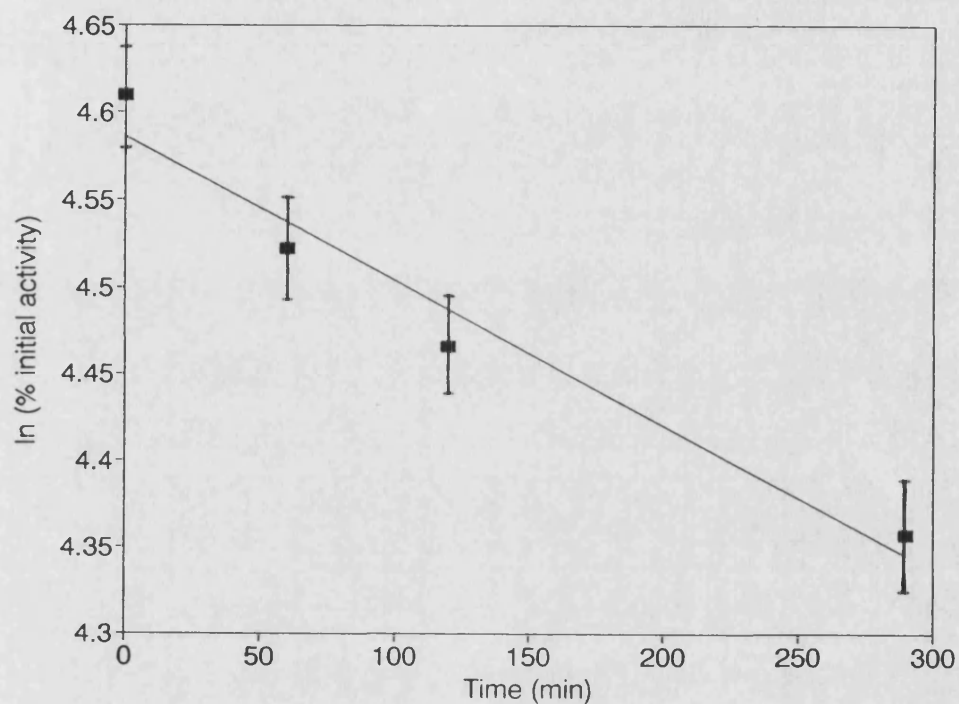


**Figure 3.2 Thermal inactivation of citrate synthase at 60°C**

The graph shows  $\ln$  (% initial activity) plotted against time in minutes. The rate constant of the inactivation  $k$ , equal to  $-(\text{slope})$ , is  $8.3 \times 10^{-4} \text{ min}^{-1}$ . Each point is the mean of triplicate independent inactivations; error bars indicate 1 standard deviation.



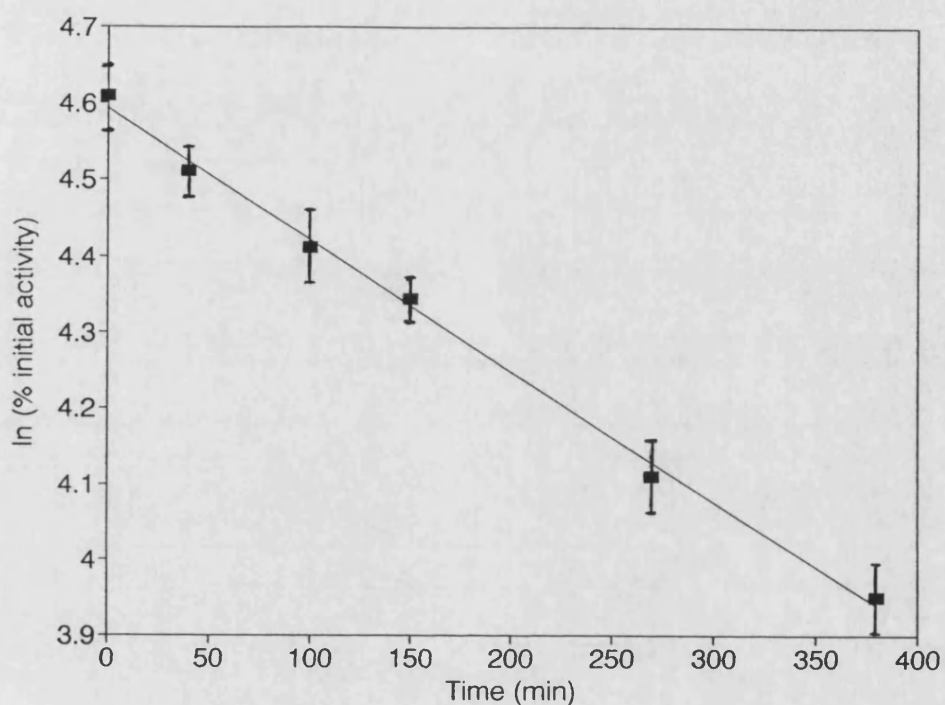


**Figure 3.3 Thermal inactivation of citrate synthase at 62°C**

The graph shows  $\ln$  (% initial activity) plotted against time in minutes. The rate constant of the inactivation  $k$ , equal to  $-(\text{slope})$ , is  $1.7 \times 10^{-3} \text{ min}^{-1}$ . Each point is the mean of triplicate independent inactivations; error bars indicate 1 standard deviation.

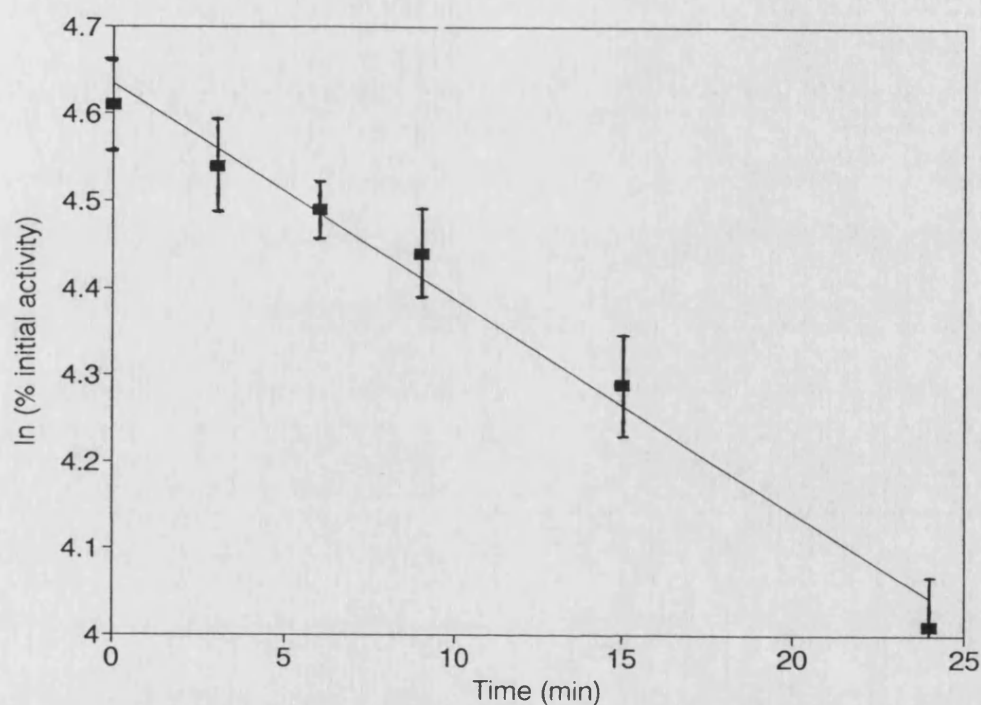


**Figure 3.4 Thermal inactivation of citrate synthase at 64°C**

The graph shows  $\ln$  (% initial activity) plotted against time in minutes. The rate constant of the inactivation  $k$ , equal to  $-(\text{slope})$ , is  $0.025 \text{ min}^{-1}$ . Each point is the mean of triplicate independent inactivations; error bars indicate 1 standard deviation.

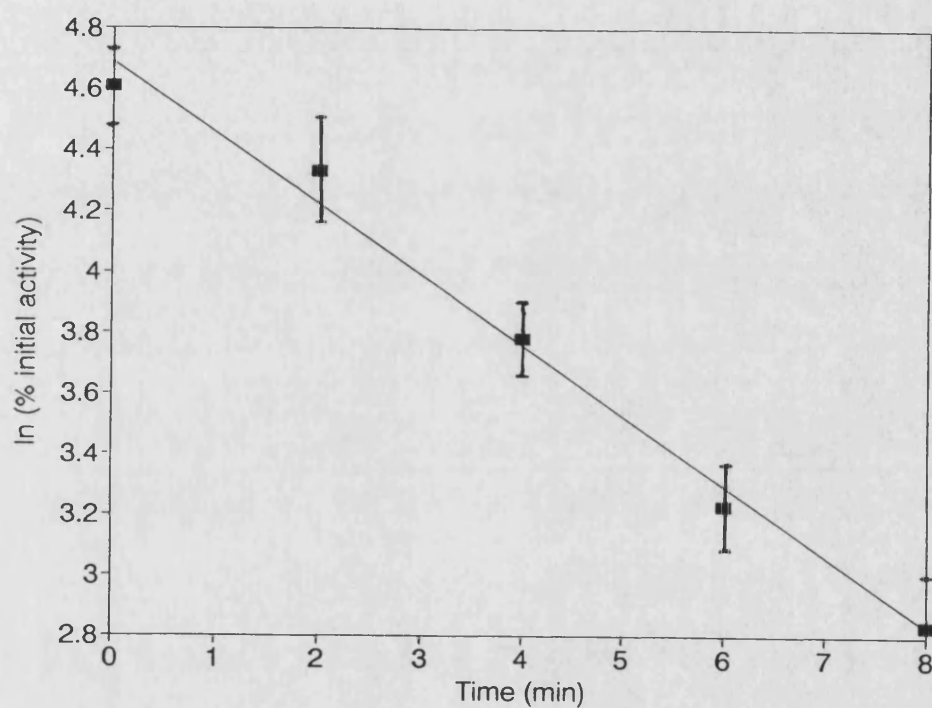


**Figure 3.5 Thermal inactivation of citrate synthase at 66°C**

The graph shows  $\ln$  (% initial activity) plotted against time in minutes. The rate constant of the inactivation  $k$ , equal to  $-(\text{slope})$ , is  $0.233 \text{ min}^{-1}$ . Each point is the mean of triplicate independent inactivations; error bars indicate 1 standard deviation.

Another form of this equation may be obtained by substituting:

$$\Delta G^{\circ*} = \Delta H^{\circ*} - T\Delta S^{\circ*}$$

Hence:

$$k = k_B T/h \cdot e^{-\Delta H^{\circ*}/RT} \cdot e^{\Delta S^{\circ*}/R}$$

Over small temperature ranges  $\Delta S^{\circ*}/R$  can be taken as a constant.

Since, with any change in temperature,  $k$  varies proportionally to  $k_B T/h$ , whereas it varies exponentially with  $-\Delta H^{\circ*}/RT$ , the term  $k_B T/h$  may be regarded as constant. Therefore the equation can be expressed:

$$\ln k = [\ln(k_B T/h) + \Delta S^{\circ*}/R] - \Delta H^{\circ*}/R \cdot (1/T)$$

This shows that under these assumptions the natural logarithm of the rate constant is a linear function of the reciprocal of the absolute temperature.

The natural logarithm of each rate constant was plotted against the reciprocal of the appropriate inactivation temperature (in degrees Kelvin) to produce a straight line (An Arrhenius plot). This plot is shown in Figure 3.6a, while Figure 3.6b shows for comparison similar data obtained in our laboratory for the citrate synthases of *Sulfolobus solfataricus*, *Thermoplasma acidophilum* and pig heart (unpublished data).

Inactivations were carried out at 64°C in 20 mM Tris-HCl (pH 8.0), 2 mM EDTA containing 1.0, 1.6, 1.7, 1.8, 2.0, 2.2 and 3.0 M KCl, to investigate the effect of KCl concentration on the thermostability of the enzyme. The rate constants of inactivation were determined as above and the combined data are plotted in Figure 3.7. Inactivation in 1.0 M KCl was too rapid to measure, while no inactivation was observed in the presence of 3 M KCl.

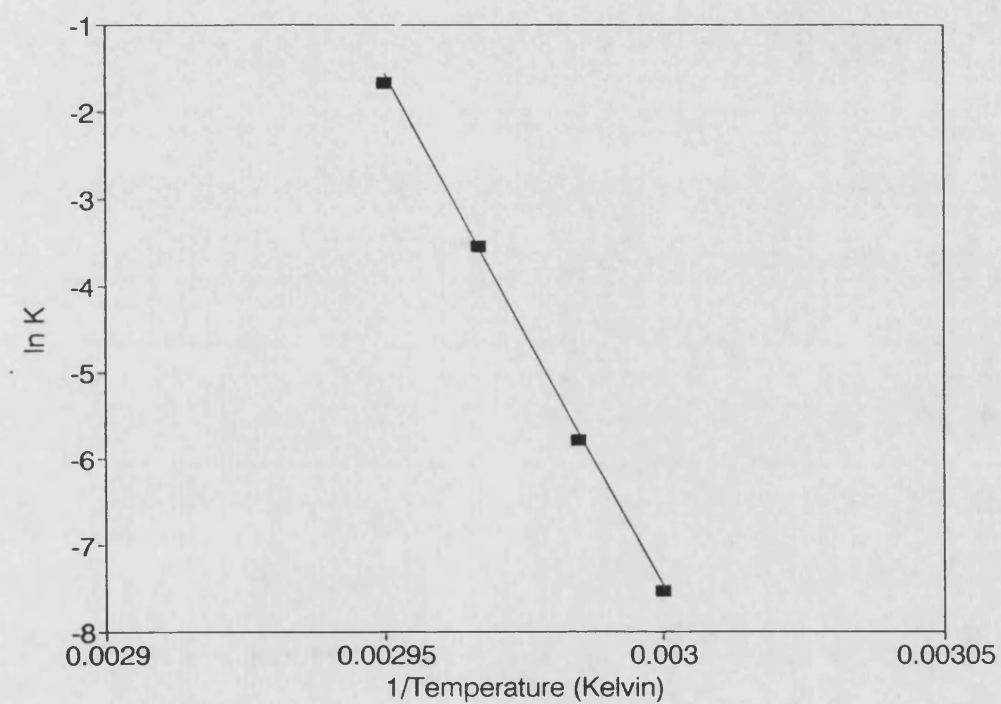


**Figure 3.6a Arrhenius plot of thermal inactivation of citrate synthase**

The graph shows  $\ln$  (rate constant of thermal inactivation  $k$ ) plotted against the reciprocal of the absolute temperature in  $\text{Kelvin}^{-1}$ . The slope of the graph, equal to  $-\Delta H^*/R$ , is  $-117870 \text{ JK}$  (standard error = 1960).

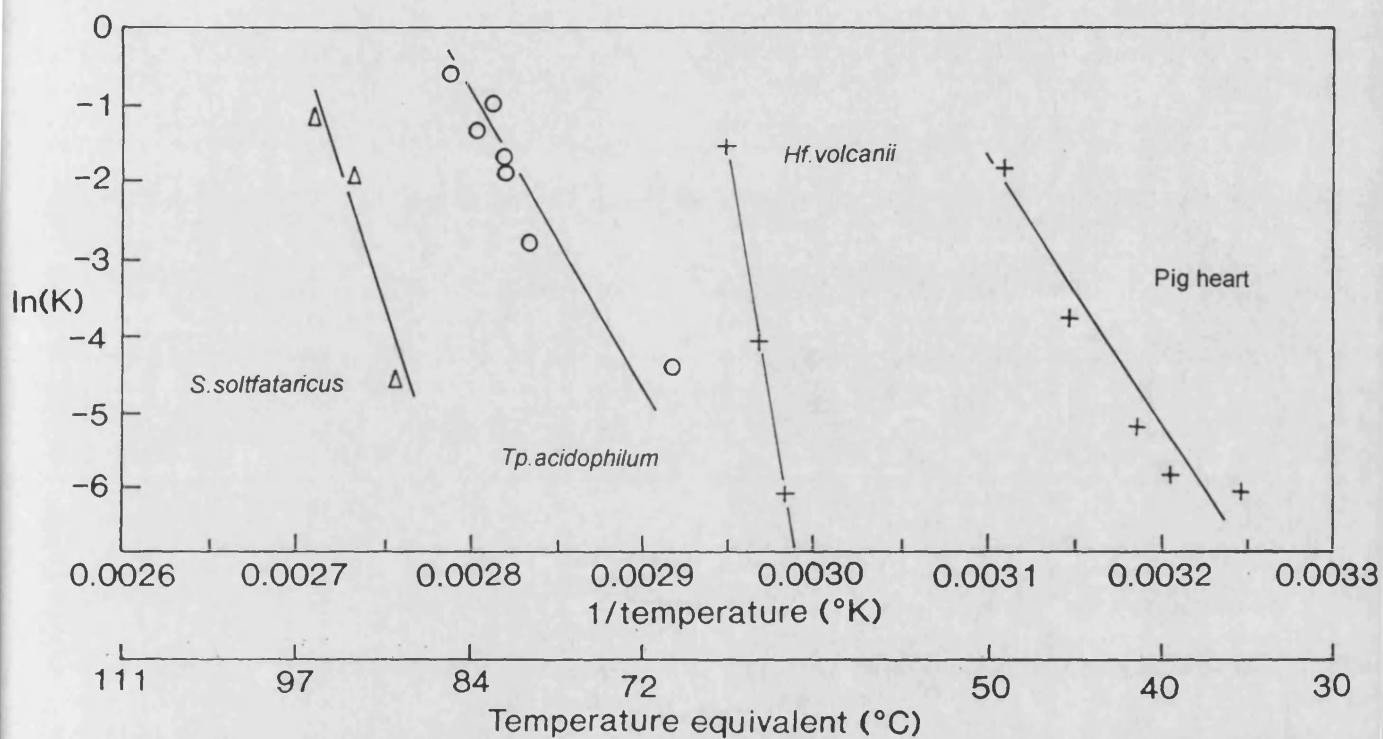


**Figure 3.6b Arrhenius plot of thermal inactivation of citrate synthases**

This graph compares the Arrhenius data for the *Hf. volcanii* citrate synthase with those obtained in our laboratory for citrate synthases from other sources (unpublished data).

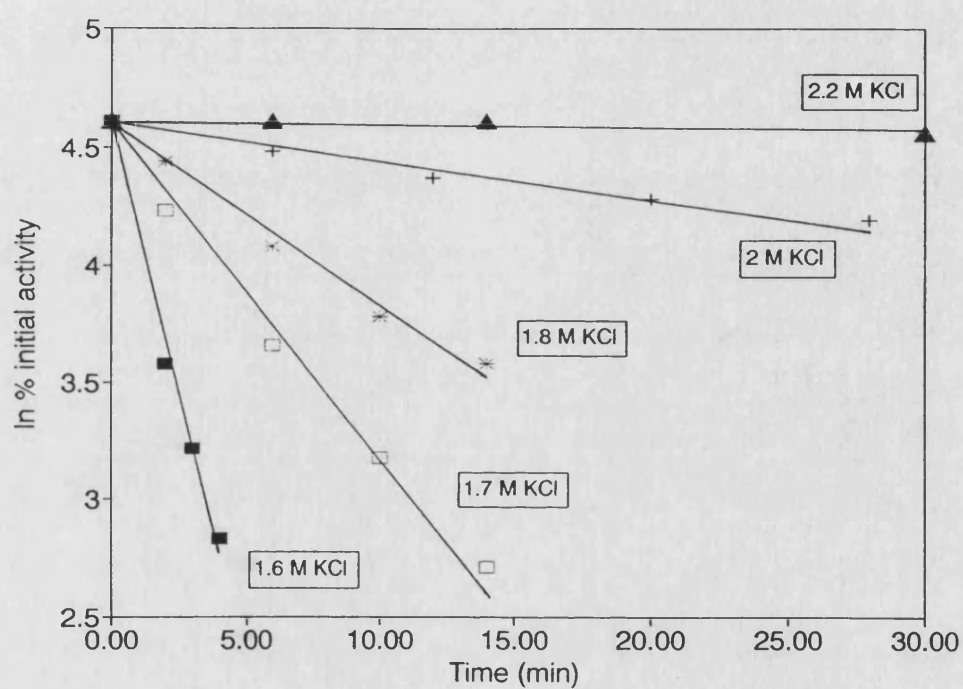


**Figure 3.7 Effect of KCl concentration on thermal inactivation of citrate synthase at 64°C**

The graph shows  $\ln$  (% initial activity) plotted against time in minutes for a range of KCl concentrations.

### 3.5 Discussion

At 30–40°C *Hf.volcanii* grows optimally at 1.7–2.5 M NaCl, with a minimum requirement of about 1.0 M NaCl (Mullakhanbhai & Larsen, 1975). Its internal KCl concentration is likely to fall into a similar range. The data show that citrate synthase is active at KCl and NaCl concentrations significantly below this range; approximately 50% of the activity observed at 2 M NaCl or KCl is retained at 0.1 M (Figure 3.1).

The activity profiles for the two cations are very similar up to a concentration of 1 M, at which point further increases in  $K^+$  exert no change on activity, while increases in  $Na^+$  give a proportional reduction in activity. The higher concentrations of  $Na^+$  probably induce structural changes that affect activity through changes in the way the enzyme binds hydrated salt ions. The significantly greater strength of the hydration interactions of  $Na^+$  over those of  $K^+$  may contribute to this. The absence of high-salt inactivation in KCl solutions is not surprising, considering the presence within *Hf.volcanii* of high KCl concentrations *in vivo*.

At 25°C *Hf.volcanii* citrate synthase is remarkably stable at low salt concentrations, even considering the organism's moderate salt requirements. The enzyme remains stable at salt concentrations in which it is active, down to 0.1 M KCl. In contrast, the citrate synthase of the extreme halophile *Halobacterium cutirubrum* exhibits some activity at 0.1 M KCl but has a half-life of only 4 minutes at 1 M KCl (Higa & Cazzulo, 1975).

The inactivation temperatures were increased from 25°C until measurable inactivation rates were observed in 2 M KCl. The inactivation data, displayed as Arrhenius plots in Figures 3.6a and 3.6b, show that



*Hf.volcanii* citrate synthase is stable up to approximately 60°C. This value is of the order expected for an organism growing at up to 45°C. The rate of activity loss changes uniformly with the small variation in temperature, the slope of the graph giving the enthalpy change involved in formation of the transition state from the native enzyme during the inactivation process (980 kJ mol<sup>-1</sup> in this case, values for pig heart, *Tp.acidophilum* and *S.solfataricus* being 331, 364 and 635 kJ mol<sup>-1</sup> respectively). The displacement of the slope along the X-axis gives an indication of thermostability of the enzyme relative to those of *S.solfataricus*, *Tp.acidophilum* and pig heart.

The slope of the *Hf.volcanii* citrate synthase Arrhenius plot is significantly greater than those of the enzymes from pig heart or *Tp.acidophilum*. It is thought that the enthalpy change required to go from the native protein to the transition state is related to the breaking of electrostatic interactions, while the entropy change is related to the disruption of hydrophobic interactions. This suggests that heat denaturation of the *Hf.volcanii* enzyme requires more electrostatic interactions to be broken in reaching the transition state than in the others. It may be that surface and internal electrostatic interactions make a greater contribution to thermostability in the halophilic enzyme than in the pig heart or *Tp.acidophilum* enzymes..

At 2 M KCl and 66°C the rate constant of inactivation of the *Hf.volcanii* citrate synthase is 0.23 min<sup>-1</sup>, while at 3 M KCl and 40°C the rate constant of inactivation of the *H.cutirubrum* citrate synthase is 0.35 min<sup>-1</sup> (Higa & Cazzulo, 1975). Thus the *Hf.volcanii* enzyme is much more stable at high salt concentrations as well as at low salt concentrations.

Once measurable rates of inactivation had been achieved, the effect of KCl concentration on stability was investigated. The data in Figure 3.7 indicate that stability is highly dependent on KCl concentration between 1.6 and 3 M. Figure 3.8 displays the same data, relating half-life to salt concentration. It is possible that at high salt concentrations (> 3 M) *Hf.volcanii* citrate synthase is more thermostable than would be expected (i.e. remaining stable for periods of hours at temperatures more than 20°C above the parent organism's maximum growth temperature); however, this was not investigated. It is interesting to note that an increased requirement for NaCl has been observed when the growth temperature of *Hf.volcanii* is raised (Mullakhanbhai & Larsen, 1975).

Once *Hf.volcanii* citrate synthase is over-expressed in either a mesophilic or halophilic host, it will be necessary to compare its physico-chemical characteristics with those of the wild-type enzyme. This comparison must cover both its kinetic parameters and its salt requirements for stability and activity. Techniques such as differential scanning calorimetry, to determine  $\Delta G$  of stability, coupled with circular dichroism or fluorescence to measure unfolding, are required for a detailed analysis of enzyme stability. The methods described above are limited in that they rely upon enzyme activity as a measure of unfolding; however, they could provide a simple means of investigating the salt requirements of over-expressed halophilic citrate synthases.

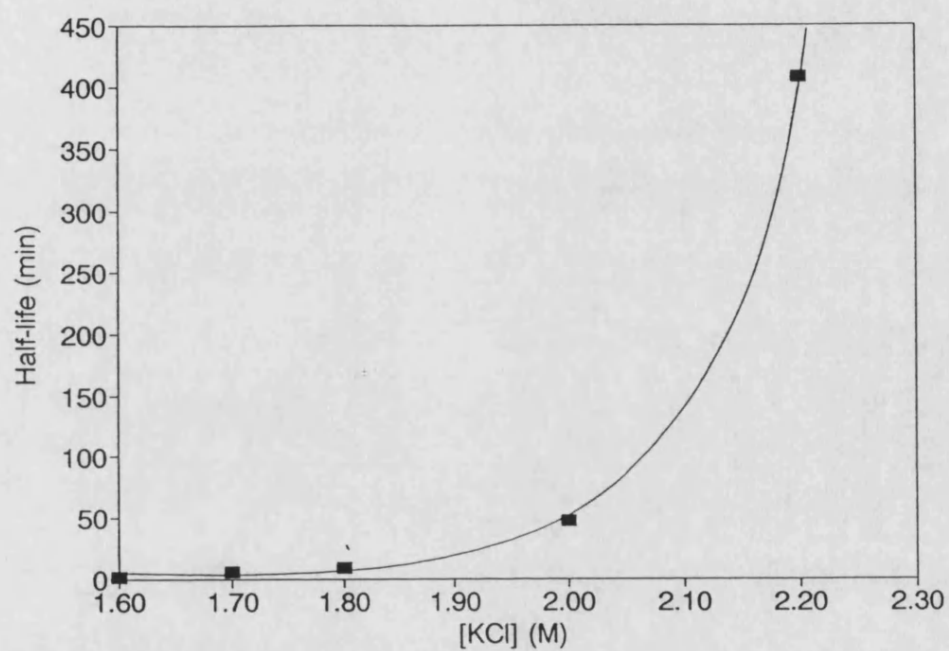


**Figure 3.8 Effect of KCl concentration on the half-life of citrate synthase at 64°C**

The graph shows half-life in minutes plotted against KCl concentration (Molar).

## Creation of size-restricted genomic libraries and screening for the citrate synthase gene

### 4.1 Introduction

Citrate synthase from *Hf.volcanii* was purified in our laboratory by Dr. M.J. Bonete, University of Alicante, Spain using a scheme based on that used to purify the *H.halobium* citrate synthase (James, 1990). SDS-PAGE of the purified enzyme revealed the presence of two major protein bands of apparent molecular weight 45 kD and 55 kD. These were Western blotted onto Immobilon P membrane and both bands were cut out and sequenced directly from the membrane.

Sequences were obtained for both bands. These are shown below, using single letter amino acid codes where X indicates an unknown residue and residues in parentheses are tentative assignments.

55 kD XXXXVIAAAYRTPFGKAA

45 kD (S)GELKRGLEGVLVAESKLSFIDGDAGQLVYXGYDIEDL

The 45 kD band appears to be citrate synthase as judged by a SWISSPROT database search and sequence alignment described in the Appendix. Outlines of the purification scheme, blotting and sequencing are also given in the Appendix.

From the N-terminal peptide sequence of the protein, oligonucleotide probes were designed and used to screen Southern blots of restriction digested genomic DNA. A suitable size range of positively-hybridising fragments were identified and used to create a size-restricted genomic library in the pUC18 plasmid vector. This was in turn screened by hybridisation and positive clones were further analysed by restriction digests and sequencing of the plasmid DNA.

## **4.2 Oligonucleotide design**

Oligonucleotides were designed from the N-terminal sequence with a bias towards G and C at the third base of each codon, reflecting the high G+C content of the *Hf.volcanii* genome. In order to aid selection of third bases a composite codon usage table was compiled from the dihydrolipoamide dehydrogenase (Vettakkorumakankav *et al.*, 1992), dihydrofolate reductase (Zusman *et al.*, 1989), his C (Conover & Doolittle, 1990) and trp cluster (Lam *et al.*, 1990) genes of *Hf.volcanii*. Figure 4.1 summarises this information.

## **4.3 Southern blot analysis**

Initially 10 µg aliquots of genomic DNA were digested with single restriction enzymes. Once restriction fragments were separated by agarose gel electrophoresis and immobilised on nylon membranes by Southern transfer, hybridisation to a  $\gamma$  <sup>32</sup>P end-labelled oligonucleotide was carried out. The sizes of hybridising fragments were calculated from autoradiographs of the blots.

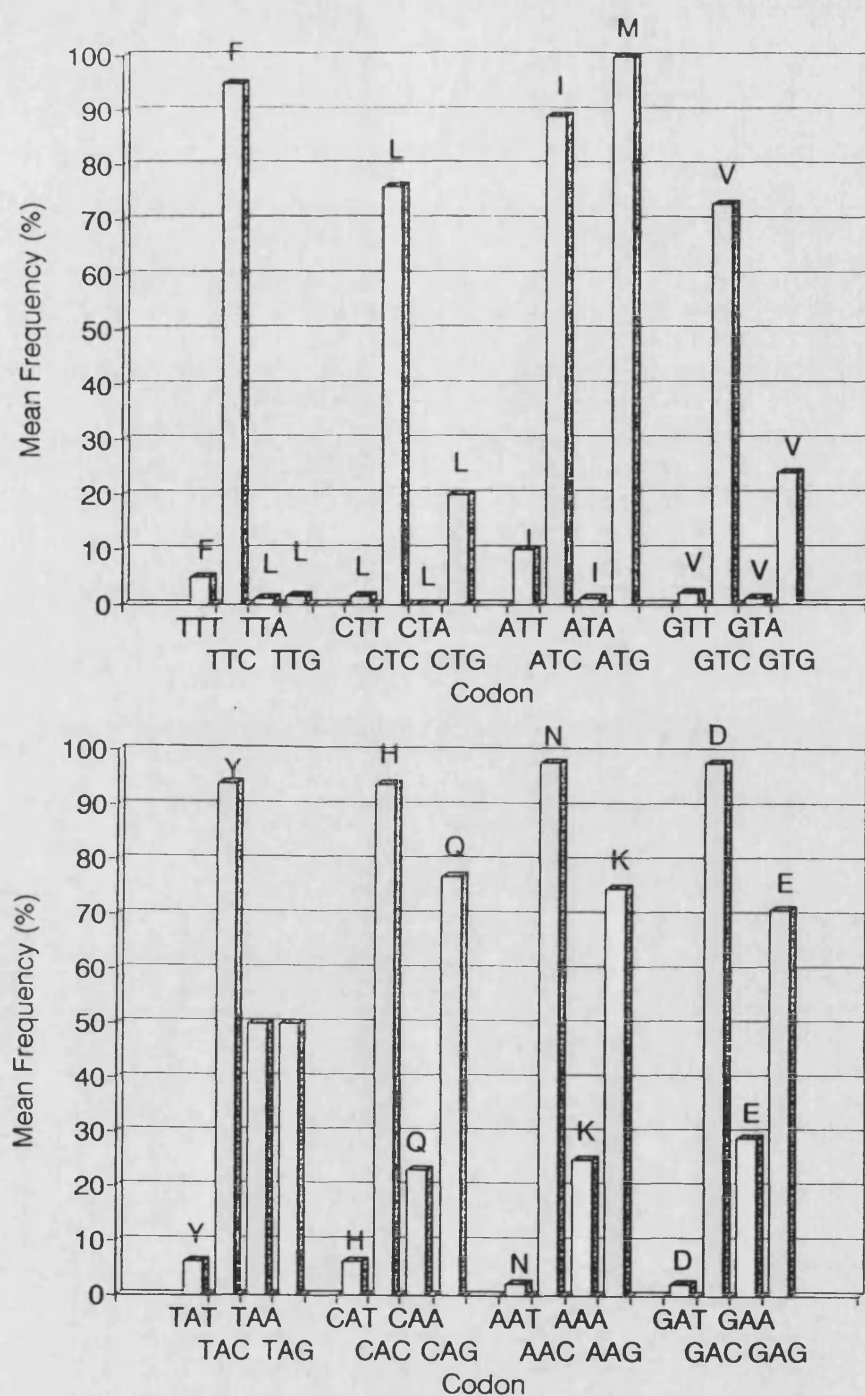


**Figure 4.1 Codon preference in *Hf.volcanii***

The frequency of each codon is expressed as a percentage of the total number coding for a particular amino acid.

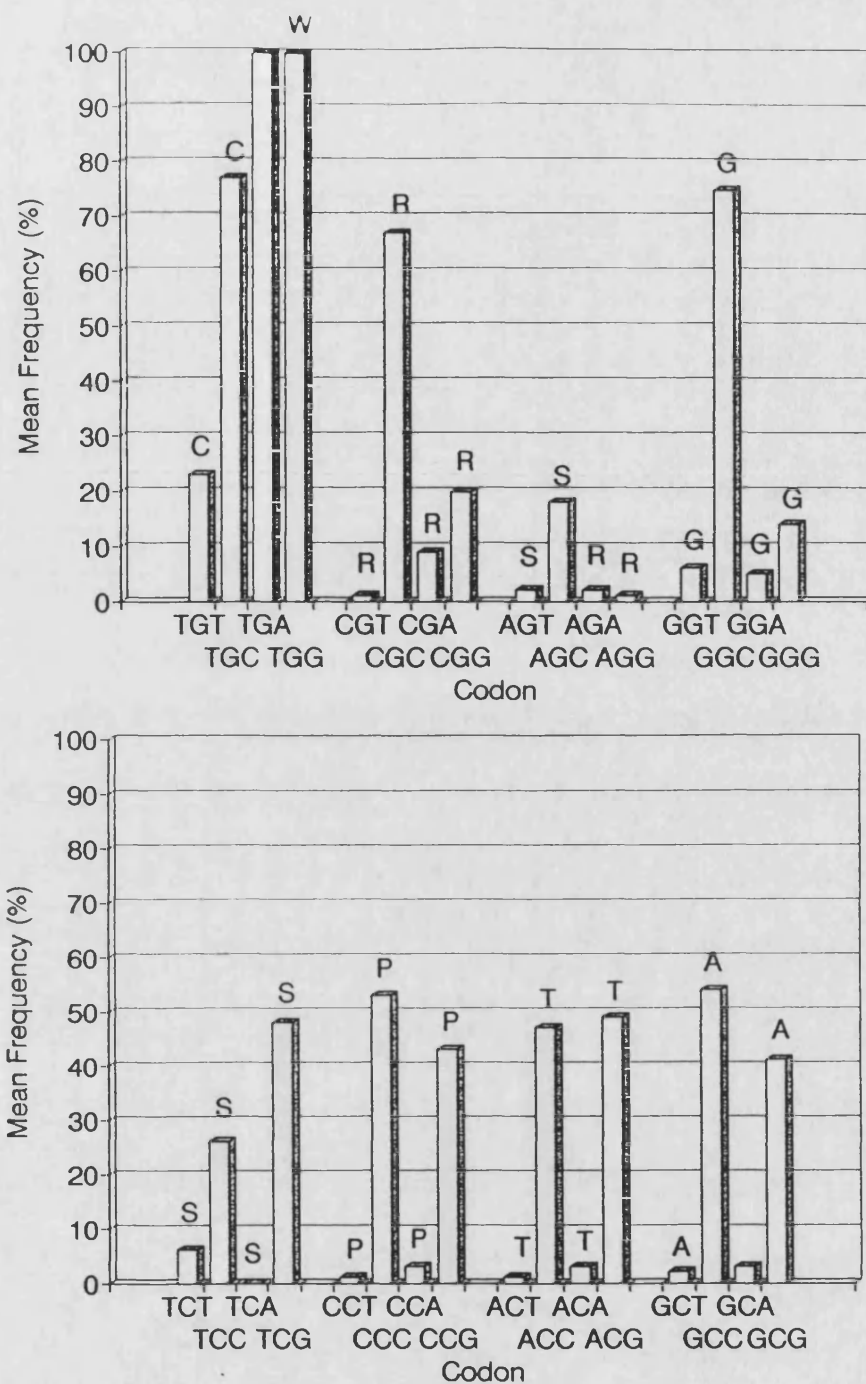


**Figure 4.1 Codon preference in *Hf.volcanii* (continued)**

The process was repeated for genomic DNA digested with pairs of restriction enzymes in order to identify hybridising fragments smaller than those produced by single enzymes ie. fragments that were doubly digested.

#### **4.4 Creation of a size-restricted genomic library**

Approximately 150 µg genomic DNA was digested with the required pair of restriction enzymes and the fragments were separated on a 1% agarose gel. A gel slice containing fragments of approximately the desired size was cut and the DNA recovered by freeze-squeeze. The fragments were purified using a NENsorb cartridge.

A 100 ng aliquot of commercially prepared pUC18 *Eco*RI / BAP plasmid (ie. digested with *Eco*RI and treated with alkaline phosphatase) was digested with *Pst*I and purified using a NENsorb cartridge. Ligations were set up using 10 ng plasmid DNA with 10%, 1% and 0.1% of the purified fragments, each in a volume of 20 µl.

Competent *E.coli* JM103 were prepared by the calcium chloride method and a 200 µl volume transformed with 8 µl ligated DNA. Transformants were selected by plating out on 2xYT agar containing ampicillin (100 µg ml<sup>-1</sup>).

#### **4.5 Screening for positive clones**

Transformants were streaked onto gridded 2xYT agar plates containing ampicillin (100 µg ml<sup>-1</sup>). From these master plates transformants were streaked onto gridded nylon membranes which were treated as described in section 2.3.9.3 Colony Hybridisation. Positive clones were purified by plating out and screening single colonies by



streaking onto gridded membranes and hybridising as above. This was repeated until all the colonies screened gave a positive signal. Clones were stored as glycerol stocks at -20°C.

## **4.6 Results**

### **4.6.1 Screening Southern blots with a non-degenerate 44 base oligonucleotide probe**

Figure 4.2 shows the sequence of a 44 base oligonucleotide designed from the citrate synthase N-terminal sequence. Its estimated  $T_m$  is in excess of 100°C (using the formula  $T_m = 4(\text{Number of G and C bases}) + 2(\text{Number of A and T bases})$ ).

When used to probe a Southern blot of the restriction digests shown in Figure 4.3a, a *Pst*I fragment of approximately 7.2 kb and a *Pst*I / *Eco*RI fragment of approximately 2.9 kb were identified as shown in Figure 4.3b (lanes 2 and 5 respectively). Hybridisations and washes were carried out at 60°C.

A library of *Pst*I / *Eco*RI fragments in the 3 kb size range were cloned into pUC18 as described in Section 5.4. Ligation of inserts into the cut vector yielded 534 transformants. Control transformations with ligations containing vector plus insert (no ligase), vector only (plus ligase) and insert only (plus ligase) yielded a total of 4 transformants between them. A control transformation with 1ng of uncut pUC18 gave an estimated transformation efficiency of  $1.5 \times 10^7 \mu\text{g}^{-1}$ .

<b>G</b>	<b>E</b>	<b>L</b>	<b>K</b>	<b>R</b>	<b>G</b>	<b>L</b>	<b>E</b>	<b>G</b>	<b>V</b>	<b>L</b>	<b>V</b>	<b>A</b>	<b>E</b>	<b>S</b>	<b>K</b>	<b>L</b>	<b>S</b>	<b>F</b>	<b>I</b>	<b>D</b>	<b>G</b>	<b>D</b>	<b>A</b>	<b>G</b>	<b>Q</b>	<b>L</b>	<b>V</b>	<b>Y</b>	<b>X</b>	<b>G</b>	<b>Y</b>	<b>D</b>	<b>I</b>	<b>E</b>	<b>D</b>	<b>L</b>			
GTA	GCA	GAA	TCA	AAA	CTA	TCA	TTT	ATA	GAT	GGA	GAT	GCA	GGA	CAA																									
<b>G</b>	<b>G</b>	<b>G</b>	<b>G</b>	<b>G</b>	<b>G</b>	<b>G</b>	<b>C</b>	<b>C</b>	<b>C</b>	<b>G</b>	<b>C</b>	<b>G</b>	<b>G</b>	<b>G</b>																									
<b>C</b>	<b>C</b>		<b>C</b>		<b>C</b>	<b>C</b>		<b>T</b>		<b>C</b>		<b>C</b>	<b>C</b>																										
<b>T</b>	<b>T</b>		<b>T</b>			<b>T</b>				<b>T</b>		<b>T</b>		<b>T</b>																									
			AGC			TTA	AGC																																
			<b>T</b>			<b>G</b>	<b>T</b>																																
<b>GTC</b>	<b>GCC</b>	<b>GAC</b>	<b>TCG</b>	<b>AAG</b>	<b>CTT</b>	<b>TCG</b>	<b>TTC</b>	<b>ATC</b>	<b>GAC</b>	<b>GGC</b>	<b>GAC</b>	<b>GCC</b>	<b>GGC</b>	<b>CA</b>																									

**Figure 4.2 Sequence of 44 base oligonucleotide probe**

The citrate synthase N-terminal sequence is shown, with all possible codons below each residue. The probe sequence is shown in **bold**.

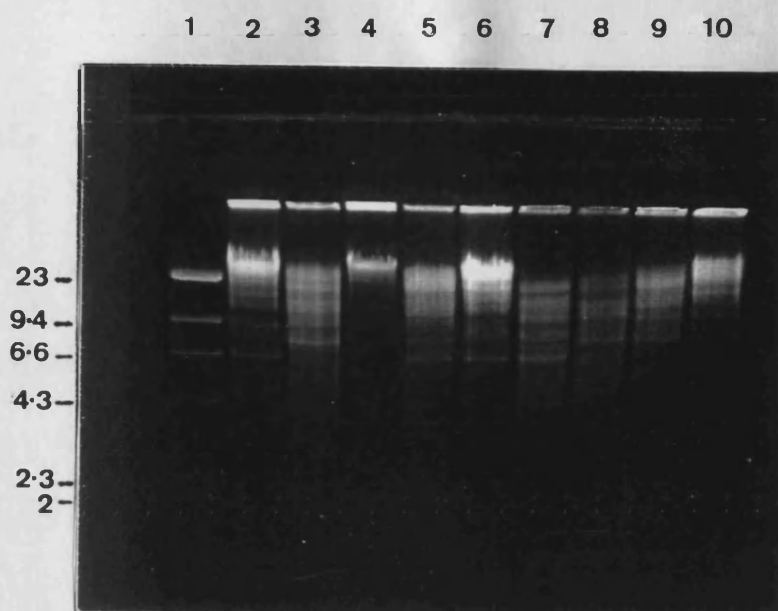


**Figure 4.3a Electrophoresis of genomic DNA restriction digests on 0.6% agarose gel**

Lane 1:  $\lambda$  *Hind*III

Lane 2: *Pst*I

Lane 3: *Sma*I

Lane 4: *Bam*HI

Lane 5: *Pst*I / *Eco*RI

Lane 6: *Pst*I / *Bam*HI

Lane 7: *Pst*I / *Sma*I

Lane 8: *Sma*I / *Eco*RI

Lane 9: *Sma*I / *Bam*HI

Lane 10: *Bam*HI / *Eco*RI

Fragment sizes are indicated in kilobases. Figure 4.3b shows an autoradiograph of the corresponding Southern blot.

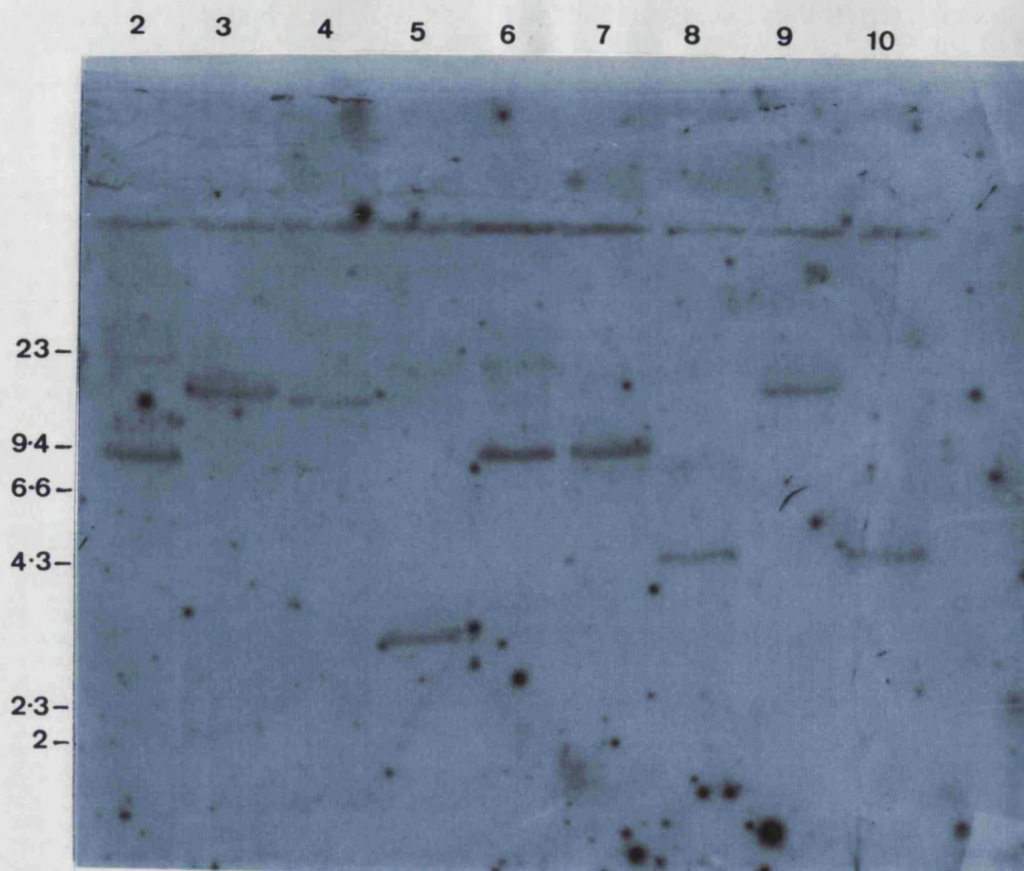


**Figure 4.3b** Autoradiograph of Southern blot probed with non-degenerate 44 base oligonucleotide (4 day exposure)

Lane 1: Not shown

Lane 2: *Pst*I

Lane 3: *Sma*I

Lane 4: *Bam*HI

Lane 5: *Pst*I / *Eco*RI

Lane 6: *Pst*I / *Bam*HI

Lane 7: *Pst*I / *Sma*I

Lane 8: *Sma*I / *Eco*RI

Lane 9: *Sma*I / *Bam*HI

Lane 10: *Bam*HI / *Eco*RI

The blot was washed at 60°C. Fragment sizes are indicated in kilobases. Figure 4.3a shows the corresponding agarose gel.

The transformants were screened by colony hybridisation as described above, using the same 44 base oligonucleotide. Hybridisations and washes were carried out at 60°C. Four strongly hybridising clones were identified, plus ten that hybridised less strongly. Examples of each are shown in Figure 4.4.

All twelve positive clones were purified as described in Section 5.5, using the same hybridisation and washing conditions as the initial screening. After the first round of purification it became apparent that only the four strongly hybridising clones were true positives, as the others did not demonstrate reproducible hybridisation. Plasmid DNA was prepared from the four positive clones by the caesium chloride 'Maxiprep' method.

#### **4.6.2 Restriction and hybridisation analysis of positive clones**

Initially a dot-blot of 1 µg DNA from each positive clone was prepared, together with 1 µg pUC18 DNA as a control. This was probed with the 44 base oligonucleotide, hybridising and washing at 60°C in 2xSSC. Hybridisation to the plasmids containing the insert was observed, while there was no detectable hybridisation to pUC18 alone. Restriction digests were carried out using the enzymes *Pst*I, *Eco*RI, *Hind*III and *Ava*I. All of the positive clones appeared to contain the same insert, as judged by the restriction pattern.

Figure 4.5a shows the restriction fragments of one positive clone separated by agarose gel electrophoresis. These were transferred to nylon membrane by Southern blotting and probed with the 44 base oligonucleotide (Figure 4.5b).



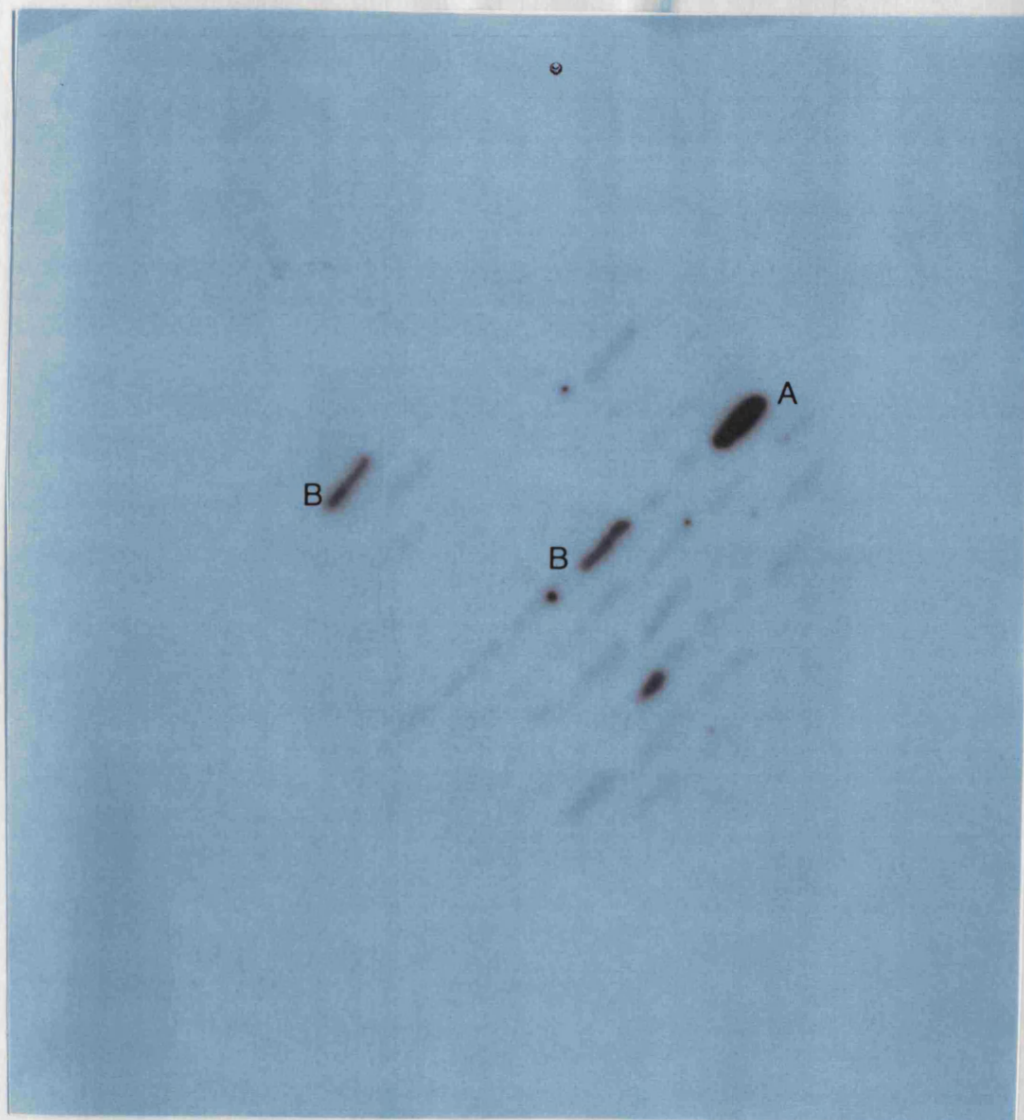


**Figure 4.4** Autoradiograph of colony blot probed with 44 base non-degenerate oligonucleotide (2 day exposure): screening transformants

A: Strong hybridisation (true positive)

B: Weaker hybridisation (later identified as false positive)

The blot was washed at 60°C.

Further restriction digests were carried out the enzymes *AccI*, *AvaI* and *HindIII*. In Figure 4.6a the restriction fragments are shown, separated by agarose gel electrophoresis. Figure 4.6b shows a Southern blot of those fragments, probed with the 44 base oligonucleotide.

From these data an initial restriction map was drawn (Figure 4.7), although the exact binding site of the probe cannot be deduced. Fragments of the 2.9 kb insert were therefore sub-cloned into pUC18 for a more detailed analysis.

#### **4.6.3 Sub-cloning fragments from the 2.9kb positive clone**

Aliquots of 5 µg plasmid DNA were digested with *AvaI* and *HindIII*. A 1.5 kb *AvaI* fragment, 1.5 kb *HindIII* fragment and 1.2 kb *HindIII* fragment were gel purified and cleaned by passing through a NENsorb cartridge. Vector was prepared by digesting 1 µg aliquots of pUC18 DNA with either *AvaI* or *HindIII*, treating with alkaline phosphatase and cleaning using a NENsorb cartridge. Each of the fragments was ligated into appropriately cut vector.

Sub-clones of the two *HindIII* fragments were obtained. The *AvaI* fragment proved difficult to clone, and despite several attempts no transformants were obtained. Since the only sub-fragment of the 2.9 kb clone to retain full hybridisation is that produced by *AvaI* digestion, cloning and sequencing this fragment is particularly important with regard to locating the hybridisation site of the probe.

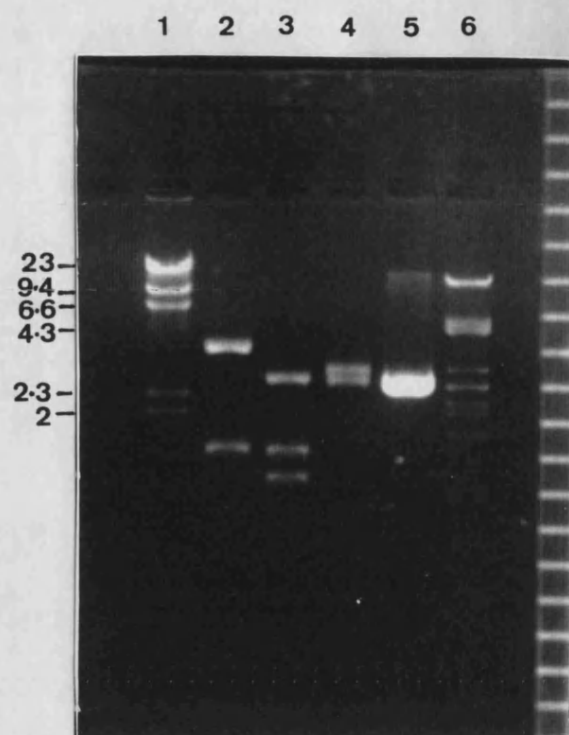


**Figure 4.5a Electrophoresis of restriction digests of 2.9 kb *Pst*I / *Eco*RI clone on 1% agarose gel**

Lane 1: $\lambda$ <i>Hind</i> III	
Lane 2: <i>A</i> vaI	Fragment sizes: (3.7), 1.5 kb
Lane 3: <i>Hind</i> III	(2.7), 1.5, 1.2 kb
Lane 4: <i>Pst</i> I / <i>Eco</i> RI	2.9, (2.7) kb
Lane 5: pUC18 <i>Eco</i> RI	(2.7) kb
Lane 6: $\lambda$ <i>Pst</i> I	

Restriction fragment sizes are indicated in kilobases (the fragment containing the pUC18 vector in parentheses).

Figure 4.5b shows the corresponding autoradiograph.



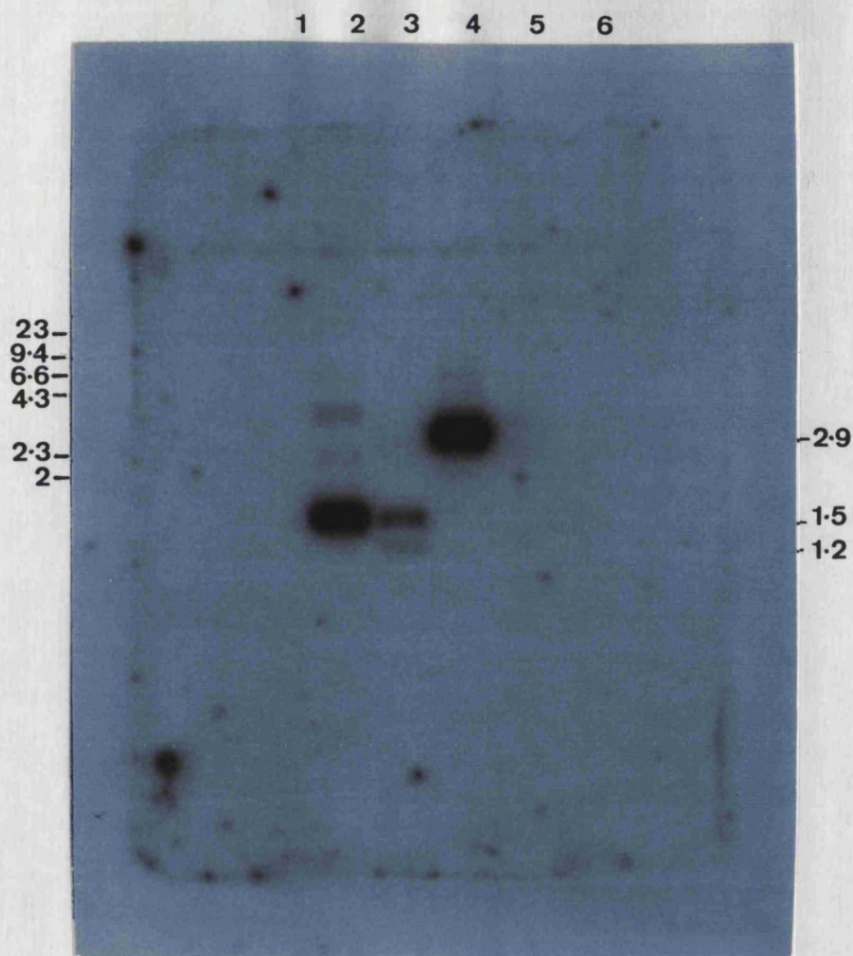


**Figure 4.5b** Autoradiograph of Southern blot probed with 44 base non-degenerate oligonucleotide (4 day exposure)

Lane 1: λ *Hind*III

Lane 2: *Ava*I

Lane 3: *Hind*III

Lane 4: *Pst*I / *Eco*RI

Lane 5: pUC18 *Eco*RI

Lane 6: λ *Pst*I

Restriction fragment sizes are indicated in kilobases. Figure 4.5a shows the corresponding agarose gel. The blot was washed at 60°C.

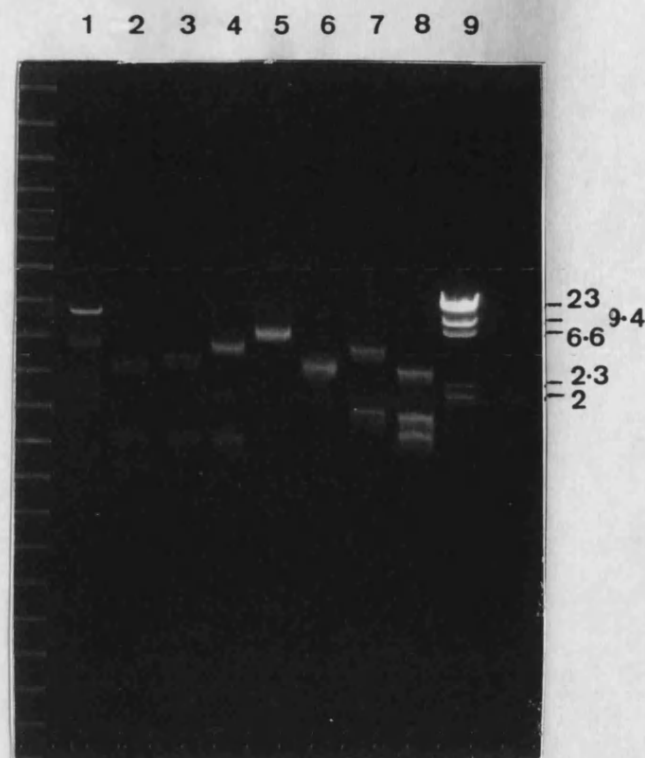


**Figure 4.6a Electrophoresis of restriction digests of 2.9 kb *Pst*I / *Eco*RI clone on 1% agarose gel**

Lane 1: $\lambda$ <i>Pst</i> I	
Lane 2: <i>Ava</i> I / <i>Hind</i> III	Fragment sizes: (2.7), 1.2, 0.95 kb
Lane 3: <i>Ava</i> I / <i>Acc</i> I	(3.3), 1.2, 0.7 kb
Lane 4: <i>Acc</i> I	(4.0), 1.2 kb
Lane 5: <i>Eco</i> RI	(5.7) kb
Lane 6: <i>Pst</i> I / <i>Eco</i> RI	(2.8) kb
Lane 7: <i>Ava</i> I	(3.8), 1.5 kb
Lane 8: <i>Hind</i> III	(2.7), 1.5, 1.2 kb
Lane 9: $\lambda$ <i>Hind</i> III	

Restriction fragment sizes are indicated in kilobases (the fragment containing the pUC18 vector in parentheses). Figure 4.6b shows the corresponding autoradiograph.

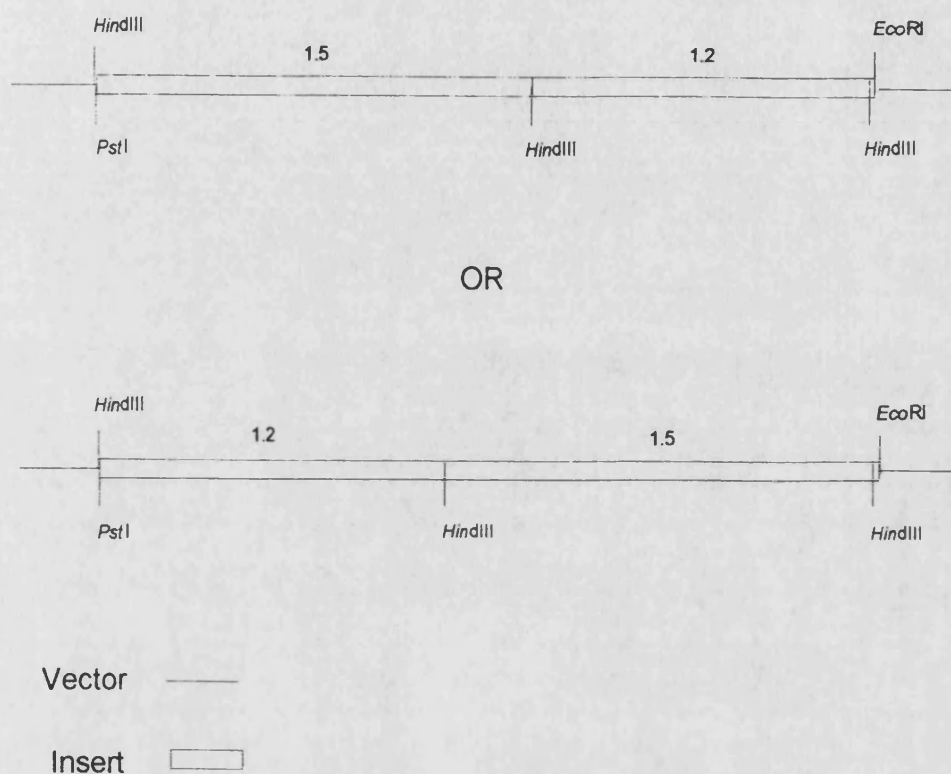


**Figure 4.7 Summary of initial restriction site information obtained from 2.9 kb *Pst*I / *Eco*RI clone in pUC18**

No sites within the clone could be mapped unambiguously at this stage. In addition to the *Hind*III sites are: a pair of *Ava*I sites 1.5 kb apart and a pair of *Acc*I sites 1.2 kb apart. There are no *Ava*I or *Acc*I sites in the vector.

#### **4.6.4 Restriction analysis of sub-cloned *HindIII* fragments**

Both the cloned 1.5 kb and 1.2 kb *HindIII* fragments were digested with *HindIII*, *AvaI* and *AccI*. Figures 4.8 and 4.9 show the restriction fragments separated by agarose gel electrophoresis.

#### **4.6.5 Sequence analysis of 2.9 kb *PstI* / *EcoRI* clone and *HindIII* sub-clones**

In order to orientate the two *HindIII* sub-clones and to make an initial search for citrate synthase sequence, the ends of the 2.9 kb *PstI* / *EcoRI* clone and *HindIII* subclones were sequenced, initially using the Forward and Reverse universal primers of pUC18 and then using synthetic 17 base primers to extend the sequenced region. The locations of the regions sequenced are shown in Figure 4.10, which also indicates the deduced orientations of the subclones.

The sequences determined were translated in all reading frames (including those for the complementary strand) and used to search the Swissprot protein database via the FASTA program from the GCG package. The translated sequences did not show any significant identity with citrate synthase, although a putative open reading frame of an unrelated gene was identified. This open reading frame was sequenced and is described in more detail in Chapter 7.

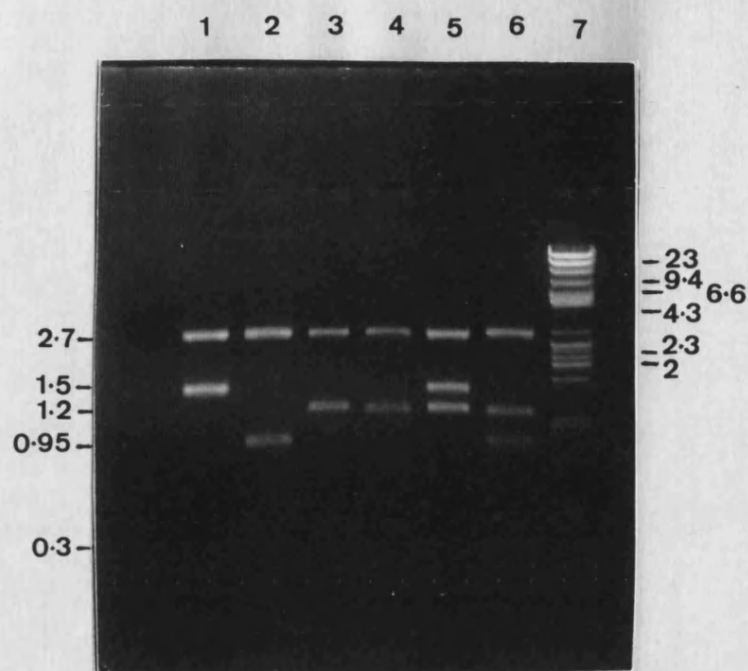


**Figure 4.8** Electrophoresis of restriction digests of 2.9 kb *Pst*I / *Eco*RI clone and *Hind*III subclones on 1% agarose gel

Lane 1: 1.5 kb <i>Hind</i> III subclone: <i>Hind</i> III digest	(2.7), 1.5 kb
Lane 2: 1.5 kb <i>Hind</i> II subclone: <i>Hind</i> III / <i>Ava</i> I digest	(2.7), 0.95, 0.3 kb
Lane 3: 1.2 kb <i>Hind</i> III subclone: <i>Hind</i> III digest	(2.7), 1.2 kb
Lane 4: 1.2 kb <i>Hind</i> III subclone: <i>Hind</i> III / <i>Ava</i> I digest	(2.7), 1.2 kb
Lane 5: 2.9 kb <i>Pst</i> I / <i>Eco</i> RI clone: <i>Hind</i> III digest	(2.7), 1.5, 1.2 kb
Lane 6: 2.9 kb <i>Pst</i> I / <i>Eco</i> RI clone: <i>Hind</i> III / <i>Ava</i> I digest	(2.7), 1.2, 0.95, 0.3 kb
Lane 7: $\lambda$ <i>Pst</i> I	

Restriction fragment sizes are indicated in kilobases (the fragment containing the pUC18 vector in parentheses).



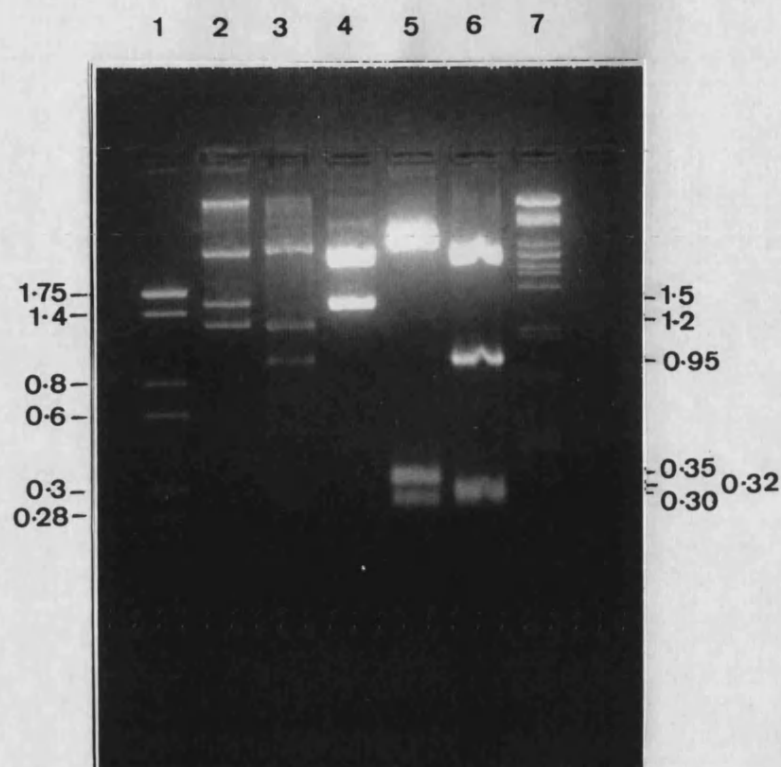


**Figure 4.9 Electrophoresis of restriction digests of 2.9 kb *Pst*I / *Eco*RI clone and 1.5 kb *Hind*III subclone on 2% agarose gel**

Lane 1: Low range DNA markers

Lane 2: 2.9 kb *Pst*I / *Eco*RI clone: *Hind*III digest (2.7), 1.5, 1.2 kb

Lane 3: 2.9 kb *Pst*I / *Eco*RI clone: *Hind*III / *Ava*I digest (2.7), 1.2, 0.95, 0.32 kb

Lane 4: 1.5 kb *Hind*III subclone: *Hind*III digest (2.7), 1.5 kb

Lane 5: 1.5 kb *Hind*III subclone: *Ava*I digest (3.3), 0.35, 0.3

Lane 6: 1.5 kb *Hind*III subclone: *Hind*III / *Ava*I digest (2.7), 0.95, 0.32

Lane 7:  $\lambda$  *Pst*I

Restriction fragment sizes are indicated in kilobases (the fragment containing the pUC18 vector in parentheses).

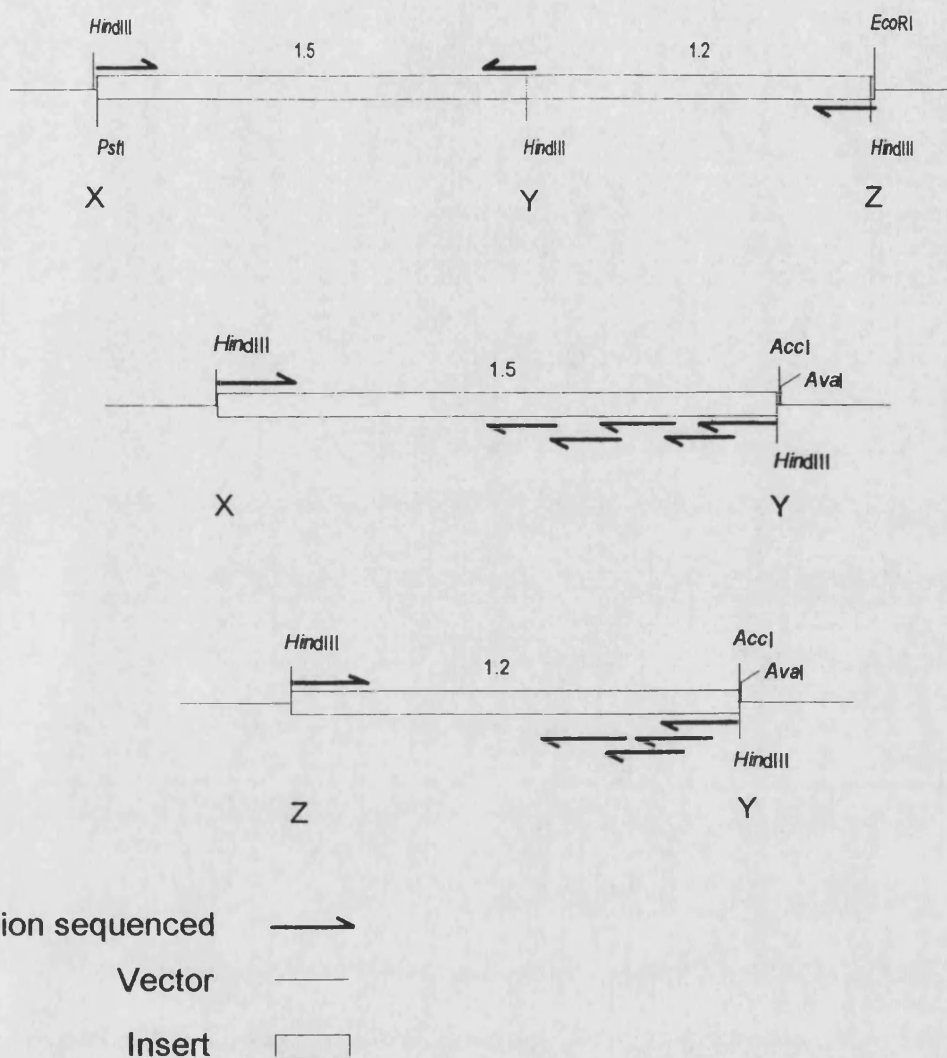


**Figure 4.10** Regions of 2.9 kb *Pst*I / *Eco*RI clone and *Hind*III subclone sequenced.

Distances are indicated in kilobases. X, Y and Z indicate the orientation of the *Hind*III fragments.

The sequence data (including that presented in Chapter 7) are combined with the results of the restriction digests described above to give the restriction maps shown in Figure 4.11.

#### **4.7 Screening with a pair of degenerate 17 base oligonucleotide probes**

As a unique 44 base oligonucleotide had failed to identify a citrate synthase gene, a different approach was taken in designing new oligonucleotides from the citrate synthase N-terminal sequence. Furthermore, as the long oligonucleotide appeared to bind to an unrelated gene, it was necessary to consider the possibility that other oligonucleotides designed to the same stretch of amino acid sequence also bind to that gene.

A pair of non-overlapping, degenerate 17 base oligonucleotides (referred to here as A and B) were designed to the citrate synthase N-terminal sequence as shown in Figure 4.12. Their  $T_m$ s were estimated as 46-56°C for oligonucleotide A and 40-52°C for oligonucleotide B, using the formula described for the 44 base probe.

These were used as probes with the aim of identifying a restriction fragment to which both would bind independently. Ideally the two non-overlapping regions of sequence used would not include the region of sequence used to design the previous 44 base probe, in order to minimise the risk of hybridisation to the unrelated gene described in Chapter 7.

In a degenerate oligonucleotide mixture the number of different species must be kept below the limit where the "correct" sequence is present in such a small proportion as to be undetectable. It was therefore



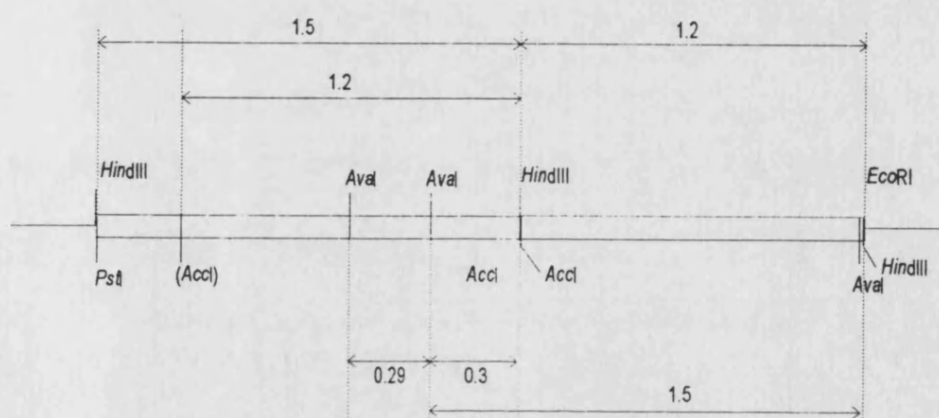


**Figure 4.11 Restriction map of 2.9 kb PstI / EcoRI clone**

This map was compiled from restriction digest and sequence data. The restriction sites in parentheses were not confirmed by sequencing. Distances are indicated in kilobases.

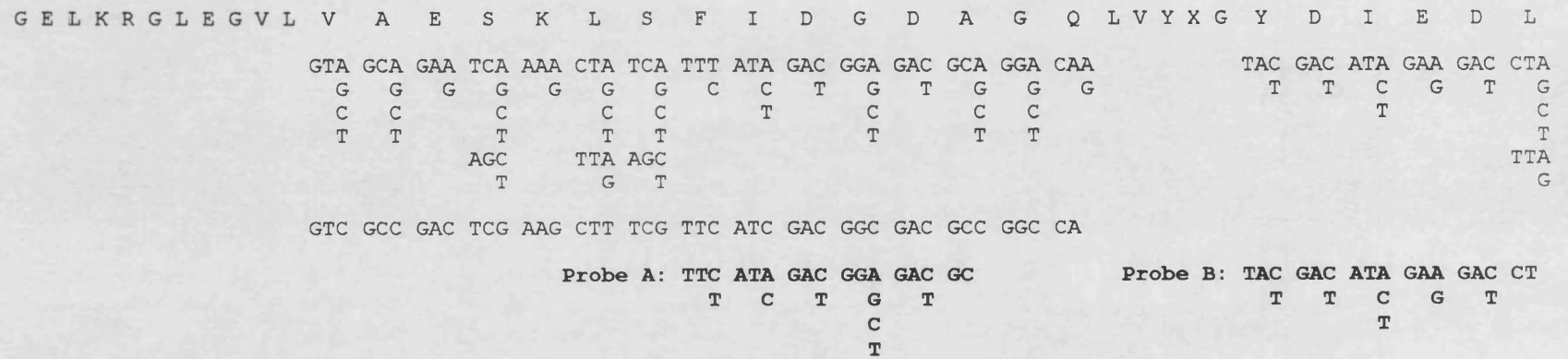


**Figure 4.12 Sequence of 17 base oligonucleotide probes**

The citrate synthase N-terminal sequence is shown, with all possible codons below each residue. The probe sequences are shown in **bold**, including degeneracies. The 44 base probe is also shown.

decided to limit the number of possible sequences for each oligonucleotide to a maximum of 96. To avoid exceeding this limit, one of the two oligonucleotides (oligo A) had to be made to a region overlapping that used to design the 44 base probe.

#### **4.7.1 Preliminary dot-blot results**

Initial hybridisations were carried out with both 17mers to dot-blots of 1 µg of the 2.9 kb *Pst*I / *Eco*RI clone and 1 µg genomic DNA to confirm that they hybridised to genomic DNA and not to the previously-cloned open reading frame. Both probes were found to hybridise to genomic DNA at 30°C, while neither hybridised to the 2.9 kb *Pst*I / *Eco*RI clone at this temperature. Oligonucleotide A hybridised more strongly than B, as judged by the intensity of the dots. In both cases hybridisation was poor, dots only becoming visible after a 14-day exposure.

#### **4.7.2 Southern blot results**

Hybridisation of oligonucleotide B was carried out at 30°C to Southern blots of genomic DNA digested with single restriction enzymes. After washing the blots at 30°C, autoradiographs showed that this probe was not hybridising under these conditions. This probe was not considered suitable for further investigation.

Oligonucleotide A was hybridised to Southern blots of genomic DNA digested with both single restriction enzymes and with pairs of enzymes. Initial blots were hybridised and washed at 37°C. Figures 4.13a and b show an example set of restriction digests and corresponding Southern

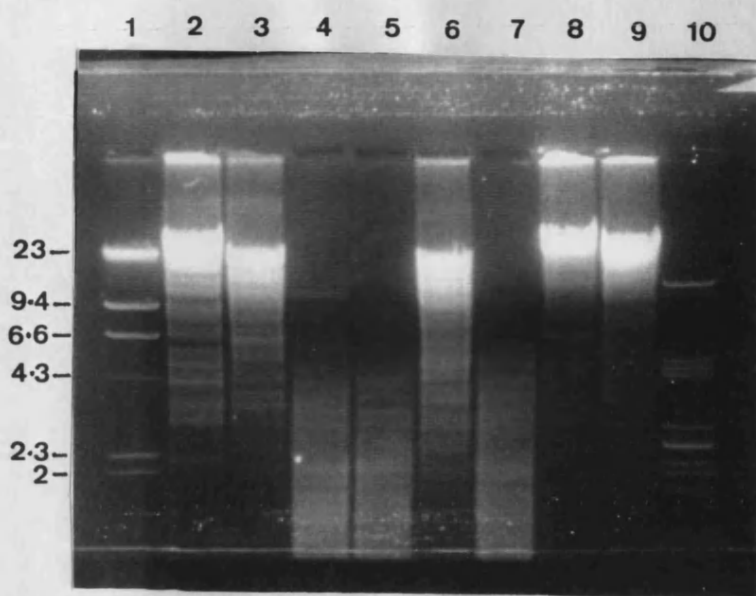


**Figure 4.13a Electrophoresis of genomic DNA restriction digests on 0.6% agarose gel**

Lane 1:  $\lambda$  *Hind*III

Lane 2: *Hind*III / *Pst*I

Lane 3: *Hind*III / *Sph*I

Lane 4: *Hind*III / *Sal*I

Lane 5: *Pst*I / *Sal*I

Lane 6: *Sph*I / *Pst*I

Lane 7: *Sph*I / *Sal*I

Lane 8: *Hind*III

Lane 9: *Sph*I

Lane 10:  $\lambda$  *Pst*I

Fragment sizes are indicated in kilobases. Figure 4.13b shows an autoradiograph of the corresponding Southern blot.

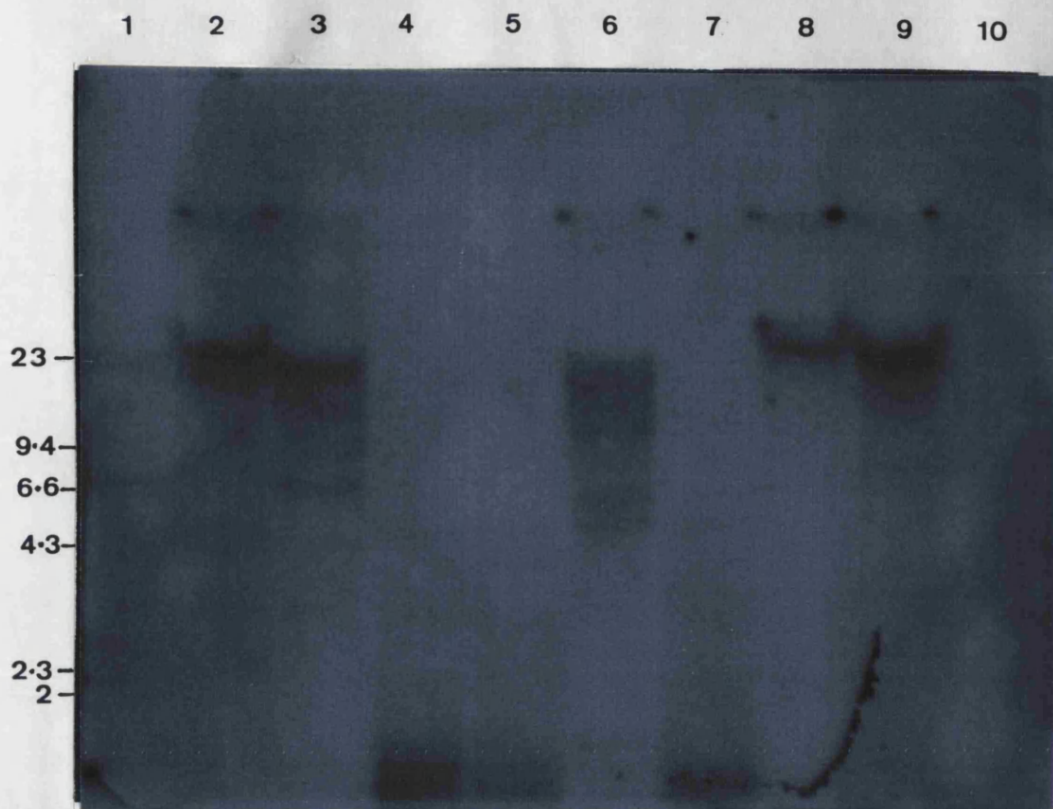


**Figure 4.13b** Autoradiograph of Southern blot probed with degenerate 17 base oligonucleotide A (9 day exposure)

Lane 1:  $\lambda$  *Hind*III

Lane 2: *Hind*III / *Pst*I

Lane 3: *Hind*III / *Sph*I

Lane 4: *Hind*III / *Sal*I

Lane 5: *Pst*I / *Sal*I

Lane 6: *Sph*I / *Pst*I

Lane 7: *Sph*I / *Sal*I

Lane 8: *Hind*III

Lane 9: *Sph*I

Lane 10:  $\lambda$  *Pst*I

Fragment sizes are indicated in kilobases. Figure 4.13a shows the corresponding agarose gel. The blot was washed at 37°C, in 2x SSC.

blot; hybridisation to a number of bands in each lane is apparent (autoradiograph exposed for 9 days).

As only one of the pair of probes (oligonucleotide A) exhibited potentially useful hybridisation, the possibility of two independent identifications of a restriction fragment containing the citrate synthase gene N-terminus was no longer viable. This meant that either such a fragment would have to be unambiguously identified from the hybridisation of the remaining 17mer (ie. single bands would have to be identified on a Southern blot), or a new probe would have to be designed.

Before taking the step of involving new probes, the possibility of identifying single restriction fragments using oligonucleotide A alone was investigated.

In order to eliminate non-specific hybridisation and to obtain single bands in each lane, further blots were hybridised and washed at 42°C. Figures 4.14a and 4.14b show the result obtained under these conditions (autoradiograph exposed for 17 days). As multiple bands were still visible under these conditions, the stringencies of the hybridisation and wash were increased by raising the temperature of both to 45°C. This resulted in a further decrease in the intensity of all bands visible on the previous autoradiographs, without enhancement of any particular band.

In another approach to improving specificity, hybridisations were carried out at 37°C, where the oligonucleotide was known to bind efficiently, followed by washes where salt concentrations had been reduced to increase the stringency. These washes were at 37°C, in the same solution as describe in Section 2.3.9.1, except that the concentration of SSC was reduced from 2x to 0.5x. Figures 4.15a and 4.15b show that



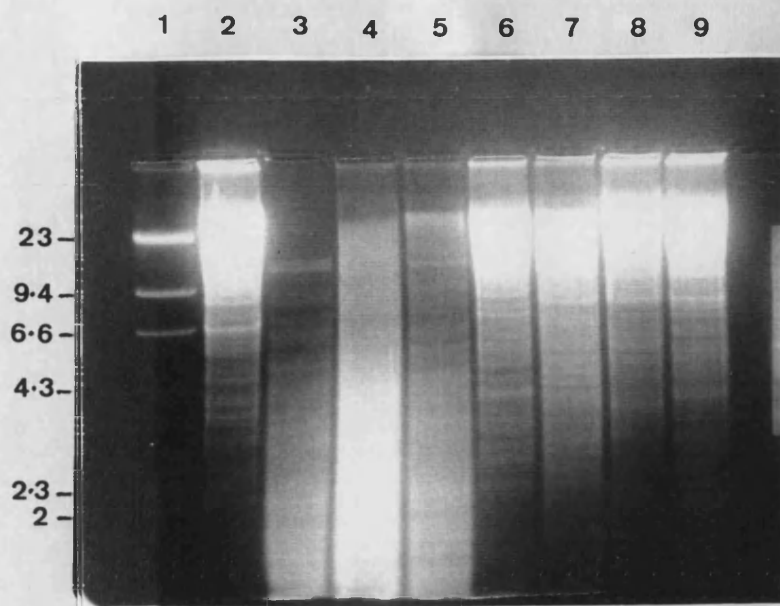


**Figure 4.14a Electrophoresis of genomic DNA restriction digests on 0.6% agarose gel**

Lane 1:  $\lambda$  *Hind*III  
 Lane 2: *Hind*III / *Sph*I  
 Lane 3: *Hind*III / *Sal*I  
 Lane 4: *Pst*I / *Sal*I  
 Lane 5: *Sph*I / *Sal*I  
 Lane 6: *Sph*I / *Pst*I

Lane 7: *Sma*I / *Eco*RI  
 Lane 8: *Sma*I / *Bam*HI  
 Lane 9: *Bam*HI / *Eco*RI

Fragment sizes are indicated in kilobases. Figure 4.14b shows an autoradiograph of the corresponding Southern blot.

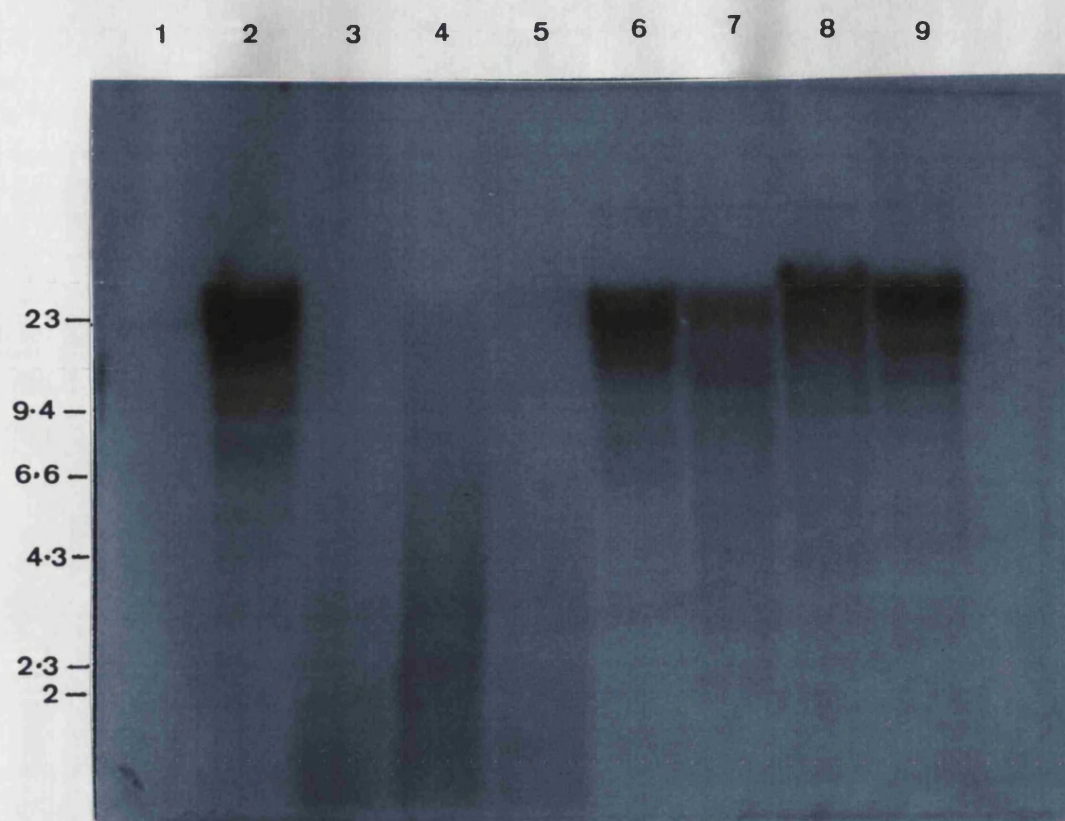


**Figure 4.14b** Autoradiograph of Southern blot probed with degenerate 17 base oligonucleotide A (17 day exposure)

Lane 1:  $\lambda$  *Hind*III

Lane 2: *Hind*III / *Sph*I

Lane 3: *Hind*III / *Sal*I

Lane 4: *Pst*I / *Sal*I

Lane 5: *Sph*I / *Sal*I

Lane 6: *Sph*I / *Pst*I

Lane 7: *Sma*I / *Eco*RI

Lane 8: *Sma*I / *Bam*HI

Lane 9: *Bam*HI / *Eco*RI

Fragment sizes are indicated in kilobases. Figure 4.14a shows the corresponding agarose gel. The blot was washed at 42°C, in 2x SSC.



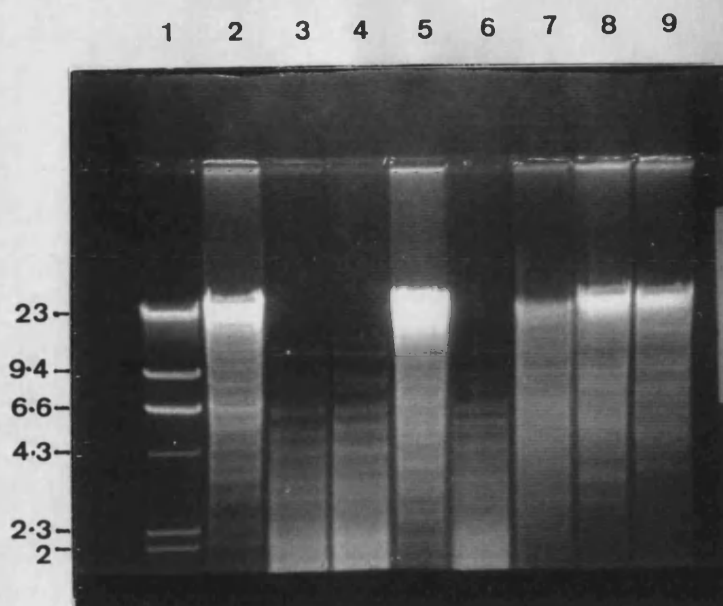


**Figure 4.15a** Electrophoresis of genomic DNA restriction digests on 0.6% agarose gel

Lane 1:  $\lambda$  *Hind*III

Lane 2: *Hind*III / *Sph*I

Lane 3: *Hind*III / *Sal*I

Lane 4: *Pst*I / *Sal*I

Lane 5: *Sph*I / *Pst*I

Lane 6: *Sph*I / *Sal*I

Lane 7: *Sma*I / *Eco*RI

Lane 8: *Sma*I / *Bam*HI

Lane 9: *Bam*HI / *Eco*RI

Fragment sizes are indicated in kilobases. Figure 4.15b shows an autoradiograph of the corresponding Southern blot.

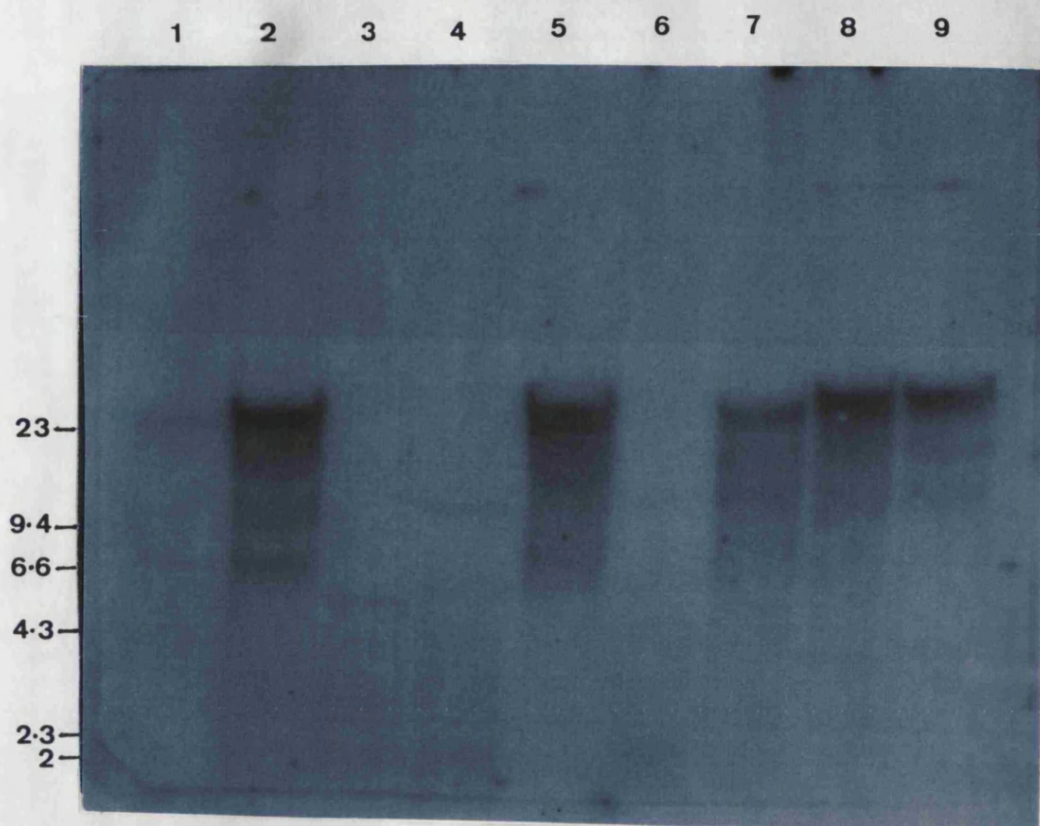


**Figure 4.15b** Autoradiograph of Southern blot probed with degenerate 17 base oligonucleotide A (30 day exposure)

Lane 1:  $\lambda$  *Hind*III

Lane 7: *Sma*I / *Eco*RI

Lane 2: *Hind*III / *Sph*I

Lane 8: *Sma*I / *Bam*HI

Lane 3: *Hind*III / *Sal*I

Lane 9: *Bam*HI / *Eco*RI

Lane 4: *Pst*I / *Sal*I

Lane 5: *Sph*I / *Sal*I

Lane 6: *Sph*I / *Pst*I

Fragment sizes are indicated in kilobases. Figure 4.15a shows the corresponding agarose gel. The blot was washed at 37°C in 0.5x SSC.

these conditions did not improve the hybridisation specificity (autoradiograph exposed for 30 days).

As a single hybridising restriction fragment could not be identified using oligonucleotide A alone, a further oligonucleotide was designed as described below.

#### **4.8 Screening Southern blots with a non-degenerate 29 base oligonucleotide probe**

A 29 base non-degenerate oligonucleotide was designed to the citrate synthase N-terminal sequence, with reference to the codon usage data previously described in Figure 4.1. It's predicted melting temperature is 102°C. The new sequence did not overlap the previous 44 base oligonucleotide and is shown in Figure 4.16.

The non-degenerate design approach was taken for two reasons: the difficulties already encountered when using degenerate oligonucleotides as probes and the lack of suitable regions to design further degenerate oligonucleotides.

The new oligonucleotide was made shorter than the previous 44 base non-degenerate probe to reduce the possibility of hybridisation to sequences other than the citrate synthase gene. The 44 base probe may have been excessively long, contributing to its ability to hybridise to an unrelated gene.

##### **4.8.1 Preliminary dot-blot results**

The 29 base probe was observed to hybridise to dot-blots of 1 µg genomic DNA when hybridisation and washing were carried out at 55°C.

```

      G   E   L   K   R   G   L   E   G   V   L V A E S K L S F I D G D A G Q L V Y X G Y D I E D L
GGA GCA CTA AAA CGA GGA CTA GCA GGA GTA
  G   G   G   G   G   G   G   G   G   G
  C   C   C       C   C   C   C   C   C
  T   T   T       T   T   T   T   T   T
      TTA       AGA       TTA
      G         G         G
GGC GAG CTC AAG CGC GGC CTC GAG GGC GT

```

**Figure 4.16 Sequence of 29 base oligonucleotide probe**

The citrate synthase N-terminal sequence is shown, with all possible codons below each residue. The probe sequence is shown in **bold**.

#### 4.8.2 Southern blot results

Hybridisation was carried out at 55°C to Southern blots of genomic DNA digested with single restriction enzymes. Washing was also carried out at 55°C. Figures 4.17a and 4.17b show the result (autoradiograph exposed for 30 days). The majority of the probe hybridised to high molecular weight restriction fragments or undigested DNA. Smaller hybridising fragments are visible, notably a 4 kb *EcoRI* fragment (Figure 4.17a, lane 7).

As it was necessary to expose each autoradiograph for a long period (30 days) it was considered impractical to use the Southern blotting technique to follow up this result in a reasonable timescale. At these hybridisation and washing stringencies, exposure times were prohibitively long, while use of less stringent conditions would run the risk of introducing non-specific hybridisation without greatly decreasing the necessary exposure time.

From this point onwards the 29 base oligonucleotide was applied as a PCR primer as described in Chapter 6. This technique had the potential to be optimised in a much shorter time.



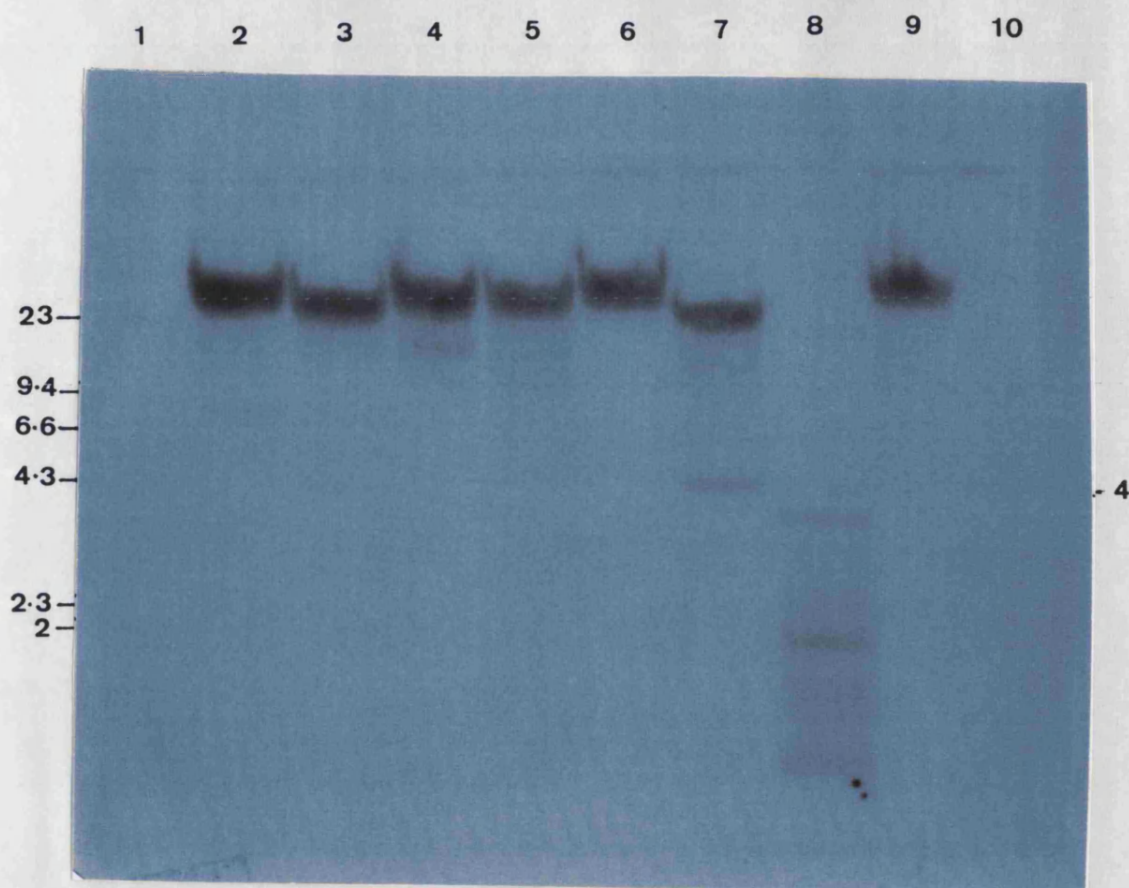


**Figure 4.17b** Autoradiograph of Southern blot probed with non-degenerate 29 base oligonucleotide (30 day exposure)

Lane 1:  $\lambda$  *Hind*III

Lane 2: *Hind*III

Lane 3: *Pst*I

Lane 4: *Sph*I

Lane 5: *Sma*I

Lane 6: *Bam*HI

Lane 7: *Eco*RI

Lane 8: *Sal*I

Lane 9: *Kpn*I

Lane 10:  $\lambda$  *Pst*I

Fragment sizes are indicated in kilobases. Figure 4.17a shows the corresponding agarose gel. The blot was washed at 55°C, in 2x SSC.

## 4.9 Discussion

This chapter describes the hybridisation results obtained with two different types of oligonucleotide probe designed to an N-terminal peptide sequence: long, non-degenerate probes designed with reference to codon usage and shorter, degenerate probes incorporating all possible sequences in the synthetic mixture. The former relies on its length to give specificity, under the assumption that the percentage of mis-matches in its sequence will be low and hybridisation will occur despite their presence. An accurate estimate of codon usage is a pre-requisite. This approach has the advantage that if the probe is a good match, all of the oligonucleotide molecules have the potential to hybridise to the target, as they all have the same sequence.

The latter approach relies on the use of a probe mixture containing all possible sequences, thereby guaranteeing that some are perfect matches to the target. However, only a small percentage of the molecules have the potential to hybridise, reducing the maximum signal that it is possible to obtain.

The 44 base probe hybridises to a non-citrate synthase sequence, a problem that may have been avoided by the use of a shorter oligonucleotide (Figure 4.18). The hybridisation data in Figure 4.5b shows that the binding site of the probe lies within the 1.5 kb *Ava*I fragment. When this fragment is cut with *Hind*III the strong hybridisation is lost and a small, weakly hybridising *Ava*I / *Hind*III is released. This fragment is visible in Figure 4.6b (lane 2). From the sequencing data this fragment is 310 base pairs in length.

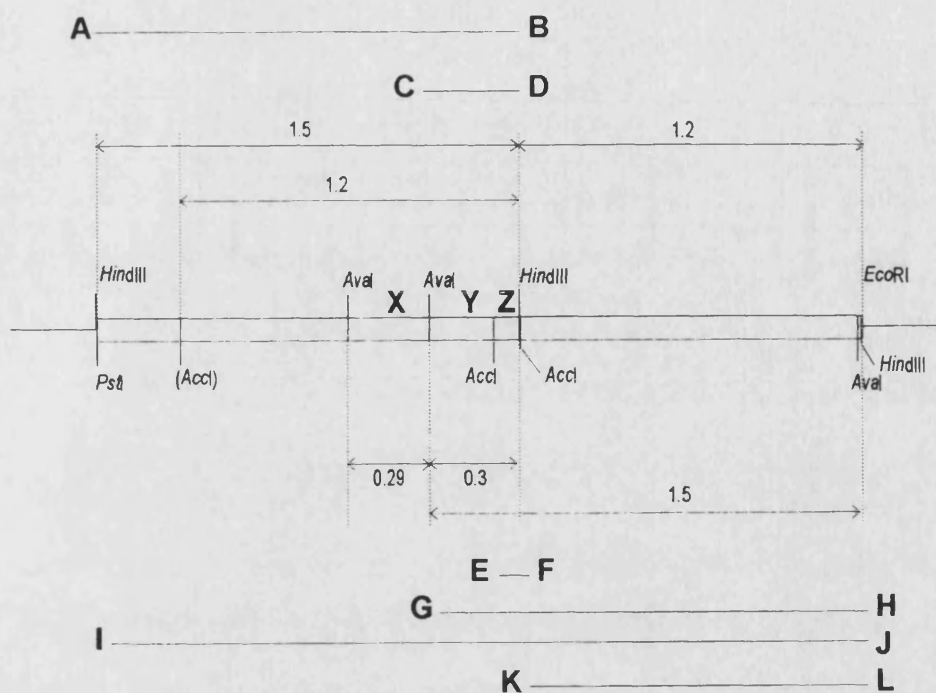


**Figure 4.18 Possible probe binding sites within 2.9 kb *PstI* / *EcoRI* clone**

All distances are in kilobases. X, Y and Z indicate the positions of the sites. Their sequences, including identity with the probe, are shown below (the probe would hybridise to the complementary strand):

**X (24/44 matches):**

870

ORF: ATCGAACTCGCGGAGTCAGCGACCATCGAAGACGGCGCAGTCGT  
 \*\*\* \* \* \* \* \*\* \* \* \* \* \*  
 Probe: GTCGCCGACTCGAAGCTTTCGTTTCATCGACGGCGACGCCGCCA

**Y (25/44 matches):**

687

ORF: ATCACGGACGCGATTTCAGTCACTCCTCGAAGACGGCTACGCCAT  
 \* \* \* \* \* \* \* \* \* \* \* \* \* \* \* \* \* \* \*  
 Probe: GTCGCCGACTCGAAGCTTTCGTTTCATCGACGGCGACGCCGCCA

**Z (24/44 matches):**

507

ORF: GTCGAGAACCCACAGCAGTTCGGCATTGCGGACGTCGACGACCA  
 \* \* \* \* \* \* \* \* \* \* \* \* \* \* \* \* \* \* \*  
 Probe: GTCGCCGACTCGAAGCTTTCGTTTCATCGACGGCGACGCCGCCA

*HindIII* fragment AB hybridises weakly  
*HindIII*/*AvaI* fragment CD hybridises weakly  
*AccI* fragment EF fragment hybridises weakly

*AvaI* fragment GH hybridises strongly  
*PstI*/*EcoRI* fragment IJ hybridises strongly  
*HindIII* fragment KL does not hybridise



subclones were sequenced such that the presence of a citrate synthase gene could be discounted.

The second approach used to locate the citrate synthase gene used mixed pools of probes. It is difficult to predict hybridisation conditions for mixed sequences as their  $T_m$  values vary considerably within the pool. Initial experiments were therefore carried out using hybridisation and washing temperatures below the lowest predicted  $T_m$  and the stringency of subsequent experiments was gradually increased.

If the perfectly-matched probe has a  $T_m$  in the lower part of the pool's  $T_m$  range it is unlikely that its specific hybridisation will be retained after all the non-specifically hybridised probes have been washed off. This effect may have contributed to the poor hybridisation results obtained with the pair of 17 base probes. The long exposure times required could suggest inefficient end-labelling of the probe, although approximately 40% or more of the oligonucleotides were labelled in all cases. Normally one would expect about 50% of the oligonucleotides to be labelled. Efforts were made to increase incorporation by re-cleaning the oligonucleotide solutions by ethanol precipitation, increasing the molar excess of ATP over oligonucleotides and using fresh reagents; however no improvement in incorporation was observed.

The second non-degenerate oligonucleotide was designed with reference to the results obtained for the 44 base probe. For the reasons described above, it was made shorter than the previous non-degenerate probe and to a different region of the N-terminal sequence. There was no reason from previous observations to suggest that a second attempt at this approach to probe design would be unsuccessful, provided that these changes were made. Despite reasonable levels of ATP incorporation when

end-labelling (approximately 40% of the oligonucleotides labelled), autoradiograph exposure times were very long. Although the hybridisation appeared to be fairly specific, analysis of further Southern blots and screening of cloned restriction fragments under these conditions would be very time consuming. Subsequent cloning strategies were centred around a PCR approach as this appeared to offer a more efficient way forward for the project.

## **Affinity purification of citrate synthase and determination of internal peptide sequence**

### **5.1 Introduction**

It is clear from the results presented in Chapter 4 that the identification of a genomic fragment containing the citrate synthase gene by hybridisation to oligonucleotides designed from the N-terminal amino acid sequence met with limited success. Knowledge of a suitable internal peptide sequence would therefore be highly valuable as it provides the opportunity to attempt PCR amplification using primers designed entirely from peptide sequences. An oligonucleotide can be designed from its corresponding peptide sequence with far greater confidence than is possible when designing a consensus probe from a multiple sequence alignment. The chance of successful PCR amplification is greatly enhanced when using such oligonucleotides as primers. The strategies used to design PCR primers are discussed in greater detail in Chapter 6.

Due to lack of material, re-purification of citrate synthase was required before further sequence analysis could be made. The original purification procedure gave a poor recovery of partially pure enzyme. An alternative was sought at this stage in an effort to improve recovery and purity in the final preparation.

Matrex Gel Red A is an agarose support to which the triazine dye ligand Procion Red HE-3B is covalently bound. The structure of Procion

Red is shown in Figure 5.1. This dye has a high affinity for NADP-linked enzymes, but a lower affinity for NAD-linked enzymes. It has found applications in the purification of dehydrogenases where it is thought to bind to the nucleotide-binding site. The structural basis of this binding is unknown, although from studies on lactate dehydrogenase (Kirchberger *et al.*, 1989) it appears that the rigid conformation of the terminal rings and the presence of the terminal ring sulphonate groups are important. Coenzyme A shares structural similarities with NADP, both having an adenine moiety linked to a phosphorylated ribose, although the two are phosphorylated at different positions on the sugar.

Based on this information, studies have previously been carried out on the binding of the coenzyme A-linked enzymes citrate synthase and succinate thiokinase, from six different organisms (Weitzman & Ridley, 1983). Significant purifications were achieved for both enzymes using a simple salt gradient elution.

Matrex Gel Red A has been used with success in the purification of citrate synthase from *Acinetobacter calcoaceticus* (Mitchell & Weitzman, 1983) and *Bacillus coagulans* (Schendel *et al.*, 1992), eluting ligand-bound enzyme with either a salt gradient or biospecifically with oxaloacetate and coenzyme A. More recently the citrate synthases of a number of Archaea, including *Sulfolobus solfataricus* (James *et al.*, 1994) and *Pyrococcus furiosus* (Muir *et al.* 1994a) have also been purified using this ligand. This method therefore appeared to be a good candidate for purification of the *Hf. volcanii* citrate synthase. Salt gradients (0-800 mM KCl in the case of *B.coagulans* above) have been found to elute bound citrate synthase from Red A; however, given that halophilic citrate synthases only achieve native

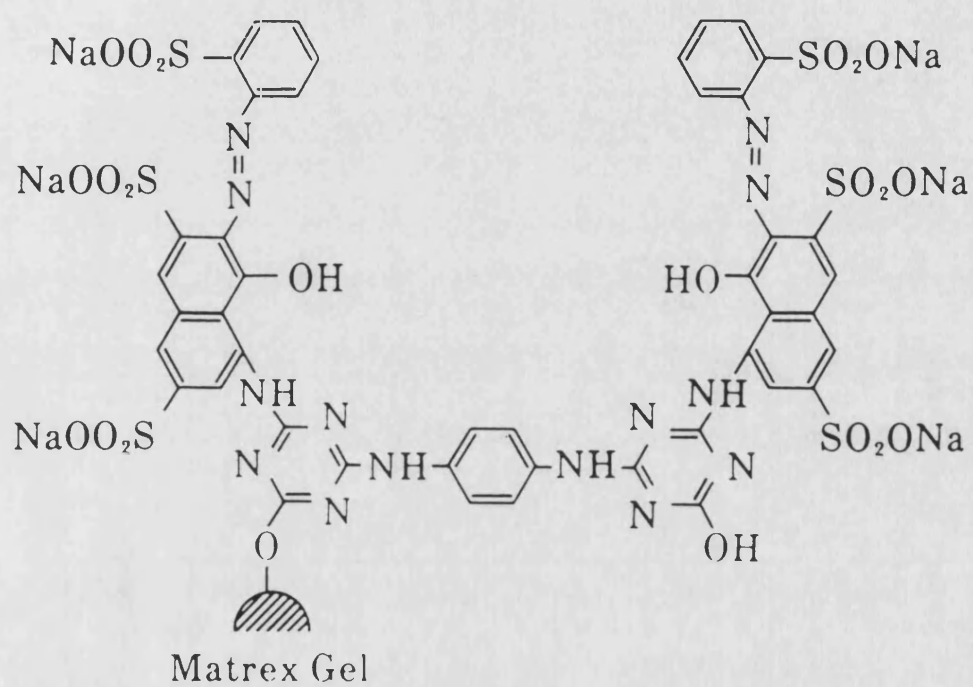


**Figure 5.1 Partial structure of Matrex Gel Red A**

conformation in high salt conditions the possibility of specific binding and elution in high salt warranted investigation.

## **6.2 Outline of the purification scheme**

*Hf.volcanii* (2 g wet weight) was resuspended in 10 ml 20 mM Tris-HCl (pH 8.0), 2 mM EDTA, 0.1 M KCl and a cell extract prepared by sonication as described in Section 2.1.1.2.

The cell extract was applied to a 10 ml column of Matrex Gel Red A equilibrated with the same buffer. After washing, citrate synthase was eluted with 1 mM oxaloacetate, 0.2 mM coenzyme A in the same buffer. Fractions containing citrate synthase activity were pooled and concentrated to a total volume of 2 ml using solid polyethylene glycol as described in Section 2.2.3. This method was found to give > 90% recovery of citrate synthase activity after concentration.

Microsep microconcentrators (10 kD cutoff) were also tried as a method of protein concentration but proved unsuitable as the flow rate through the filter decreased rapidly after the first 10 minutes of centrifugation, suggesting that the protein was adhering to the filter membrane. Only 50% of the citrate synthase activity applied to the concentrator could be recovered when using this method.

The concentrated solution was adjusted to 2 M KCl by addition of solid KCl and was then applied to an FPLC Superdex-200 gel filtration column equilibrated with 20 mM Tris-HCl (pH 8.0), 2 mM EDTA, 2 M KCl. Fractions containing citrate synthase activity were pooled, dialysed against 10 mM ammonium bicarbonate, 0.01% (w/v) SDS and dried in a Savant Speedvac concentrator.

### **5.3 Cyanogen bromide cleavage**

Cyanogen bromide cleavage and N-terminal sequencing were carried out by Mrs. Janice Young at Zeneca Pharmaceuticals, Macclesfield. An estimated 20 µg protein was dissolved in 250 µl 70% (v/v) formic acid, in a polypropylene tube and 186 µl cyanogen bromide solution (10 mg ml<sup>-1</sup> in 70% (v/v) formic acid) added. After purging with nitrogen, the sample was incubated in the dark for 24 hours, at room temperature.

The sample was dried, after addition of 5 µl 10% (w/v) SDS to prevent fragments sticking to the tube. The sample was re-dissolved in water and dried again to remove the acid. The sample was dissolved in reduced tris-tricine sample buffer, run on a 16.5% tris-tricine polyacrylamide minigel and blotted onto Problott membrane. A band of approximately 6 kD was cut out.

### **5.4 N-terminal sequencing**

To repeat the N-terminal sequencing of the intact protein, 5-10 µg was dissolved in reducing sample buffer, subjected to SDS-polyacrylamide gel electrophoresis and blotted onto Problott membrane. The single band was cut out and sequenced using an Applied Biosystems 477 Sequencer (modified to run blot cycles) with a gas phase TFA delivery.

The cyanogen bromide fragment was sequenced using an Applied Biosystems 475 Sequencer. In both cases the sequencers were coupled to an Applied Biosystems 120A Phenylthiohydantoin analyser.

## 5.5 Results

### 5.5.1 Purification

The purification is summarised in the table below

Step	Protein mg	CS Activity U	Sp Activity U mg <sup>-1</sup>	Purification	Yield
Cell-free extract	160	13.5	0.085	1	100
Red A	0.66	10.8	16.42	196	81
PEG concentration	-	10.7	-	-	-
Superdex-200	0.21	9.5	45.2	532	70

Figures 5.2 and 5.3 show elution profiles of the Red A column and Superdex-200 column respectively. Figure 5.4 shows an SDS-polyacrylamide gel of the cell extract, the pooled fractions from the Red A column and the pooled fractions from the Superdex-200 column after dialysis and drying.

CoA in the Red A gel fractions was assayed by addition of DTNB to an aliquot of the fraction, in the absence of oxaloacetate. The reaction was followed to completion spectrophotometrically as for a citrate synthase assay and the CoA concentration calculated from the final absorbance at 512 nm.



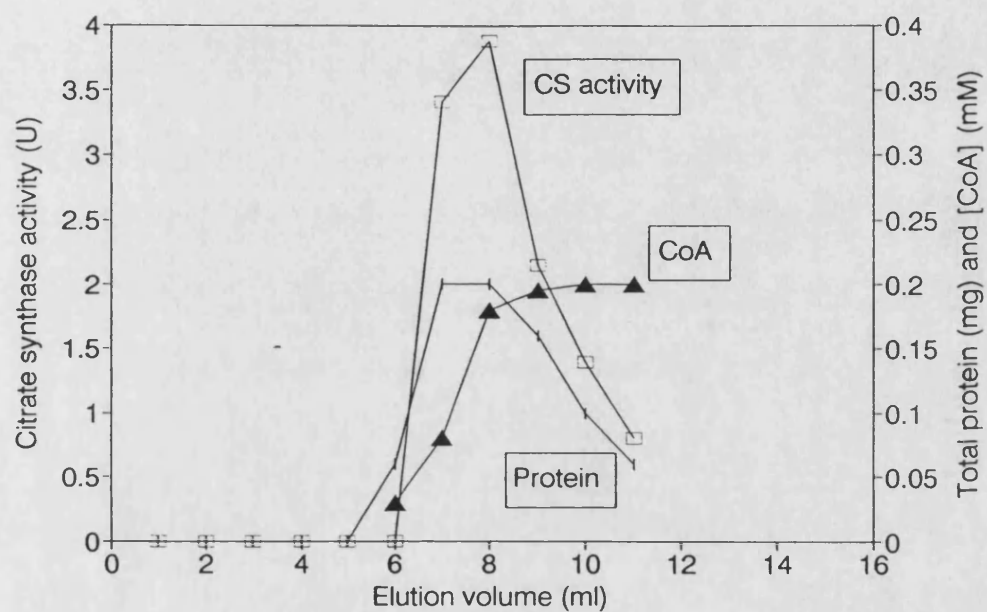


**Figure 5.2 Matrex gel Red A chromatography of citrate synthase**

The elution profile of a 10 ml column is shown. Citrate synthase activity (U), total protein (mg) and Coenzyme A concentration (mM) in each 1 ml fraction are plotted against elution volume (ml).

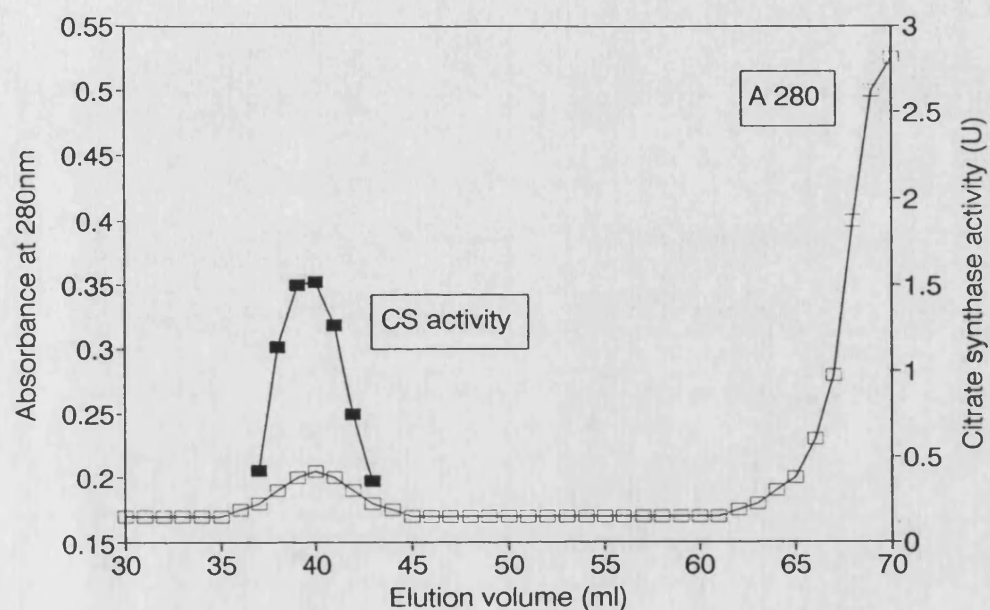


**Figure 5.3 FPLC Superdex-200 gel filtration of citrate synthase**

Citrate synthase activity (U) and absorbance at 280 nm are plotted against elution volume (ml) for each 1 ml fraction. The void volume of the column is 30 ml. The absorbance peak at 60 - 70 ml is caused by CoA eluting from the column.

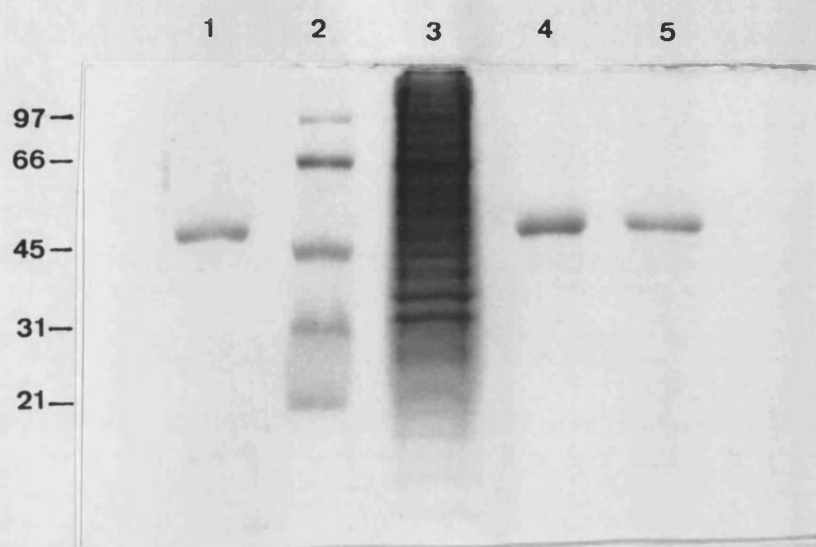


**Figure 5.4 SDS-PAGE of citrate synthase**

Lane 1: Pig heart citrate synthase

Lane 2: Molecular weight markers

Lane 3: *Hf. volcanii* cell extract

Lane 4: Matrex gel Red A eluent

Lane 5: Superdex-200 eluent

Sizes are indicated in kD.

### 5.5.2 N-terminal sequencing

The re-sequencing of the N-terminus of the uncleaved protein confirmed the 38 residue sequence previously obtained. The yield of fragments from cyanogen bromide treatment was unexpectedly low: on SDS-PAGE only a single band 6 kD band was visible. The N-terminal sequence of the 6 kD band was determined and is shown below. Residues in parentheses are tentative assignments and X indicates an unknown residue.

6 kD XIPIDLYTPIFAVSRAG(G)

### 5.6 Discussion

In terms of final purity and recovery of citrate synthase the revised purification scheme is a significant improvement on that previously used. The dried citrate synthase appeared pure as judged by the appearance of a single band on SDS gels. The most significant loss of material occurred during the concentration step, where the protein appeared to bind to the filtration membrane.

Trials of the Red A column were carried out on small (1 ml bed volume) columns using a variety of different loading and elution conditions. Initially the procedure described above was carried out in buffers containing 1 M KCl, the concentration at which the enzyme has maximum activity, since if the Red A dye is acting as nucleotide analogue it is likely

to bind at the acetyl coenzyme A binding site and a fully active enzyme ensures correct conformation of that site. Under these conditions citrate synthase bound irreversibly to the column, resisting elution with concentrations of oxaloacetate and coenzyme A as high as 10 mM and 1 mM respectively. The binding appeared to be specific as the vast majority of the protein loaded onto the column could be accounted for in the initial wash.

Reducing the KCl concentration to 0.1 M, the minimum KCl concentration at which the enzyme retains both activity and stability, resulted in modified specific binding which could be overcome by addition of 1 mM oxaloacetate and 0.2 mM coenzyme A as described. The difference in binding could be due to non-specific interactions between citrate synthase and the dye-ligand matrix which occur in addition to the specific binding, in the presence of 1 M KCl. Alternatively the change in binding with KCl concentration may be caused by a change in the enzyme's affinity for the ligand, coenzyme A or oxaloacetate.

It has since been shown in our laboratory that as the KCl concentration is decreased from 1 M to 0.1 M, the  $K_m$  of oxaloacetate decreases and the  $K_m$  of acetyl coenzyme A increases (Henderson, 1994). This suggests that oxaloacetate may become a more efficient eluant at lower salt concentrations, where its  $K_m$  is lower. If the  $K_m$  of coenzyme A increases at lower KCl concentrations, the binding to the column may be weaker under these conditions.

The internal peptide sequence was aligned by hand to the same citrate synthase multiple sequence alignment as was used to align the N-terminal sequence. Figure 5.5 shows the relevant region of the alignment. The sequence shows very high identity with the other citrate synthases

and includes four residues that are conserved in all the enzymes. The cyanogen bromide cleavage site is likely to be a methionine in the equivalent position to that observed in the *E.coli*, *A.aceti*, *R.prowazekii*, *M.smegmatis* and *Tp.acidophilum* sequences. These sequence data were used to design an oligonucleotide primer for use in PCR as described in Chapter 6.

```

                                401                                450
Chicken heart  aanpwPNvDa hsgvllqyyg mt.emnyYTv lFgvsRalGv laqli.wsra
Pig kidney    aknpwPNvDa hsgvllqyyg mt.emnyYTv lFgvsRalGv laqli.wsra
Yeast (cytoplasm) tknpwPNvDa hsgvllqyyg lk.essfYTv lFgvsRafGi laqli.tdra
Yeast (mitoch) tknpwPNvDs hsgvllqyyg lt.easfYTv lFgvaRaiGv lpqli.idra
Tetrahymena   ianpyPNvDc hsgvllyslgt lt.eyqyYTv vFavsRalGc manli.wsra
Mycobacterium ..rikPNlD. fptgayylmd fpi..esFTp lFvmsRitGw tahimeqaas
Bacillus      ..glfPNlDy yaapvywklg ipi..plyTtp iFfssRtvGl cahvmeqhen
Acinetobacter ..klyPNvDf ysgiiikaig ip..temFTv iFalaRtvGw ishwlemhsg
Pseudomonas   ..nlyPNvDf ysgiiikaig ip..tsmFTv iFalaRtvGw ishwqemlsg
Escherichia   ..klyPNvDf ysgiiikamg ip..ssmFTv iFamaRtvGw iahwsemhsd
Acetobacter   ..klyPNvDf ysgiiikamg ip..tsmFTv lFavaRttGw vsqwkemiee
Coxiella      ..klyPNvDf ysgltlnaig ip..snmFTv iFalsRtvGw ishwmemmss
Rickettsia    ..klyPNvDf ysgiiykamg ip..sqmFTv lFaiaRtvGw maqwkemhed
Thermoplasma  ..giyPNtDy fsgivymsig fplrnniYTa lFalsRvtGw qahfieyvee
Haloferax                                           IP IDLYTP IFAVSRAG
Consensus     -----PN-D- -----T- -F---R--G- -----

```

**Figure 5.5 Alignment of 6kD peptide N-terminal sequence with citrate synthase multiple sequence alignment**

# Chapter 6

## **Amplification of the citrate synthase gene of *Haloferax volcanii* from genomic DNA by PCR**

### **6.1 Introduction**

The amplification of genomic DNA by the polymerase chain reaction provides an alternative to the Southern blot screening approach in gene cloning. The success of a PCR reaction relies heavily on the specificity of the primers used, which in turn requires careful primer design at the planning stage.

Primers may be designed with reference to a known amino acid sequence and codon-usage table, or alternatively an alignment of related protein sequences may be created and used to identify highly conserved regions of sequence, which are in turn used for primer design. The first method is far superior as it relies on only one set of assumptions (the codon-usage table), while the second relies on two (both the primary amino acid sequence and the codon use are inferred). Both of these strategies were applied in this project.

### **6.2 PCR amplification of an 830 bp sequence from genomic DNA using N-terminal and consensus amino acid sequences for primer design**

The aim of the reactions described in this section was to amplify a large part of the citrate synthase gene for cloning and sequencing. From these sequence data a restriction map could be made and long, perfectly matched



oligonucleotide probes designed with which to screen Southern blots as described in Chapter Four, but with much greater efficacy.

### 6.2.1 Primer design

These reactions were carried out before the internal protein sequence data described in Chapter Five had been determined. The sense primer used was the non-degenerate 29 base oligonucleotide made to the citrate synthase N-terminal amino acid sequence (described in Figure 4.16).

The anti-sense primer was therefore made with reference to an alignment of citrate synthase amino acid sequences, shown in Figure 6.1. The alignment was created by M. McCormack, in our laboratory using the program PILEUP in the GCG program package. There are four particularly well conserved regions apparent in the alignment (designated R1 to R4 in Figure 6.1), each containing a number of residues conserved in all citrate synthases so far sequenced.

The only Archaeal citrate synthase sequence available is that of *Thermoplasma acidophilum* (Sutherland *et al.*, 1991) which shows 19-20% identity with eukaryotic sequences and 27-28% with bacterial sequences. The citrate synthase sequences currently available show higher identity within a domain than between domains (Sutherland *et al.*, 1991). The N-terminal sequence of the *Hf.volcanii* enzyme shows highest identity with the corresponding region of the *E.coli* enzyme (50%) and the *Tp.acidophilum* enzyme (42%). This was considered in choosing residues from the conserved regions of the alignment (R1 to R4) most likely to occur in the *Hf.volcanii* enzyme, as shown in Figure 6.2.

The most probable DNA sequences corresponding to these regions were estimated using the codon use data in Figure 4.1 and are given in Figure 6.3.

	1				50
Chicken heart	...asstnlk	dvlaalipke	qariktfrqq	hggtaglqgit	v.dms.....
Pig kidney	...asstnlk	diladlipke	qariktfrqq	hgntvvggit	v.dmm.....
Yeast (cytoplasm)	...sqektlk	erfseippih	aqdvrqfvke	hgktkisdl	l.eqv.....
Yeast (mitoch)	...aseqtlk	erfaeiipak	aqeikkfkke	hgktvigevl	leeqa.....
<i>Tetrahymena</i>	....sqtnlk	kviaeiipqk	qaelkevkek	ygdkvvgqyt	v.kqv.....
<i>Mycobacterium</i>	.....apq	qalrtaalrr	lqpvrllrlq	lrraggesmt	tateseapri
<i>Bacillus</i>	.....	.....	.....	.....	....vntnqf
<i>Acinetobacter</i>	....seatgk	kavlhlldgke	.ielpiysgt	lgpdvidvkd	vlas.ghftf
<i>Pseudomonas</i>	.....adk	kaqliiegss	pvelpvlsgt	mgpdvvdvrg	ltat.ghftf
<i>Escherichia</i>	.....adt	kakltlngdt	aveldvkgt	lgqdvidirt	lgsk.gvftf
<i>Acetobacter</i>	sasqkegkls	tatisvdgks	a.empvlsgt	lgpdvidirk	lpaqlgvftf
<i>Coxiella</i>	.....snr	kaklsfenqs	.vefpiyspt	lgkdvidvkt	l.gnhgayal
<i>Rickettsia</i>	.tngnnnnle	faelkirgk.	lfklpilkas	igkdvidisr	vsaeadyfty
<i>Thermoplasma</i>	.....	.....	.....	.....	....peteei
Consensus	-----	-----	-----	-----	-----
	51				100
Chicken heart	ygGmrqmkgl	vyetsvldpd	egi.rfrGfs	ipeqcqllpk	gg.....xg
Pig kidney	ygGmrqmkgl	vyetsvldpd	egi.rfrGys	ipeqcqmlpk	ak.....gg
Yeast (cytoplasm)	ygGmrqgpgs	vwegsvldpe	dgi.rfrGrt	iadiqkdlpk	ak.....gs
Yeast (mitoch)	ygGmrqgikgl	vwegsvldpe	egi.rfrGrt	ipeiqrelpk	ae.....gs
<i>Tetrahymena</i>	igGmrqmkgl	msdlsrcdpy	qgi.ifrGyt	ipqlkeflpk	adpkaadqan
<i>Mycobacterium</i>	hkGlagvvvd	ttaiskvvp	tnsltyrGyp	vqd.l.....	.....a
<i>Bacillus</i>	ipGlegvias	etkisfldtv	nseivikGyd	lla.l.....	.....s
<i>Acinetobacter</i>	dpGfmatasc	eskitfidgd	kgillhrGyp	idq.l.....	.....a
<i>Pseudomonas</i>	dpGfmstasc	eskityidgd	kgvllhrGyp	ieq.l.....	.....a
<i>Escherichia</i>	dpGftstasc	eskitfidgd	egillhrGfp	idq.l.....	.....a
<i>Acetobacter</i>	dpGygetaac	nskitfidgd	kgvllhrGyp	iaq.l.....	.....d
<i>Coxiella</i>	dvGfyystaac	eskitfidge	kgillyrGyp	idq.l.....	.....a
<i>Rickettsia</i>	dpGfmstasc	qstityidgd	kgilwyrGyd	ikd.l.....	.....a
<i>Thermoplasma</i>	skGledvnik	wtrlttidgn	kgilrygGys	vedii.....	.....a
Consensus	--G-----	-----d--	-g----rG--	-----	-----
	101				150
Chicken heart	geplpeglfw	lLvtGqiPtg	aqvswLskew	akraalpshv	vtmldnFptn
Pig kidney	eeplpeglfw	lLvtGqiPte	eqvswLskew	akraalpshv	vtmldnFptn
Yeast (cytoplasm)	sqplpealfw	lLltGevPtq	aqvenLsadi	msrselpshv	vqllldnLpkd
Yeast (mitoch)	teplpealfw	lLltGeiPtd	aqvkaLsadi	aarseipehv	iqllldsLpkd
<i>Tetrahymena</i>	qeplpegifw	lLmtGqlPth	aqvdaLkhew	qnrgrtvnqdc	vnfilnLpkd
<i>Mycobacterium</i>	.aqcsfeqv	lLwhGelPtd	.qlalFsqre	rasrridrs	qallakLpdn
<i>Bacillus</i>	ktkgyldivh	lLleGtiPne	aekqhLeetl	kqeydvpdei	iqvlslLpkt
<i>Acinetobacter</i>	tqadyletcy	lLlnGelPta	eqkveFdakv	rahtmvhdqv	srffngFrdd
<i>Pseudomonas</i>	eksdyletcy	lLlnGelPta	aqkeqFvgti	knhtmvheql	ktffngFrdd
<i>Escherichia</i>	tdsnylevcy	iLlnGekPtq	eqydeFkttv	trhtmiheqi	trlfhaFrdd
<i>Acetobacter</i>	enasyeeyiy	lLlnGelPnk	vqydtFtnl	tnhtllheqi	rnffngFrdd
<i>Coxiella</i>	dksdymevcy	lLmyGelPnk	gekekFvrti	kehtsvyeqv	tkffngFhyd
<i>Rickettsia</i>	eksdflevay	lMiyGelPss	dqycnFtkkv	ahhslvnerl	hylfqtFcsc
<i>Thermoplasma</i>	sgaqdeeiqy	lFlyGnlPte	qelrkYketv	qkgykipdfv	inairqLpre
Consensus	-----	lL--G--P--	-----	-----	-----

**Figure 6.1 Multiple sequence alignment of citrate synthases.**

	151			•	200
Chicken heart	lhpmSQLsaa	itaLnsesnf	arayaeg.il	rtkywemvye	samdLiaklp
Pig kidney	lhpmSQLsaa	itaLnsesnf	arayaeg.ih	rtkyweliye	dcmdLiaklp
Yeast (cytoplasm)	lhpmAQfsia	vtaleSeskf	akayaqg.is	kqdywsytfe	dsldLlgklp
Yeast (mitoch)	lhpmAQfsia	vtaleSeskf	akayaqg.vs	kkeywsytfe	dsldLlgklp
Tetrahymena	lhsmtmlsma	llyLqkdskf	aklydegkis	kkdywepfye	dsmdLiakip
Mycobacterium	chpmdvvrta	isyLg.....	aedleedvdt	aeanya....	kslrMfavlp
Bacillus	ahpmdalrtg	vsvLa.....	sfdtellnre	hstnlk....	rayqLlgkip
Acinetobacter	ahpmaimvgv	vgaLs.....	afyhnnldie	dinhrei...	tairLiakip
Pseudomonas	ahpmavmcgv	igaLs.....	afyhdsldit	npkhrqv...	sahrLiakmp
Escherichia	shpmavmcgi	tgaLa.....	afyhdsldvn	nprhrei...	aafrLlskmp
Acetobacter	ahpmailcgt	vgaLs.....	afypdandia	ipanrdl...	aamrLiakip
Coxiella	ahpmamvlst	igaLs.....	afyhdaldit	kpadrel...	sairLiakmp
Rickettsia	shpmaimlaa	vgsLs.....	afypdllnfn	etdy.el...	tairMiakip
Thermoplasma	sdavamqmaa	vaaMa.....	as.etkfkwn	ktdtdrdv...	aa.eMigrms
Consensus	-h-m-----	---L-----	a-----	-----	-----k-p
	201				250
Chicken heart	cvaakiyrnl	yragssigai	dskldWshnF	tnmlgyt...	.....daqft
Pig kidney	cvaakiyrnl	yregssigai	dskldWshnF	tnmlgyt...	.....daqft
Yeast (cytoplasm)	viaakiyrnv	fkdg.kmgev	dpnadYaknL	vnligsk...	.....dedfv
Yeast (mitoch)	viaskiyrnv	fkdg.kitst	dpnadYgknL	aqllyge...	.....nkdfi
Tetrahymena	rvaaiiyrhk	yrdsklids.	dskldWagnY	ahmmgfe...	.....qhvvk
Mycobacterium	tivatdir..	rrqgltpipp	hsqLgYaqnF	lnmcfgevpe	.....pvvv
Bacillus	nivansyh..	ilhseepvqp	lqdlSyanF	lymitgkkpt	.....elee
Acinetobacter	tlaawsyk..	ytvgqpfiiy	rndlnYaenF	lhmmfatpad	rdykvnpvla
Pseudomonas	tiaamvyk..	yskgepmmyy	rndlnYaenF	lhmmfntpce	tk.pispvla
Escherichia	imaamcyk..	ysigqpfvyp	rndlsYagnF	lnmmfstpce	p.yevnpile
Acetobacter	tiaawayk..	ytqgeafiyp	rndlnYaenF	lsmmfarmse	p.ykvnpvla
Coxiella	tlaamsyk..	ysigqpfmhp	rramnYaenF	lhmlfgtpye	et.epdpvla
Rickettsia	tiaamsyk..	ysigqpfiiy	dnsldFtenF	lhmmfatpc.	tkykvnpik
Thermoplasma	aitvnvyr..	himmpaelp	kpsdsYaesF	lnaafgrkat	ke.....ei
Consensus	-----y--	-----	-----	-----	-----
	251		•		300
Chicken heart	elmrlYltih	sDHeggnvSa	htshlvGsal	sdpYlsfaaa	mngLaGplHG
Pig kidney	elmrlYltih	sDHeggnvSa	htshlvGsal	sdpYlsfaaa	mngLaGplHG
Yeast (cytoplasm)	dlmrlYltih	sDHeggnvSa	htshlvGsal	sspYlslasg	lngLaGplHG
Yeast (mitoch)	dlmrlYltih	sDHeggnvSa	htthlvGsal	sspYlslaag	lngLaGplHG
Tetrahymena	ecirgyLsih	cdHeggnvSa	htthlvGsal	sdpYlsysag	vngLaGplHG
Mycobacterium	rafeqsMvly	aEHs.fnaSt	faarvvStq	sdiYsavtaa	igaLkGslHG
Bacillus	kifdrsLvly	sEHe.lpnSt	ftarviaStl	sdlyGaltga	vasLkGhlHG
Acinetobacter	ramdriFtlh	adHe.qnaSt	stvrLagStg	anpYacisag	isaLwGpaHG
Pseudomonas	kamdriFilh	adHe.qnaSt	stvrLagSsg	anpFaciaag	iasLwGpaHG
Escherichia	ramdriLilh	adHe.qnaSt	stvrtagSsg	anpFaciaag	iasLwGpaHG
Acetobacter	ramnrililh	adHe.qnaSt	stvrLagStg	anpFaciaag	iasLwGpaHG
Coxiella	ramdriFilh	adHe.qnaSt	ttvrvagStg	anpFacisag	isaLwGpaHG
Rickettsia	nalnkiFilh	adHe.qnaSt	stvriagSsg	anpFacistg	iasLwGpaHG
Thermoplasma	damntaLily	tdHe.vpaSt	taglvavStl	sdmYsgitaa	laaLkGplHG
Consensus	-----	-EHe--n-S-	-----S--	-----	---L-Gp-HG
					←---R1-

**Figure 6.1 Multiple sequence alignment of citrate synthases.**

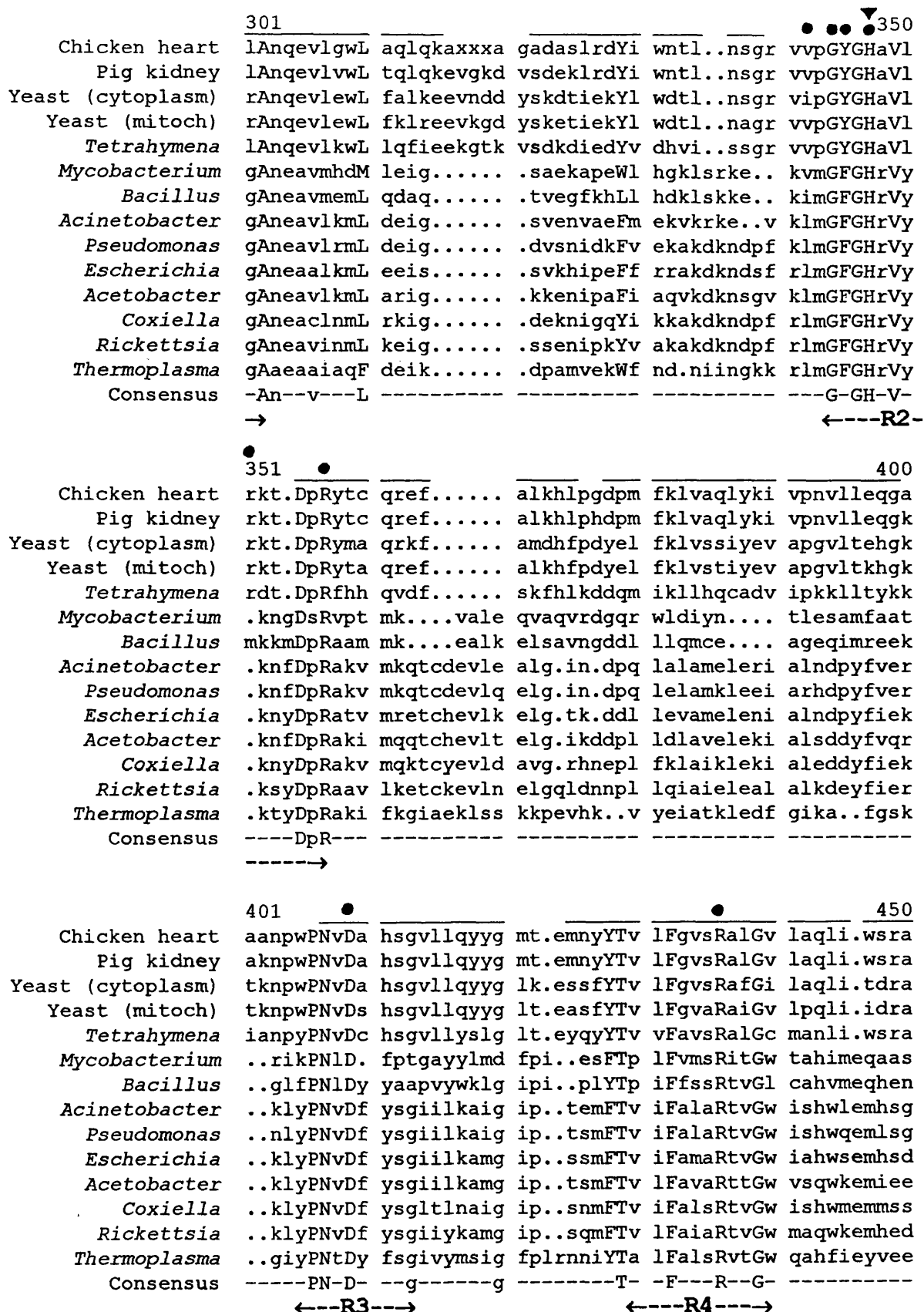


Figure 6.1 Multiple sequence alignment of citrate synthases.

	451	●		478
Chicken heart	lgfpleRPks	mstd...gli	al.....	
Pig kidney	lgfpleRPks	mstd...gli	klvds..	
Yeast (cytoplasm)	igasieRPks	ystekykely	knieskl.	
Yeast (mitoch)	vgapieRPks	fstekykely	kkieskn.	
<i>Tetrahymena</i>	fglpieRPgs	adlkwfhdky	re.....	
<i>Mycobacterium</i>	..naliRPls	eysgqpqrsl	v.....	
<i>Bacillus</i>	..nrifRPrv	lytgarnlr	ed.....	
<i>Acinetobacter</i>	p.ykigRPrq	lytgevqr	di kr.....	
<i>Pseudomonas</i>	p.ykigRPrq	lytghtqrdf	talkdrg.	
<i>Escherichia</i>	g.mkiaRPrq	lyigyekr	df ksdikr..	
<i>Acetobacter</i>	pgqrisRPrq	lyigapqr	dy vplakr..	
<i>Coxiella</i>	pdhrlaRPrq	lytgeterev	isldkrqa	
<i>Rickettsia</i>	peqkisRPrq	lytgyvhrey	kciverk.	
<i>Thermoplasma</i>	q.qrliRPra	vyvgpaerky	vpiaerk.	
Consensus	-----RP--	-----	-----	

## Figure 6.1 Multiple sequence alignment of citrate synthases.

Residues with Dayhoff matches of 1.2 or greater are in Upper Case (Schwartz & Dayhoff, 1979). The Dayhoff match between two amino acids reflects the probability of changing from one amino acid to any other, taking into account factors such as the required change in codon. It's value may vary from -1.2 to 1.5, where 1.5 indicates identity.

The consensus contains residues that occur in at least 12 of the 14 sequences, regardless of their relative Dayhoff values.

Regions of secondary structure in the Pig enzyme are indicated by the horizontal bar above the alignment. Active site residues (▼) and substrate-binding residues (●) in the Pig enzyme are indicated.

Conserved regions considered for PCR primer design are marked R1 to R4.

### Region 1:

```

300
Chicken heart LaGplHG lA
Pig kidney LaGplHG lA
Yeast (cytoplasm) LaGplHG rA
Yeast (mitoch) LaGplHG rA
Tetrahymena LaGplHG lA
Mycobacterium LkGslHG gA
Bacillus LkGhlHG gA
Acinetobacter LwGpaHG gA
Pseudomonas LwGpaHG gA
Escherichia LwGpaHG gA
Acetobacter LwGpaHG gA
Coxiella LwGpaHG gA
Consensus L-G--HG gA
(Haloferax?) LwGpaHG gA

```

### Region 2:

```

350
Chicken heart GYGHaVl rkt.DpR
Pig kidney GYGHaVl rkt.DpR
Yeast (cytoplasm) GYGHaVl rkt.DpR
Yeast (mitoch) GYGHaVl rkt.DpR
Tetrahymena GYGHaVl rdt.DpR
Mycobacterium GFGHrVy .kngDsR
Bacillus GFGHrVy mkkmDpR
Acinetobacter GFGHrVy .knfDpR
Pseudomonas GFGHrVy .knfDpR
Escherichia GFGHrVy .knyDpR
Acetobacter GFGHrVy .knfDpR
Rickettsia GFGHrVy .ksyDpR
Thermoplasma GFGHrVy .ktyDpR
Consensus G-GH-V-----D-R
(Haloferax?) GFGHrVy .k?yDpR

```

### Region 3:

```

401
Chicken heart wPNvDa hsg
Pig kidney wPNvDa hsg
Yeast (cytoplasm) wPNvDa hsg
Yeast (mitoch) wPNvDs hsg
Tetrahymena yPNvDc hsg
Mycobacterium kPNlD. fpt
Bacillus fPNlDy yaa
Acinetobacter yPNvDf ysg
Pseudomonas yPNvDf ysg
Escherichia yPNvDf ysg
Acetobacter yPNvDf ysg
Coxiella yPNvDf ysg
Rickettsia yPNvDf ysg
Thermoplasma yPNtDy fsg
Consensus -PN-D- ---
(Haloferax?) yPNvDf ysg

```

### Region 4:

```

431
Chicken heart Tv lFgvsRalG
Pig kidney Tv lFgvsRalG
Yeast (cytoplasm) Tv lFgvsRafG
Yeast (mitoch) Tv lFgvaRaiG
Tetrahymena Tv vFavsRalG
Mycobacterium Tp lFvmsRitG
Bacillus Tp iFfssRtvG
Acinetobacter Tv iFalaRtvG
Pseudomonas Tv iFalaRtvG
Escherichia Tv iFamaRtvG
Acetobacter Tv lFavaRttG
Coxiella Tv iFalsRtvG
Rickettsia Tv lFaiaRtvG
Thermoplasma Ta lFalsRvtG
Consensus T- -F---R--G
(Haloferax?) Tv iFa??Rt?G

```

**Figure 6.2 Regions conserved in all known citrate synthase sequences**

The possible corresponding sequences in *Hf.volcanii* are indicated. Question marks indicate positions where it was not possible to determine a likely residue for *Hf.volcanii*. Note that only completely conserved residues have been retained in the consensus for this analysis.

### Region 1:

	L	w	G	p	a	H	G	q	A
5' -	CTC	TGG	GGC	CCC	GCC	CAC	GGC	GGC	GC

88% G+C

### Region 2:

	G	F	G	H	r	V	y	k
5' -	GGC	TTC	GGC	CAC	CGC	GTC	TAC	AA

65% G+C

### Region 3:

	y	P	N	v	D	f	y	s	q	
5' -	TAC	CCC	AAC	GTC	GAC	TTC	TAC	TCG	GG	
Antisense	ATG	GGG	TTG	CAG	CTG	AAG	ATG	AGC	CC	-5'

52% G+C

**Figure 6.3 Predicted DNA sequences corresponding to conserved regions in citrate synthase amino acid sequences**

Region 3 alone was chosen for PCR primer design for the reason described in Section 6.2.1. The sequence of the anti-sense primer synthesised is shown above.

Region 1 was eliminated as the predicted DNA sequence was greater than 85% G+C as such a high G+C content is likely to cause secondary structure formation, primer-dimer artefacts during PCR and possibly non-specific binding of the primer. Region 4 was also eliminated because some positions in the predicted amino acid sequence were highly uncertain. Region 3 was chosen over region 2 because a slightly longer primer could be made and a larger fragment of the gene could be amplified. A 26 base anti-sense consensus primer of the sequence given in Figure 6.3 was synthesised.

The *Tp.acidophilum* citrate synthase gene is 1152 bp in length, therefore the expected length of the PCR product is approximately 200 bp less; about 960 bp.

### **6.2.2 PCR amplification with N-terminal and consensus primers**

PCR reactions were carried out using 80 ng genomic DNA as template, 0.4  $\mu$ M primers and 50  $\mu$ M dNTPs. Thirty cycles were performed, melting at 94°C (1 minute), annealing at 55°C (1 minute 30 seconds) and extending at 72°C (2 minutes). The magnesium concentration in the reactions was varied from 0.5 to 5 mM. Figure 6.4 shows examples of the PCR products, separated by electrophoresis on a 1% agarose gel.

A PCR fragment of 830 bp is apparent in the 1 to 5 mM  $Mg^{2+}$  lanes. This is approximately 130 bp shorter than expected (corresponding to a citrate synthase some 40 residues shorter than that of *Tp.acidophilum*), and was unlikely to be an amplified citrate synthase sequence, even though control reactions carried out in 1.5 mM  $Mg^{2+}$  using single primers confirmed that this band was not an artefact caused by one primer binding at multiple sites (Figure 6.5).



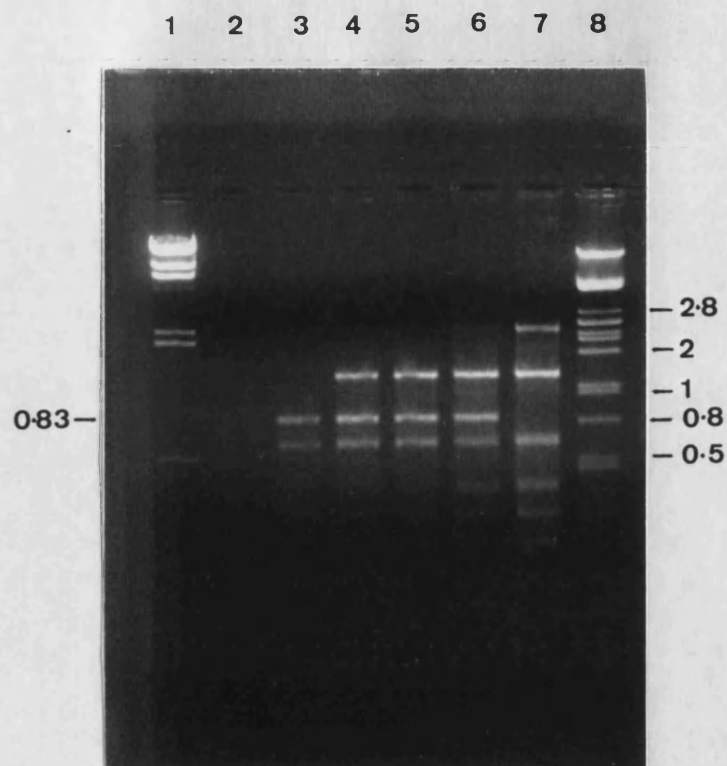


**Figure 6.4 PCR amplification of genomic DNA using 29 base N-terminal and 26 base consensus primers, annealing at 55°C**

Lane 1:  $\lambda$  *Hind*III

Lane 2: 0.5 mM  $Mg^{2+}$

Lane 3: 1.0 mM  $Mg^{2+}$

Lane 4: 1.5 mM  $Mg^{2+}$

Lane 5: 2.0 mM  $Mg^{2+}$

Lane 6: 3.0 mM  $Mg^{2+}$

Lane 7: 5.0 mM  $Mg^{2+}$

Lane 8:  $\lambda$  *Pst*I

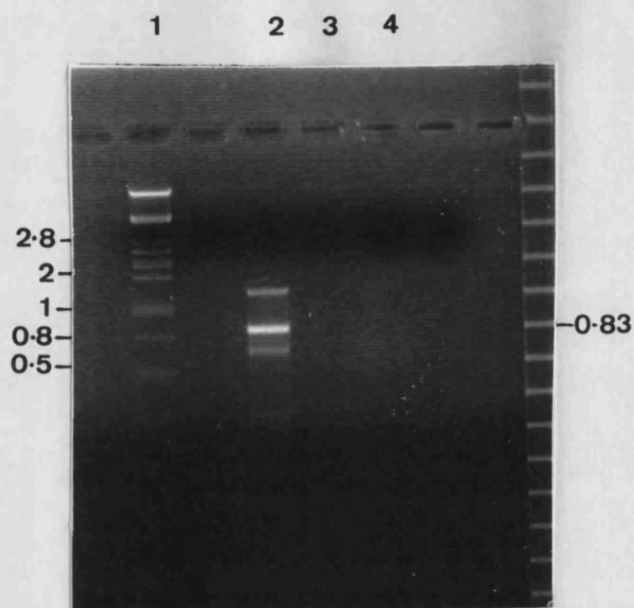


**Figure 6.5 PCR amplification of genomic DNA using 29 base N-terminal and 26 base consensus primers, annealing at 55°C**

Lane 1:  $\lambda$  *Pst*I

Lane 2: 1.5 mM  $Mg^{2+}$

Lane 3: 1.5 mM  $Mg^{2+}$

Lane 4: 1.5 mM  $Mg^{2+}$

29 base N-terminal primer control

26 base consensus primer control

The control reactions contained only the primer indicated.

To confirm whether this product was correct, both ends were sequenced by the method described below.

A 10 µl aliquot of a 100 µl PCR reaction (1.5 mM  $Mg^{2+}$ ) was run on a 1% agarose gel, the 830 bp DNA band excised, purified using GeneClean and dissolved in 50 µl sterile Milli Q water. This product was re-amplified at the same  $Mg^{2+}$  concentration, annealing at 60 or 65°C, using 0.5 µl as template (Figure 6.6).

Re-amplification at 60°C produced the highest yield of the single band. Asymmetric PCR was carried out at this annealing temperature to produce single-stranded DNA for sequencing.

### **6.2.3 Asymmetric PCR amplification of 830 bp fragment**

Asymmetric PCR was carried out as described in Section 2.3.15.2, using 0.5 µl of the purified 830 bp band as template, at an annealing temperature of 60°C and at an  $Mg^{2+}$  concentration of 1.5 mM. Thirty cycles were performed, melting at 94°C (1 minute), annealing at 55°C (1 minute 30 seconds) and extending at 72°C (2 minutes). One reaction contained 50 pmoles of the N-terminal primer and 1 pmole of the consensus primer (to produce an excess of the sense strand), while a second reaction contained 50 pmoles of the consensus primer and 1 pmole of the N-terminal primer (to produce an excess of the anti-sense strand).

The single-stranded DNA produced by both of these reactions was sequenced.

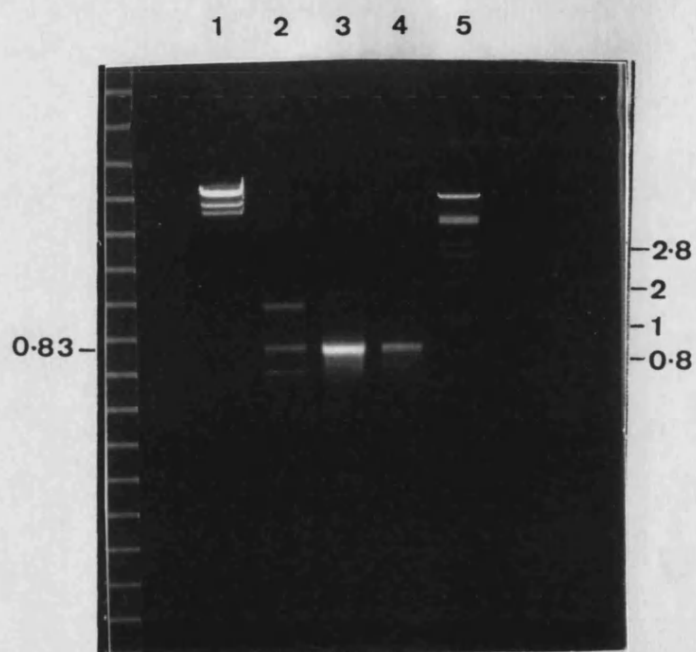


**Figure 6.6 PCR amplification of 830 bp band using 29 base N-terminal and 26 base consensus primers**

Lane 1:  $\lambda$  *HindIII*

Lane 2: Amplification from genomic DNA, 1.5 mM  $Mg^{2+}$ , annealing 55°C

Lane 3: Re-amplification of 830 bp band, 1.5 mM  $Mg^{2+}$ , annealing 60°C

Lane 4: Re-amplification of 830 bp band, 1.5 mM  $Mg^{2+}$ , annealing 65°C

Lane 5:  $\lambda$  *PstI*

#### **6.2.4 Sequencing of asymmetric PCR products**

Sequencing was carried out by the dideoxy method described in Section 2.3.16, omitting the denaturation step. The sense strand was sequenced with 1 pmole of the consensus primer, and the anti-sense strand with 1 pmole of the N-terminal primer. The Sequenase label mix was diluted 10 fold and 2 minute extension times were used in order to sequence close to the primers.

The sequence obtained by extension from the N-terminal primer was translated in three reading frames, while the sequence obtained by extension from the consensus primer was reversed and complemented (to read the sense strand) and then translated in three reading frames (Figure 6.7). No translated sequence showed any homology with any previously determined citrate synthase sequence, confirming this product to be an artefact. Both sequences were then translated in all reading frames and used to search the GenBank sequence database via the FASTA program from the GCG program package. No significant identity with any sequence in the database was observed.

#### **6.3 PCR amplification of a 960 bp sequence from genomic DNA using determined N-terminal and C-terminal amino acid sequences for primer design**

Once the internal citrate synthase protein sequence described in Chapter Five became available, improved PCR reactions were undertaken, using these data.

**Sequence of 830 bp PCR product obtained with N-terminal primer:**

```
S T L * E V S R I S R P R F R R A P S G E
R R C K R C R E S L D R D F A A L H Q A N
D A V R G V E N L S T A I S P R S I R R M
TCGACGCTGTAAGAGGTGTCGAGAATCTCTCGACCGGATTTCGCCGCGCTCCATCAGGCGAA
      10      20      30      40      50      60
AGCTGCGACATTCTCCACAGCTCTTAGAGAGCTGGCGCTAAAGCGGCGGAGGTAGTCCGCTT
R R Q L L H R S D R S R S K A A S W * A F
S A T L P T S F R E V A I E G R E M L R I
V S Y S T D L I E R G R N R R A G D P S H
```

**Sequence of 830 bp PCR product obtained with consensus primer:**

```
A E Q P R I P A R T A * R Q K L F Y P C
L N S P A F R R E P L D D R N Y F T R A
* T A P H S G A N R L T T E T I L P V P
GCTGAACAGCCCCGATTCCGGCGCGAACCGCTTGACGACAGAACTATTTTACCCGTGC
      10      20      30      40      50      60
CGACTTGTCGGGGCGTAAGGCCGCGCTTGCGAACTGCTGTCTTTGATAAAATGGGCACG
S F L G A N R R S G S S S L F * K V R A
Q V A G C E P A F R K V V S V I K G T G
S C G R M G A R V A Q R C F S N * G H R

R L D V R S Y Q T N H G D Y R H L S D E
D * M * G R T K Q I M E I T D I S A T K
I R C E V V P N K S W R L Q T S Q R R K
CGATTAGATGTGAGGTCGTACCAAACAAATCATGGAGATTACAGACATCTCAGCGACGAA
      70      80      90      100      110      120
GCTAATCTACACTCCAGCATGGTTTGTGTTAGTACCTCTAATGTCTGTAGAGTCGCTGCTT
S * I H P R V L C I M S I V S M E A V F
I L H S T T G F L D H L N C V D * R R F
N S T L D Y W V F * P S * L C R L S S F

N Q Q R V V G R V H R V P A R H
I S N E S W G E F I E F P L V T
S A T S R G A S S S S S R S S P
AATCAGCAACGAGTCGTGGGGCGAGTTCATCGAGTTCCCGCTCGTCACCA
      130      140      150      160
TTAGTCGTTGCTCAGCACCCCGCTCAAGTAGCTCAAGGGCGAGCAGTGGT
I L L S D H P S N M S N G S T V
D A V L R P A L E D L E R E D G
* C R T T P R T * R T G A R * W
```

**Figure 6.7 Sequences of each end of the 830 bp PCR fragment**

Single-stranded DNA was produced by asymmetric PCR and sequenced with the same primers as were used for the amplification.

### **6.3.1 Primer design**

The sense primer used was the non-degenerate 29 base oligonucleotide made to the citrate synthase N-terminal amino acid sequence (described in Figure 4.16).

The anti-sense primer was designed from the amino acid sequence of the cyanogen bromide cleavage fragment described in Section 5.5.2, with reference to the codon-usage data in Figure 4.1. Its sequence is shown in Figure 6.8.

The expected length of the PCR product was approximately 980 bp.

### **6.3.2 PCR amplification with N-terminal and C-terminal primers**

PCR reactions were carried out using 80 ng genomic DNA as template, 0.4  $\mu$ M primers and 50  $\mu$ M dNTPs. Thirty cycles were performed, melting at 94°C. Sequence of 830 bp PCR product obtained with N-terminal primer: (1 minute), annealing at 55°C (1 minute 30 seconds) and extending at 72°C (2 minutes). The magnesium concentration in the reactions was varied from 0.5 to 5 mM. Figure 6.9a shows examples of the PCR products, separated by electrophoresis on a 1% agarose gel. Control reactions performed at the same time indicate that at 55°C (and 20 mM  $Mg^{2+}$ ) the N-terminal primer binds at more than one position, causing products to be formed when it is the sole primer present. These products were larger than the desired fragments and while undesirable, did not interfere with their detection at this point (Figure 6.9b). At an annealing temperature of 55°C and a  $Mg^{2+}$  concentration of 5 mM, a product of 960 bp is formed. This product was of the expected size, although the amplification was not very specific.

	I	P	I	D	L	Y	T	P	I	F	A	V	S	R	A	G
	ATA	CCA	ATA	GAC	CTA	TAC	AAA	CCA	ATA	TTC	GCA	GTA	TCA	CGA	GCA	GGA
	C	G	C	T	G	T	G	G	C	T	G	G	G	G	G	G
	T	C	T		C		C	C	T		C	C	C	C	C	C
		T			T		T	T			T	T	T	T	T	T
					TTA								AGC			
					G								T			
Sense	ATC	CCG	ATC	GAC	CTC	TAC	ACG	CCC	ATC	TTC	GC					
Oligo	<b>TAG</b>	<b>GGC</b>	<b>TAG</b>	<b>CTG</b>	<b>GAG</b>	<b>ATG</b>	<b>TGC</b>	<b>GGG</b>	<b>TAG</b>	<b>AAG</b>	<b>CG</b>	<b>-5'</b>				
		G														

**Figure 6.8 Sequence of anti-sense PCR primer designed from amino acid sequence**

The amino acid sequence and potential codons are shown. The primer sequence is in **bold** and includes the degeneracy shown.



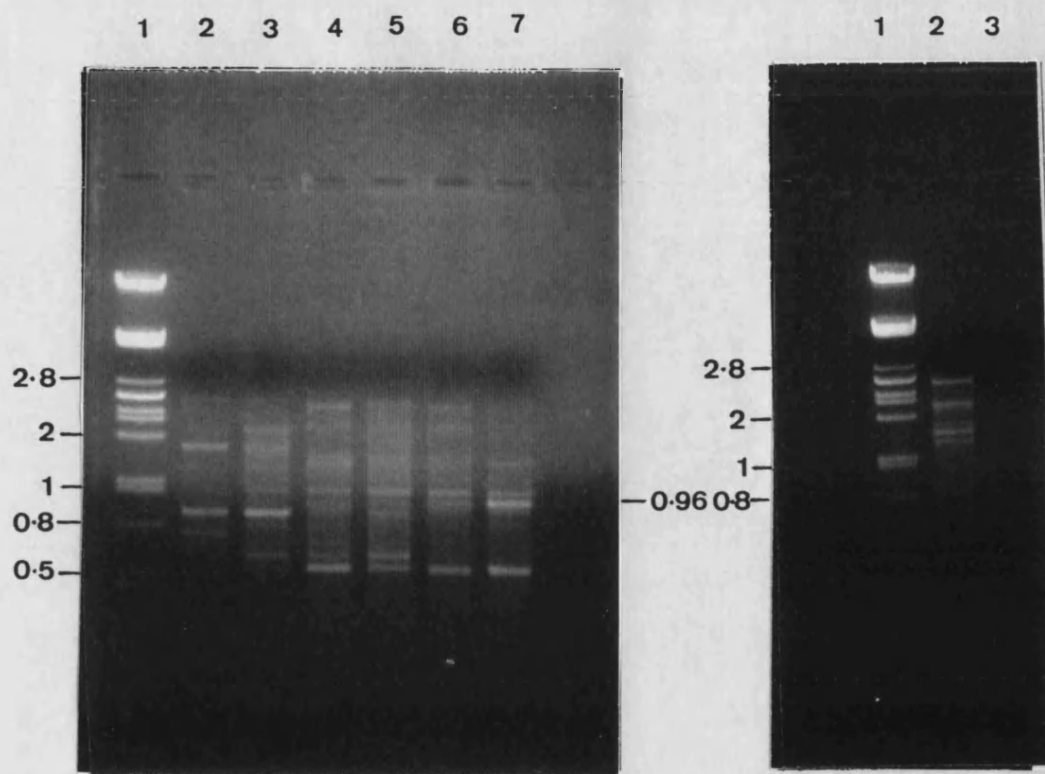


**Figure 6.9a,b PCR amplification 960 bp band using N-terminal and C-terminal primers**

a. Lane 1:  $\lambda$  *Pst*I  
 Lane 2: 0.5 mM  $Mg^{2+}$   
 Lane 3: 1.0 mM  $Mg^{2+}$   
 Lane 4: 1.5 mM  $Mg^{2+}$   
 Lane 5: 2.0 mM  $Mg^{2+}$   
 Lane 6: 3.0 mM  $Mg^{2+}$   
 Lane 7: 5.0 mM  $Mg^{2+}$

b. Lane 1:  $\lambda$  *Pst*I  
 Lane 2: 2 mM  $Mg^{2+}$ , N-terminal primer control  
 Lane 3: 2 mM  $Mg^{2+}$ , C-terminal primer control

As many PCR products were formed, the annealing temperature was raised to 60°C to reduce the level of non-specific primer binding. The result in Figure 6.10 demonstrates an improvement in the N-terminal primer control as products are no longer formed by this primer alone. The only product whose yield was improved by the higher annealing temperature is an 860 bp fragment evident in the 0.5-1.5 mM Mg<sup>2+</sup> lanes. This is approximately 120 bp (corresponding to 40 residues) shorter than would be expected and unlikely to contain the desired sequence. This product was purified and re-amplified by asymmetric PCR as described in 6.2.3, in order to confirm this assertion; however, under these conditions the yield of single-stranded DNA was too low to permit sequencing.

The 960 bp product amplified at an annealing temperature of 55°C and 5 mM Mg<sup>2+</sup> was investigated further. A 10 µl aliquot of a 100 µl PCR reaction (5 mM Mg<sup>2+</sup>) was run on a 1% agarose gel, the 960 bp DNA band excised, purified using GeneClean and dissolved in 50 µl sterile Milli Q water. This product was re-amplified over a range of Mg<sup>2+</sup> concentrations, annealing at 60°C, using 0.5 µl as template (Figure 6.11).

Asymmetric PCR was also carried out under the conditions described in 6.2.3 to confirm the presence of citrate synthase sequence. The yield of single-stranded DNA was too low to allow direct sequencing by this method.

## 6.4 Discussion

The current state of this project is that a 960 bp DNA fragment has been amplified from genomic DNA. Due to time constraints I was unable to confirm that this product contains a citrate synthase gene sequence. This is currently being undertaken by our research group by a route involving blunt-ended

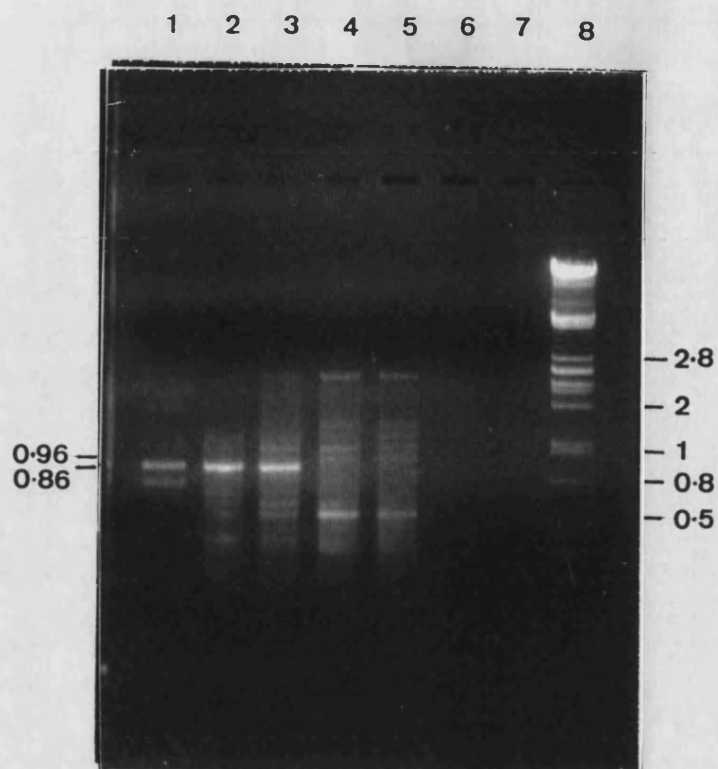


**Figure 6.10 PCR amplification 960 bp band using N-terminal and C-terminal primers, annealing at 60°C**

- Lane 1: 1.0 mM Mg<sup>2+</sup>
- Lane 2: 1.5 mM Mg<sup>2+</sup>
- Lane 3: 2.0 mM Mg<sup>2+</sup>
- Lane 4: 3.0 mM Mg<sup>2+</sup>
- Lane 5: 5.0 mM Mg<sup>2+</sup>
- Lane 6: 2.0 mM Mg<sup>2+</sup>, N-terminal primer control
- Lane 7: 2.0 mM Mg<sup>2+</sup>, C-terminal primer control
- Lane 8:  $\lambda$  *Pst*I

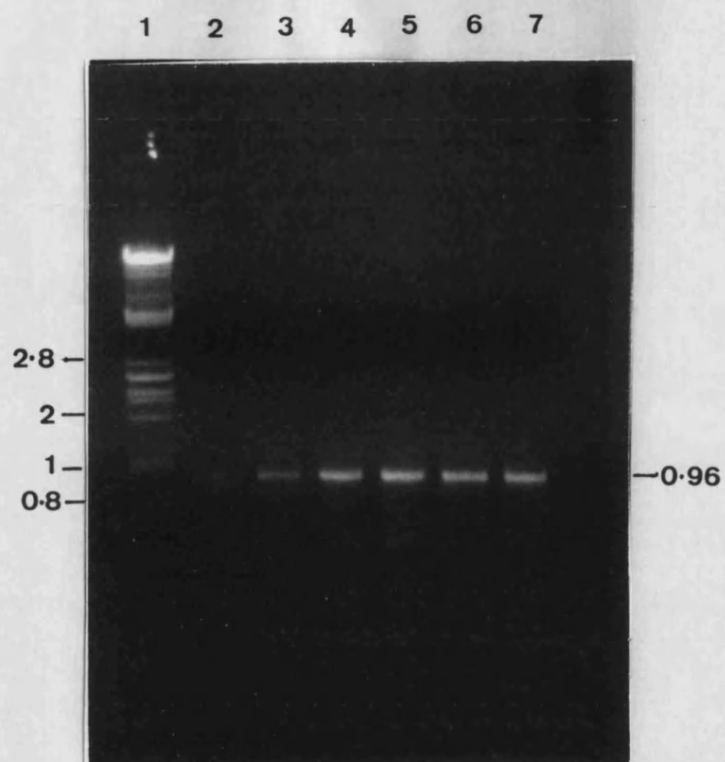


**Figure 6.11 PCR amplification 960 bp band using N-terminal and C-terminal primers, annealing at 60°C**

Lane 1:  $\lambda$  *Pst*I

Lane 2: 0.5 mM  $Mg^{2+}$

Lane 3: 1.0 mM  $Mg^{2+}$

Lane 4: 1.5 mM  $Mg^{2+}$

Lane 5: 2.0 mM  $Mg^{2+}$

Lane 6: 3.0 mM  $Mg^{2+}$

Lane 7: 5.0 mM  $Mg^{2+}$

cloning of the re-amplified product into a pUC vector. This will allow normal double-stranded DNA sequencing methods to be used. The 860 bp PCR product is shorter than one would expect for a section of a citrate synthase gene amplified between the N-terminal and C-terminal primers. The expected length of a product is some 120 bp greater, corresponding to about 40 amino acids in the protein. This difference is too small to dismiss this product as an artefact and should therefore be sequenced and retained or discarded on the basis of sequence data.

Once a gene sequence is obtained, perfectly matched oligonucleotide probes will be synthesised and used to probe restriction digested genomic DNA on Southern blots. By making probes close to both the N-terminal and C-terminal ends of the gene, a restriction fragment that has a high probability of containing the entire gene and flanking regions can be identified. Such a fragment would be at least 2 kb in length and hybridise to both probes.

## **Analysis of 939 bp open reading frame within the 2.9 kb *Pst*I / *Eco*RI clone**

### **7.1 Introduction**

Chapter Four describes the screening of genomic DNA restriction fragments with a 44 base oligonucleotide probe designed from the N-terminal sequence of *Hf.volcanii* citrate synthase. A 2.9 kb *Pst*I / *Eco*RI fragment was isolated and cloned using this probe. Sequence analysis of this clone revealed that it did not contain the citrate synthase gene, although a FASTA search (GCG program package) of the Swissprot protein database with the translated DNA sequence revealed a putative open reading frame of an unrelated gene. This chapter describes the sequencing and analysis of the 939 bp open reading frame.

### **7.2 Sequence analysis**

Sequencing was carried out as described in Chapter Four using the protocols given in Section 2.3.16. As the full characterisation and expression of this gene was outside the scope of this project, the sequence was determined in a single direction only. Figure 7.1 shows the position of the gene within the 2.9 kb insert and indicates the regions sequenced.

The gene sequence and corresponding amino acid sequence are given in Figure 7.2.

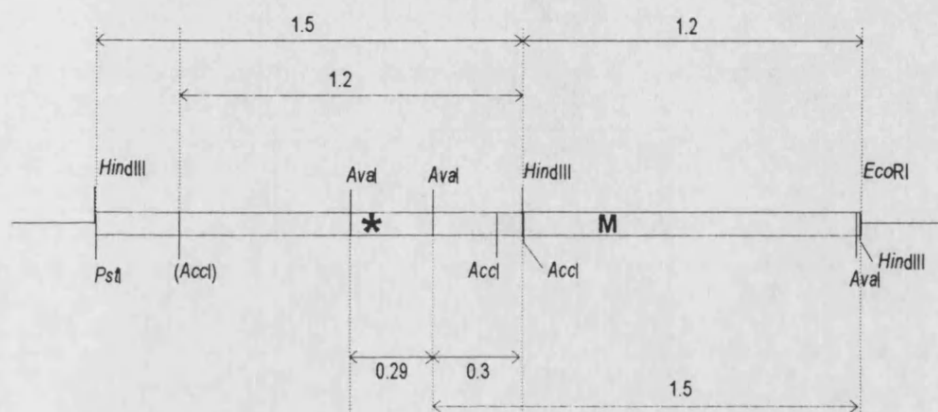


**Figure 7.1** Position of the open reading frame within the 2.9 kb *Pst*I / *Eco*RI clone

The positions of the start codon (M) and stop codon (\*) are indicated. The open reading frame is on the reverse strand.

```

CGGATTCCGTACGACTGGAACGCGGAAATCCACGGCTAAACAGCAACCTGCCAGCAGGGC
1  -----+-----+-----+-----+-----+-----+ 60
GCCTAAGGCATGCTGACCTTGCGCCTTTAGGTGCCGATTTGTCGTTGGACGGTCGTCCCG

Box B?                               Box A?
ACAAACTTATTTAGTACCGTGTGTCAGGTATCGTCTCATATCGATGAAAGGCGTACTTCTCT
61  -----+-----+-----+-----+-----+-----+ 120
TGTTTGAATAAATCATGGCACAGTCCATAGCAGAGTATAGCTACTTTCCGCATGAAGAGA

M K G V L L S -

CAGGAGGCACGGGCTCCCGTCTCCGACCCATTACCCACACCGGGCCGAAGCAACTCGTTC
121 -----+-----+-----+-----+-----+-----+ 180
GTCTCCGTGCCCGAGGGCAGAGGCTGGGTAATGGGTGTGGCCCGGCTTCGTTGAGCAAG

G G T G S R L R P I T H T G P K Q L V P -

CGGTCGCGAATAAACCCGTCTCGAATACGCGGTGAGGACCTCAAAGAAGCGGGAATCA
181 -----+-----+-----+-----+-----+-----+ 240
GCCAGCGCTTATTTGGGCAGGAGCTTATGCGCCAGCTCCTGGAGTTTCTTCGCCCTTAGT

V A N K P V L E Y A V E D L K E A G I T -

CCGAAATCGGCGTCATTCTCGGCCACAAGGGCCGCGAGGAGATTGAGAACCTCCTCGGCG
241 -----+-----+-----+-----+-----+-----+ 300
GGCTTTAGCCGAGTAAGAGCCGGTGTTCCCGGCGCTCCTCTAAGTCTTGAGGAGCCGC

E I G V I L G H K G R E E I Q N L L G D -

ATGGTTCGGACTACGGCGTCGAGATTACCTACATCGTCCAAGGGAACCCCTCGGCCTCG
301 -----+-----+-----+-----+-----+-----+ 360
TACCAAGCCTGATGCCGCAGCTCTAATGGATGTAGCAGGTTCCCTTGGGGGAGCCGGAGC

G S D Y G V E I T Y I V Q G N P L G L A -

CCCACGCGGCGGGCTGTGCGAAGGACTTCGTGCGGCGACGACGACTTCGTGATGTACCTCG
361 -----+-----+-----+-----+-----+-----+ 420
GGGTGCGCCGCCGACACGCTTCCTGAAGCAGCCGCTGCTGCTGAAGCACTACATGGAGC

H A A G C A K D F V G D D D F V M Y L G -

GAGATAACATCCTCAAAGAGGGCGTCGTGACCTCGTCGAAAGCTTCGAGTCGGGCGACT
421 -----+-----+-----+-----+-----+-----+ 480
CTCTATTGTAGGAGTTTCTCCCGCAGCAGCTGGAGCAGCTTTTGAAGCTCAGCCCGCTGA

D N I L K E G V V D L V E S F E S G D F -

TCGGTGCGGGCATCGCCCTACAGGAAGTCGAGAACCCACAGCAGTTCGGGATTGCGGACG
481 -----+-----+-----+-----+-----+-----+ 540
AGCCACGCCCCGTAGCGGGATGTCCTTCAGCTCTTGGGTGTCGTCGAAGCCCTAACGCCTGC

G A G I A L Q E V E N P Q Q F G I A D V -

```

**Figure 7.2 Sequence of open reading frame and corresponding amino acid sequence**

The start codon is shown in bold. Putative promotor regions (Box A and B) are underlined.



```

TCGACGACCAGGGTAACGTACCCCAACTCATCGAGAAGCCGGACGAGCCGCCGACGAATC
541 -----+-----+-----+-----+-----+-----+ 600
AGCTGCTGGTCCCATTGCAGTGGGTTGAGTAGCTCTTCGGCCTGCTCGGCGGCTGCTTAG

  D D Q G N V T Q L I E K P D E P P T N L -

TCGCACTCATCGGGATGTACGTCTTCTCGCCCCGGTCTTCGACGCCATCGAGCAACTCG
601 -----+-----+-----+-----+-----+-----+ 660
AGCGTGAGTAGCCCTACATGCAGAAGAGCGGGCGCCAGAAGCTGCGGTAGCTCGTTGAGC

  A L I G M Y V F S P A V F D A I E Q L E -

AACCTCGTGGCGCGGCGAACTCGAAATCACGGACGCGATTCACTCACTCCTCGAAGACG
661 -----+-----+-----+-----+-----+-----+ 720
TTGGGAGCACCGCGCCGCTTGAGCTTTAGTGCCTGCGCTAAGTCAGTGAGGAGCTTCTGC

  P S W R G E L E I T D A I Q S L L E D G -

GCTACGCCATCGACTCGCACGTCGTGGAAGGCTGGTGGAAAGACACCGGCAAGCCCGAAG
721 -----+-----+-----+-----+-----+-----+ 780
CGATGCGGTAGCTGAGCGTGACGAGCTTCCGACCACCTTTCTGTGGCCGTTCTGGGCTTC

  Y A I D S H V V E G W W K D T G K P E D -

ACATCCTCGAGGCGAACCAACTCGTCCTCGAAGACAAGTCGCTCAAAAAGCGGGGCACCG
781 -----+-----+-----+-----+-----+-----+ 840
TGTAGGAGCTCCGCTTGTTGAGCAGGAGCTTCTGTTTCAGCGAGTTTTTCGCCCCGTGGC

  I L E A N Q L V L E D K S L K K R G T V -

TCAGCGACGATGAGACCGTCGATGGACGTATCGAACTCGCGGAGTCAGCGACCATCGAAG
841 -----+-----+-----+-----+-----+-----+ 900
AGTCGCTGCTACTCTGGCAGCTACCTGCATAGCTTGAGCGCCTCAGTCGCTGGTAGCTTC

  S D D E T V D G R I E L A E S A T I E D -

ACGGCGCAGTCGTCCGTGGCCCGGTCTCTATCGCGGATGGCGCGGTCATCAAATCGGGCA
901 -----+-----+-----+-----+-----+-----+ 960
TGCCGCGTCAGCAGGCACCGGGCCAGAGATAGCGCTACCGCGCCAGTAGTTTAGCCCGT

  G A V V R G P V S I A D G A V I K S G T -

CCTACGTCGGCCCGTACACGTTTCGGTCCGAACTCGACACTCGAAGGCGTCCACATCGAG
961 -----+-----+-----+-----+-----+-----+ 1020
GGATGCAGCCGGGCATGTGCAAAGCCAGGCTTGAGCTGTGAGCTTCCGCAGGTGTAGCTC

  Y V G P Y T F R S E L D T R R R P H R E -

AACTCGGTCGTCATCGGTGAGTCGAGCATCAACACCTCCGGCCGCATCGTTGACAGCCTC
1021 -----+-----+-----+-----+-----+-----+ 1080
TTGAGCCAGCAGTAGCCACTCAGCTCGTAGTTGTGGAGGCCGGCGTAGCAACTGTCGGAG

  L G R H R *

```

**Figure 7.2 Continued**

```

CTCGGGAAGGGTCGCGAACATCGGCAGTGCGGACGACTTCCTCCCGGAGGGTCGTCGCCT
1081 -----+-----+-----+-----+-----+-----+ 1140
GAGCCCTTCCCAGCGCTTGTAGCCGTCACGCCTGCTGAAGGAGGGCCTCCCAGCAGCGGA

CGTCGTTGGCGAGGGCTCCCAACTGAAACTCTAACCATGCACATCATCACCCACGCCTGT
1141 -----+-----+-----+-----+-----+-----+ 1200
GCAGCAACCGCTCCCGAGGGTTGACTTTGAGATTGGTACGTGTAGTAGTGGGTGCGGACA

ACGCAGTGCGGAACCGTCGTCTCCGCGAACGAACTCGAATCGAACCGCGTGATGAAGTGC
1201 -----+-----+-----+-----+-----+-----+ 1260
TGCGTCACGCCTTGGCAGCAGAGGCGCTTGCTTGAGCTTAGCTTGGCGCACTACTTCACG

CCC GGA
1261 ----- 1266
GGGCCT

```

**Figure 7.2 Continued**

### 7.3 Database search results

The Genbank and EMBL databases were searched with the complete translated sequence of the open reading frame. The results of the search are given in Table 7.1 below.

Sequence	Organism	% identity with ORF	GenBank Accession No.	Reference
strD (putative glucose-1-phosphate thymidyltransferase)	<i>Streptomyces griseus</i>	47.1% in 293 aa overlap	Y00459	Distler <i>et al.</i> (1987)
Capsule gene complex UDP-glucose-4-epimerase	<i>Neisseria meningitidis</i>	36.9% in 244 aa overlap	L09188	Hammerschmidt <i>et al.</i> (1992)
Genomic region 84.5 to 86.5	<i>Escherichia coli</i>	36.3% identity in 237 aa overlap	M87049	Daniels <i>et al.</i> (1992)
Genomic region 325 to 333	<i>Bacillus subtilis</i>	40.6% in 244 aa overlap	X73124	Glaser <i>et al.</i> (1993)
rfbG (putative glucose-1-phosphate thymidyltransferase)	<i>Yersinia enterocolitica</i>	33.3% in 273 aa overlap	Z18920	Zhang <i>et al.</i> (1993)
rfbB (dTDP-glucose 4,6-dehydratase)	<i>Shigella flexneri</i>	36.9% in 236 aa overlap	L14842	Rajakumar <i>et al.</i> (1994)
rfbC or rfbD (dTDP-6-deoxy-D-glucose-3,5 epimerase OR dTDP-6-deoxy-L-mannose dehydrogenase)	<i>Salmonella typhimurium</i>	36.9% in 236 aa overlap	X56793	Jiang <i>et al.</i> (1991)
rfbA (glucose-1-phosphate thymidyltransferase)	<i>Salmonella enterica</i>	36.9% in 236 aa overlap	X60665	Wang <i>et al.</i> (1992)
rfbA (glucose-1-phosphate thymidyltransferase)	<i>Azorhizobium caulinodans</i>	40.4% in 208 aa overlap	Z22611	Goethals <i>et al.</i> (1993)
rfbA (putative glucose-1-phosphate thymidyltransferase)	<i>Xanthomonas campestris</i>	38.6% in 236 aa overlap	L23941	Koeplin <i>et al.</i> (1993)

	1					50
<i>Hf.volcanii</i> ORF	.....	.....	.....	.....	mKgvLsGGt	
<i>S.griseus</i>	.....	.....	.....	.....	mKalvLaGGt	
<i>E.coli</i>	.....	.....	.....	.....	mKgimLaGGs	
<i>N.meningitidis</i>	vakcierqls	fgtfrywkiv	frrhpdamps	enpsqrkke	mKgiiLaGGs	
<i>B.subtilis</i>	.....	.....	.....	.....	vKgvLaGGn	
Consensus	-----	-----	-----	-----	-K---L-GG-	
	51					100
<i>Hf.volcanii</i> ORF	GsRLrPiTh	gpKqLvPVan	kPvleYaved	lkeAGItEIg	vIlghkgree	
<i>S.griseus</i>	GtRLrPiTh	saKqLvPVan	kPvlfYglea	iraAGIiDVg	iVvgdta.de	
<i>E.coli</i>	GtRLhPiTrg	vsKqLlPIyd	kPmiYpIsv	lmlAGIrEIl	iIttpekdgy	
<i>N.meningitidis</i>	GtRLyPiTrg	vsKqLlPVyd	kPmiYpIsv	lmlAGIrDIl	vItapednas	
<i>B.subtilis</i>	GsRLmPlTka	vnKhLlPVgp	yPmiYwsimk	lqeAGIkDIl	lIsqkehmpq	
Consensus	G-RL-P-T--	--K-L-PV--	-P---Y----	---AGI-DI-	-I-----	
	101					150
<i>Hf.volcanii</i> ORF	iqnllGdgds	YGveitYivQ	gnplGlahaa	gcakdFvgdD	dfvMyLGDNi	
<i>S.griseus</i>	ivaavGdgSr	FGlkvsYipQ	skplGlahcv	lisrdFlgeD	dfiMyLGDnf	
<i>E.coli</i>	fqrllGdvge	FGiqleYaeQ	pspdGlaqaf	iigetFlngE	pscLvLGDNi	
<i>N.meningitidis</i>	fkrllGdgds	LGisisYavQ	pspdGlaqaf	iigeeFignD	nvcLvLGDNi	
<i>B.subtilis</i>	fykllGngee	LGvtitYqvQ	paasGisdgl	syakrFtkkE	sfiLlLGDNi	
Consensus	-----G----	-G---Y--Q	----G-----	-----F---D	---L-LGDN-	
	151					200
<i>Hf.volcanii</i> ORF	lke.gv.vlv	esfesgdfiga	gialqeVenP	qqFGiaDvdD	qg.nvtqliE	
<i>S.griseus</i>	vvg.vvedsv	refraarpda	hlmltrVpeP	rsFGvaElsD	sg.qvlgLE	
<i>E.coli</i>	ffgqgfspkl	rhvaartegp	.vfgyqVmdP	erFGxvEfdD	.nfraisleE	
<i>N.meningitidis</i>	fygqsftqtl	kqaarqthga	tvfayqVknP	erFGvvEfnE	.nfravsieE	
<i>B.subtilis</i>	f.edslkpyt	erfeqqgkga	kvllkeVddP	erFGiaEide	knkrirsiiE	
Consensus	-----	-----	-----V--P	--FG--E--D	-----E	
	201					250
<i>Hf.volcanii</i> ORF	KPdePptnla	liGmYvFspa	vfdaieqleP	SwRGELEITd	aiqslleDgy	
<i>S.griseus</i>	KPahPkSdla	lvGvYlFspa	iheavaaitP	SwRGELEITd	avqwliDagr	
<i>E.coli</i>	KPkqPkSdna	vtGlyfYdsk	vveyakqvKp	SeRGELEITs	inqmyLEagn	
<i>N.meningitidis</i>	KPqrPkSdwa	vtGlyfYdnr	avefakqikP	SaRGELEITd	lnrmyLEdgs	
<i>B.subtilis</i>	KPeqPptnlc	vtGiYmYdae	vfsyieqisP	SkRGELEITd	vnnlyiEnsQ	
Consensus	KP--P-----	--G-Y-Y---	-----P	S-RGELEIT-	-----E---	
	251					300
<i>Hf.volcanii</i> ORF	aidshvveGW	.WkDtGkped	ileanqLVle	dkslkkrgrtv	sddetvdgri	
<i>S.griseus</i>	dvrstvisGY	.WkDtGnvtd	mlevnrLVle	tteprcdglv	dersdligrv	
<i>E.coli</i>	ltvellgrGF	aWlDtGthds	lieastFV.q	tvekrqgfki	acleeiawrn	
<i>N.meningitidis</i>	lsvqilgrGF	aWlDtGthes	lheaasFV.q	tvqniqdlqi	acleeiawrn	
<i>B.subtilis</i>	ltydvls.GW	.WvDaGthes	lylasqLVhq	alrkqgdek*	.....	
Consensus	-----G-	-W-D-G---	-----LV--	-----	-----	

**Figure 7.3 Alignment of the *Hf.volcanii* open reading frame (ORF) with the four sequences of highest identity from the database search**

The uppercase letters denote conserved or conservatively replaced residues. The alignment was produced using PILEUP. Refer to Table 7.1 for the functions of these genes.

	301				350
<i>Hf.volcanii</i> ORF	elaesatied	gavvrgpvs	adgaviksgt	yvgpytfrse	.....
<i>S.griseus</i>	lveegaevrn	srvmgptvig	agtrvtns..	yvgpftslae	dcvvedseve
<i>E.coli</i>	gwlddegvkr	aasslaktgy	gqyllellra	rprqy*....	.....
<i>N.meningitidis</i>	gwlekkdvet	rakplektay	gqyllhligk	*.....	.....
<i>B.subtilis</i>	.....	.....	.....	.....	.....
Consensus	-----	-----	-----	-----	-----
	351				400
<i>Hf.volcanii</i> ORF	.....	ldtrrrphre	lgrhr*....	.....	.....
<i>S.griseus</i>	fsivlrgasi	sgvrrieasl	igrhqvtsa	pevphanrlv	lgdhsraqis
<i>E.coli</i>	.....	.....	.....	.....	.....
<i>N.meningitidis</i>	.....	.....	.....	.....	.....
<i>B.subtilis</i>	.....	.....	.....	.....	.....
Consensus	-----	-----	-----	-----	-----
	401				
<i>Hf.volcanii</i> ORF	..				
<i>S.griseus</i>	s*				
<i>E.coli</i>	..				
<i>N.meningitidis</i>	..				
<i>B.subtilis</i>	..				
Consensus	--				

**Figure 7.3 Continued**

13%. This is consistent with the theory that halophilic proteins contain acidic residues that stabilise them under high salt conditions, as described in Section 1.6.

Of the sequences given in Table 7.1, two are of unknown function (*B.subtilis* genomic region 325-333 and *E.coli* genomic 84.5-86.5), one is a UDP-glucose-4-epimerase, one a dTDP-glucose 4,6-dehydratase and one either a dTDP-6-deoxy-D-glucose-3,5 epimerase or a dTDP-6-deoxy-L-mannose dehydrogenase. The remainder are putative (*S.griseus*, *Y.enterocolitica* and *X.campestris*) or confirmed (*S.enterica*) glucose-1-phosphate thymidyltransferases.

The *S.griseus* glucose-1-phosphate thymidyltransferase is proposed to be involved early in the biosynthetic pathway of streptomycin (Distler *et al*, 1987, Distler *et al.*, 1992). With the exception of the *S.flexneri* dTDP-glucose 4,6-dehydratase, roles have been proposed for all of the other activities in the biosynthesis of lipopolysaccharides. In *Y.enterocolitica* and the *Salmonella* species the lipopolysaccharide in question is a surface antigen, while the *A.caulinodans* gene is part of a lipopolysaccharide operon involved in nodule formation.

The *Hf.volcanii* open reading frame may code for an enzyme that has glucose-1-phosphate thymidyl or uridylyl transferase activity, activating a carbohydrate moiety by nucleotidylation prior to its polymerisation into a polysaccharide. Alternatively the gene product may accept a nucleotidylated sugar as a substrate and act as an epimerase or dehydratase.

If the *Hf.volcanii* open reading frame codes for a sugar-activating enzyme, it is likely to have a fundamental role in polysaccharide biosynthesis. It has been proposed that nucleotide-activated sugars (UDP-glucose, UDP-mannose and UDP-galactose) are added to an unidentified glycolipid precursor during the biosynthesis of glycolipids in *Hf.volcanii*



(Kates, 1994). The biosynthesis of the *Hf.volcanii* S-layer glycoprotein also utilises nucleotide-activated sugars (Kandler & Konig, 1994).

Further study of this open reading frame requires confirmation of its sequence by sequencing both strands, followed by characterisation of the activity of the protein which it encodes. This could be approached by PCR amplification of the gene using primers containing restriction sites which would allow it to be cloned into an *E.coli* expression vector. The gene could then be expressed in *E.coli* under the control of a powerful, inducible promoter (such as *tac*) and the enzyme activated by addition of salt. If the expressed protein is found to be insoluble, solubility may be improved by growing the transformed *E.coli* at 30-32°C. Activation of the enzyme may not be achieved by the simple addition of KCl to a cell extract. It may be necessary to partially unfold the expressed enzyme and allow it to refold into an active conformation by addition of guanidine hydrochloride followed by dialysis against a high KCl buffer, or by heating the inactive enzyme in a high KCl buffer and allowing it to cool.

The development of an assay to determine the activity of the expressed enzyme should be undertaken with care as the enzyme may be inactive due to incorrect folding. Adding 2 M KCl to a cell extract (produced by sonication) acts as an initial purification as many *E.coli* proteins are precipitated under these conditions. A subsequent dialysis step would then remove nucleotide triphosphates and nucleotidylated sugars which could interfere with assays.

Simple spectrophotometric assays for glucose-1-phosphate thymidyltransferase rely on addition of pyrophosphate and dTDP-glucose as substrates, catalysing the formation of glucose-1-phosphate, which is in turn converted to glucose-6-phosphate by phosphoglucomutase (in the presence of its activator, glucose-1,6-bisphosphate) which is coupled to glucose-6-phosphate dehydrogenase and the reduction of NAD is followed

spectrophotometrically (Kornfeld & Glaser, 1961). This type of coupled assay is unsuitable for use with a halophilic enzyme. An alternative system has been developed using HPLC analysis of aliquots taken from a reaction between glucose-1-phosphate and dTTP, forming dTDP-glucose and pyrophosphate (Lindquist *et al.*, 1993). This method is also unsuitable as it relies on a non-halophilic pyrophosphatase to affect the equilibrium of the reaction.

A possible method for a halophilic enzyme would be to incubate the cell extract (prepared as described above) with a radiolabelled sugar-phosphate and dTDP or UDP, stop the reaction and purify the nucleotide diphosphate sugar by adsorption to charcoal, eluting with a solution of ammonia in ethanol/water (Okazaki *et al.*, 1961). The incorporation of radiolabel could be measured for a variety of different combinations of sugar-phosphates and dTDP or UDP, to determine the preferred substrate.

An epimerase activity may be detected by incubation of the enzyme with a potential substrate, followed by purification of the substrate-product mixture by adsorption as above. Analysis by HPLC of aliquots taken at various time points during the incubation would reveal any reaction that had taken place.



## Conclusions and suggested further work

The strategy of purifying a protein, determining its N-terminal amino acid sequence and using a corresponding synthetic oligonucleotide probe to screen for its gene is well established. In our laboratory this route has been successfully taken in cloning the citrate synthase gene (Sutherland *et al.*, 1990) and the glucose dehydrogenase gene (Bright *et al.*, 1991) from the Archaeon *Thermoplasma acidophilum*. In each case both long, unique probes and short, degenerate probes were used, the citrate synthase gene being identified using the former type of probe and the glucose dehydrogenase with the latter. Both of these approaches to the design of probes were therefore considered appropriate for this project.

Short, degenerate probes designed to *Hf.volcanii* citrate synthase amino acid sequence were found to lack the required specificity when hybridising to genomic DNA. Longer, unique probes appear to offer a greater chance of success in following up this work. The marked preference for certain codons in the *Hf.volcanii* genome makes their design easier.

Trieselmann and Charlebois (1992) have shown by cDNA hybridisation to genomic DNA that regions of the relatively A-T rich FII DNA of the *Hf.volcanii* genome are transcriptionally active. There may be protein coding genes within these areas whose codon preference differs from that described in Figure 4.1. Probes designed using codon preference data from G-C rich regions would be less likely to hybridise to such genes. This may be relevant to our search for the citrate

synthase gene. A comprehensive survey of codon preference in halophilic Archaea has recently been carried out (Soppa, 1993). The majority of the genes surveyed possessed the same G-C biased codon preference, including those used to compile Figure 4.1. To date, only the gas vacuole genes of the *Halobacteria* are known to have a significantly different (relatively A-T) rich codon preference. On balance it still appears valid to have designed the probes to the G-C rich codon preference.

The next step to be taken with this project should be the cloning and sequencing of the 960 bp PCR product described in Section 6.3.2. A pair of 20-30 base oligonucleotides designed to match the ends of a correctly amplified product could be used to probe restriction-digested genomic DNA. A fragment of 2 to 3 kb to which both probes bound would be highly likely to contain the entire gene. Should both of the PCR products described in Section 6.3.2 prove to be artefacts, the 29 base PCR primer designed from the amino acid sequence at the C-terminal end of the protein has the potential to be used as a probe.

At the outset of this project it was our intention eventually to express the *Hf.volcanii* citrate synthase in *E.coli*, prepare crude cell extracts by sonication and use the addition of salt to both activate the *Hf.volcanii* enzyme and concomitantly to precipitate many of the contaminating *E.coli* proteins. Cendrin *et al.* (1993) have since demonstrated that it is possible to achieve high level expression of a halophilic malate dehydrogenase in a soluble form in *E.coli*. The enzyme was fully activated by the addition of NaCl to a concentration of 3 M. The *Hf. volcanii* dihydrofolate reductase has also been expressed in *E.coli*, but in an insoluble form that was activated by denaturing in guanidine hydrochloride, followed by dilution into high salt solutions.

If the *Hf.volcanii* citrate synthase is found to express as an incorrectly folded polypeptide that resists folding upon the addition of either high salt or guanidine, the option of expression in *Hf.volcanii* is still open. *Hf.volcanii* is a fast growing organism that reaches a high density in culture and an effective means of enzyme purification is available in the Red A affinity column. Expression in *Hf.volcanii* has the advantage that the polypeptide is likely to fold correctly, but has the drawback that expression would be from its own promotor rather than the highly efficient, inducible promoters (such as *tac*) available in *E.coli* expression systems.

In order to study the basis of halophilicity by site-directed mutagenesis one needs detailed knowledge of the structure of the enzyme under investigation. A crystal structure has yet to be determined for a halophilic enzyme, so until such time mutagenesis studies must rely upon predicted structural models, such as that for the *Hf.volcanii* dihydrofolate reductase (Bohm & Jaenicke, 1994). The crystal structure of the *Tp.acidophilum* citrate synthase has now been determined (Russell *et al.*, 1993) and may be a useful point from which to start homology modelling the *Hf.volcanii* enzyme once its sequence is known, while crystallisation trials are started. As citrate synthases are composed almost entirely of  $\alpha$ -helices it will be interesting to see if any in the *Hf.volcanii* enzyme have the "halophilic helix motif" (negative charge clusters at the N-terminal end of a helix) observed in the dihydrofolate reductase model.

The sequencing of the *Hf.volcanii* citrate synthase will provide a representative of the halophiles for phylogenetic analysis, a group so far absent from the phylogenetic tree of citrate synthases. The N-terminal amino acid sequence of the *Hf.volcanii* citrate synthase indicates that the enzyme is, like that of *Tp.acidophilum* and

*B.coagulans*, approximately 40 residues shorter than other citrate synthases. Two other *Bacillus* sequences have since been determined (A.L. Sonenshein, Tufts Univ. School of Medicine, Boston, USA, Unpublished), both of which are of the shorter type. This points to a relationship between the citrate synthases of the Archaea and the Gram positive Bacteria. The Gram positive *Mycobacterium smegmatis* also groups with the Archaea and *Bacillus* species on phylogenetic analysis (Taylor, G., Hough, D.W. and Danson, M.J., Unpublished data), although it does not lack the 40 or so N-terminal residues.

It is important in defining phylogenetic relationships between organisms to take a consensus from the phylogenetic relationships between as many of their genes as possible. Not all gene sequences will represent their parent organism in the same fashion as all have developed under slightly different conditions. It may be argued that all genes are valuable phylogenetically; however, our present techniques of analysis lack the sophistication to unlock the information within many sequences. Citrate synthase is a widespread central metabolic enzyme, functionally conserved in all organisms that possess it. It is a valuable addition to the growing range of enzymes whose gene sequences are a source of accessible phylogenetic information.

During the course of this project an open reading frame was identified within a cloned fragment of *Hf.volcanii* genomic DNA. It has been shown in Chapter Seven that this sequence bears significant homology with several enzymes from bacterial sources involved in the metabolism of nucleotide-activated hexose sugars. Such enzymes have been implicated in the biosynthesis of lipopolysaccharides and S-layer glycoproteins in halophilic Archaea. This is a subject area that has not yet been intensively studied at the genetic level and no gene coding for any of these activities has yet been cloned. Chapter Seven described

possible approaches to characterise the function of the *Hf.volcanii* open reading frame.

If this sequence is a gene involved in polysaccharide metabolism it may provide a basis for further investigation into these pathways in the halobacteria, particularly if other genes of related function in the pathway are clustered with this one, as is the case in the *Salmonella* and *Yersinia* species studied to date. The sequencing of such a gene cluster, while a major project, would provide data from which a putative metabolic pathway could be deduced.

## Appendix

### Purification of citrate synthase

Citrate synthase from *Hf.volcanii* was purified in our laboratory by Dr. M.J. Bonete, University of Alicante, Spain using a scheme based on that used to purify the *H.halobium* citrate synthase (James, 1990).

The purification is summarised in the table below.

Step	Protein mg	CS Activity U	Sp. Activity U mg <sup>-1</sup>	Purification	Yield %
Cell-extract	2105	78.3	0.037	1	100
DEAE- Sephadex	350	64.7	0.185	5	83
Hydroxylapatite	53.5	58.5	1.096	30	75
Mono-Q	7.8	37.3	4.78	129	48
Superdex-200	0.53	10.0	18.88	510	13
Superdex-200	0.13	3.4	25.8	697	4

### SDS-polyacrylamide gel electrophoresis and Western blotting

The dried citrate synthase was dissolved in 40 µl Milli Q water. SDS-polyacrylamide gel electrophoresis was carried out on 2 µl aliquots using the Bio-Rad Protean II system. An initial gel was Coomassie stained to locate the protein bands, while subsequent ones were left unstained in order to carry out Western blots. The latter were used to optimise blotting

conditions. Figure 9.1 below shows a 0.5 µl aliquot of the purified citrate synthase run on a small (Mini-Atto system) 8% SDS polyacrylamide gel. Two major protein bands are visible; one of 45 kD and another of approximately 55 kD.

The remaining 30 µl were electrophoresed as above and blotted onto Immobilon P membrane under the optimised conditions. The membranes were stained and both major protein bands (45 kD and 55 kD) were cut out. The bands were sequenced directly from the membrane.

### **N-terminal sequencing**

Both protein bands were sequenced using an Applied Biosystems 470A gas-phase Sequencer coupled to an Applied Biosystems 120 Phenylthiohydantoin analyser.

Sequences were obtained for both 45 kD and 55 kD bands. These are shown below, using single letter amino acid codes where X indicates an unknown residue and residues in parentheses are tentative assignments.

55 kD XXXXVIAAAYRTPFGKAA

45 kD (S)GELKRGLEGVLVAESKLSFIDGDAGQLVYXGYDIEDL

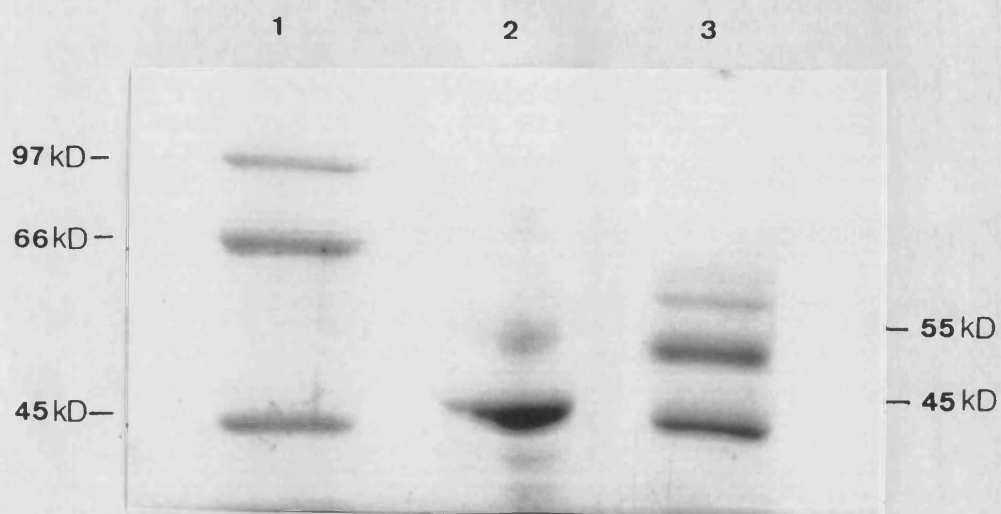


**Figure 9.1 SDS-PAGE of purified *Hf.volcanii* citrate synthase**

Lane 1: Molecular weight markers

Lane 2: Pig heart citrate synthase (4  $\mu$ g)

Lane 3: *Hf.volcanii* citrate synthase ( 0.5  $\mu$ l of 40  $\mu$ l)



Halophilic proteins are often highly acidic and thus bind less of a cationic detergent, such as SDS, than a non-halophilic protein. This results in reduced mobility on SDS gels and consequent over-estimates of protein molecular weight. It was therefore not possible to distinguish which of the two major bands was citrate synthase by migration distance alone. Based on the subunit sizes observed for citrate synthases from other sources, the 45 kD band is closest to the expected size of a citrate synthase monomer; however, the 55 kD band could be citrate synthase migrating slowly for the reasons described above. In the latter case the 45 kD band could either be a proteolytic degradation product of the larger band or a co-purified contaminant. It was therefore necessary to obtain N-terminal sequence for both of the bands.

The sequence of the 45 kD band was initially aligned by hand with a multiple sequence alignment of eight other citrate synthases. The sequences from both bands were used to search the Swissprot (1991) protein database, using the FASTA search program from the GCG program package. Only the 45 kD band showed significant homology with any of the sequences in the database. All of the best scores, with the exception of one, were obtained for matches to the N-termini of citrate synthases. The eight highest identities are shown in Table 9.1.

Sequence	Organism	Swissprot Accession No.	Reference
Citrate synthase	<i>Coxiella burnetii</i>	P18789	Heinzen <i>et al.</i> (1991)
Citrate synthase	<i>Pseudomonas aeruginosa</i>	P14165	Donald & Duckworth (1989)
Citrate synthase	<i>Acinetobacter anitratum</i>	P20902	Donald & Duckworth (1987)
Citrate synthase	<i>Rickettsia prowazekii</i>	P09948	Wood <i>et al.</i> (1987)
Citrate synthase	<i>Acetobacter aceti</i>	P20901	Fukaya <i>et al.</i> (1990)
DNA dependent RNA polymerase	<i>Sulfolobus acidocaldarius</i>	P11513	Puehler <i>et al.</i> (1989)
Citrate synthase	<i>Thermoplasma acidophilum</i>	P21553	Sutherland <i>et al.</i> (1990)
Citrate synthase	<i>Escherichia coli</i>	P00891	Bhayana & Duckworth (1984)

**Table 9.1 Results of Swissprot database search**

Alignments of available citrate synthase sequences show that the enzymes can be divided into two categories based on the presence or absence of a stretch of approximately 40 amino acids at the N-terminus (Muir *et al.*, 1994a). The gene sequences of the *Tp.acidophilum* (Sutherland *et al.*, 1991) and *Bacillus* sp. (Schendel *et al.*, 1992) citrate synthases, which are both of the shorter type, show that the absence of

these residues is not due to proteolytic cleavage, but is coded for at the DNA level.

Figure 9.2 shows the relevant part of a citrate synthase multiple sequence alignment created using the PILEUP program from the GCG package. The alignment was created using the full sequences and includes the *Hf.volcanii* 45 kD band sequence and the recently determined N-terminal sequences from *S.solfataricus* (Lill *et al.*, 1992) and *P.furiosus* (Muir *et al.*, 1994b) citrate synthases. It is evident that the *Hf.volcanii* N-terminal sequence aligns with the shorter N-termini and hence the enzyme belongs to the short category. It is unlikely that this observation is due to proteolytic cleavage of the *Hf.volcanii* N-terminus as the lack of these residues appears to be a feature of archaeal citrate synthases.

	1				50				
Chicken heart	...asstnlk	dvlaalipke	qariktfrqq	hggtalgqit	v.dms.....ygGmrgmkgl	vyetsvldpd	egi.rfrGfs	ipecq	
Pig heart	...asstnlk	diladlipke	qariktfrqq	hgntvvgqit	v.dmm.....ygGmrgmkgl	vyetsvldpd	egi.rfrGys	ipecq	
Yeast (cytoplasm)	...sqektlk	erfseiypih	aqdvrrqfvke	hgktkisdvl	l.eqv.....ygGmrgipgs	vwegsvldpe	dgi.rfrGrt	iadiq	
Yeast (mitoch)	...aseqtlk	erfaeiipak	aqeikkfkke	hgktvigevl	leeqa.....ygGmrgikgl	vwegsvldpe	egi.rfrGrt	ipeiq	
<i>Tetrahymena</i>	....sqtnlk	kviaeiipqk	qaelkevkek	ygdkvvgqyt	v.kqv.....igGmrgmkgl	msdlsrldpy	qgi.ifrGyt	ipqlk	
<i>Mycobacterium</i>	.....apq	qalrtaalrr	lqpvrllrlq	lrraggesmt	tateseaprihkGlagvvvd	ttaiskvpe	tnsltyrGyp	vqd.1	
<i>Bacillus</i>	.....	.....	.....	.....	....vntnqfipGlegvias	etkisfldtv	nseivikGyd	lla.1	
<i>Acinetobacter</i>	....seatgk	kavlhlldgke	.ielpiysgt	lgpdvidvkd	vlas.ghftfdpGfmatasc	eskitfidgd	kgillhrGyp	idq.1	
<i>Pseudomonas</i>	.....adk	kaqliiegsa	pvelpvlsgt	mgpdvvdvrg	ltat.ghftfdpGfmstasc	eskityidgd	kgvllhrGyp	ieq.1	
<i>Escherichia</i>	.....adt	kakltlngdt	aveldvkgt	lgqdvidirt	lgsk.gvftfdpGftstasc	eskitfidgd	egillhrGfp	idq.1	
<i>Acetobacter</i>	sasqkegkls	tatisvdgks	a.empvlsgt	lgpdvidirk	lpaqlgvftfdpGygetaac	nskitfidgd	kgvllhrGyp	iaq.1	
<i>Coxiella</i>	.....snr	kaklsfenqs	.vefpiyspt	lgkdvidvkt	l.gnhgayaldvGfystaac	eskitfidge	kgillyrGyp	idq.1	
<i>Rickettsia</i>	.tngnnnnle	faelkirgk.	lfklpilkas	igkdvidisr	vsaeadyftydpGfmstasc	qstityidgd	kgilwyrGyd	ikd.1	
<i>Thermoplasma</i>	.....	.....	.....	.....	....peteeiskGledvnik	wtrlttidgn	kgilrygGys	vedii	
<i>Haloferax</i>					<b>SGELKRGLEGVLVA</b>	<b>ESKLSFIDGD</b>	<b>AGQLVYAGYD</b>	<b>IED L</b>	
Consensus	-----	-----	-----	-----	-----G-----	-----	-----G--	-----	

**Figure 9.2 Multiple sequence alignment of citrate synthases showing the *Hf.volcanii* N-terminal sequence**

The alignment was created using the PILEUP from the GCG package. The entire citrate synthase sequences were used to create the alignment and the N-terminal sequence was then added by hand.

## References

- Aitken, D.M. & Brown, A.D. (1969) *Biochim. Biophys. Acta* 177, 351-354
- Alter, G.M., Casazza, J.P., Wang, Z., Nemeth, P., Srere, P. & Evans, C.T. (1990) *Biochemistry* 29, 7557-7563
- Baldacci, G., Guinet, F., Tillit, J., Zaccai, G. & de Recondo, A. (1990) *Nucleic Acid Res.* 18 No.3, 507-511
- Beanland, T.J. & Howe, C.J. (1992) *Comp. Biochem. Physiol.* 102B No.4, 643-659
- Benachenhou-Lahfa, N., Forterre, P. & Labedan, B. (1993) *J. Mol. Evol.* 36, 335-346
- Bhayana, V. & Duckworth H.W. (1984) *Biochemistry* 23, 2900-2905
- Bonnete, F., Ebel, C., Zaccai, G. & Eisenberg H. (1993) *J. Chem. Soc. Faraday Trans.* 89 No.15, 2659-2666
- Bohm, G. & Jaenicke, R. (1994) *Protein Eng.* 7, 213-220
- Bradford, M.M. (1976) *Anal. Biochem.* 72, 248-254
- Cendrin, F., Chroboczek, J., Zaccai, G., Eisenberg, H. & Mevarech, M. (1993) *Biochemistry* 32, 4308-4313
- Charlebois, R.L., Hofman, J.D., Schalkwyk, L.C., Lam, W.L. & Doolittle, W.F. (1990) *Can. J. Microbiol.* 35, 21-29
- Charlebois, R.L., Lam, W.L., Cline, S.W. & Doolittle, W.F. (1987) *Proc. Natl. Acad. Sci. USA* 84, 8530-8534
- Charlebois, R.L., Schalkwyk, L.C., Hofman, J.D. & Doolittle, W.F. (1991) *J. Mol. Biol.* 222, 509-524

- Conover, R.K. & Doolittle, W.F. (1990) *J. Bacteriol.* 172, 3244-3249
- Daniels, D.L., Plunkett, G., Burland, V. & Blattner, F.R. (1992) *Science* 257, 771-778
- Danson, M.J. (1988) *Adv. Micro.Physiol.* 29, 165-231
- Danson, M.J., Black, S.C., Woodland, D.L. & Wood, P.A. (1985) *FEBS Lett.* 179, 120-124
- Danson, M.J., McQuattie, A. & Stevenson, K.J. (1986) *Biochemistry* 25, 3880-3884
- David, M., Lubinsky-Mink, S., Ben-Zvi, A., Suissa, M., Ulitzur, S. & Kuhn, J. (1991) *Biochem. J.* 278, 225-234
- Devereux, J., Haeberli, P. & Smithies, O. (1984) *Nuc. Acids Res.* 12, 387-395
- Distler, J., Mansouri, K., Mayer, G., Stockmann, M. & Piepersberg, W. (1992) *Gene* 115, 105-111
- Distler, J., Ebert, A., Mansouri, K., Pissowotski, K., Stockmann, M. & Piepersberg, W. (1987) *Nuc. Acids Res.* 15, 8041-8056
- Donald, L.J., Molgat, G.F. & Duckworth, H.W. (1989) *J. Bacteriol.* 171, 5542-5550
- Donald, L.J. & Duckworth, H.W. (1987) *Biochem. Cell Biol.* 65, 930-938
- Eisenberg, H., Mevarech M. & Zaccari, G. (1992) *Adv. Protein Chem.*, 43, 1-63
- Evans, C.T., Owens, D.D., Sumegi, B., Kispal, G. & Srere, P.A. (1988) *Biochemistry* 27, 4680-4686
- Forterre, P., Benachenhou-Lahfa, N., Confalonieri, M.D., Elie, C. & Labedan, B. (1993) *BioSystems* 28, 15-32

Fukaya, M., Takemura, H., Okumura, H., Kawamura, Y., Horinouchi, S. & Beppu, T. (1990) *J. Bacteriol.* 172, 2096-2104

Glaser, P., Kunst, F., Arnaud, M., Coudart, M.P., Gonzales, W., Hullo, M.F., Ionescu, M., Lubochinsky, B., Marcelino, L., Moszer, I., Presecan, E., Santana, M., Schneider, E., Schweitzer, J., Vertes, A., Rapoport, G. & Danchin, A. (1993) *Mol. Microbiol.* 10, 371-384

Goethals, K.H.M., Leyman, B., Van den Eede, G., Van Montagu, M. (1993) Unpublished.

Gogarten, J.P., Kibak, H., Dittrich, P., Taiz, L., Bowman, E.J., Bowman, B.J., Manolson, M.F., Poole, R.J., Date, T., Oshima, T., Konishi, J., Denda, K. & Yoshida, M. (1989) *Proc. Natl. Acad. Sci. USA* 86, 6661-6665

Gupta, M.N. (1992) *Eur. J. Biochem.* 203, 25-32

Gupta, R., Lanter, J.M. & Woese, C.R. (1983) *Science* 221, 656-659

Hammerschmidt, S., Birkholz, C., Robertson, B.D., van Putten, J., Ebeling, O. & Frosch, M. (1992) Unpublished

Heinzen, R.A., Frazier, M.E. & Mallavia, L.P. (1991) *Gene* 109, 63-69

Henneke, C.M., Danson, M.J., Hough, D.W. & Osguthorpe, D.J. (1989) *Protein Eng.* 2, 597-604

Heinzen, R.A., Frazier, M.E. & Mallavia, L.P. (1991) *Gene* 109, 63-69

Hickson, I (1994) Final year project report, Department of Biochemistry, University of Bath

Higa, H. & Cazzulo, J.J. (1975) *Biochem J.* 147, 267-274

Holmes, M.H., Nuttall, S.D. & Dyall-Smith, M.L. (1991) *J. Bacteriol.* 173, 3807-3813

Holmes, M.L., Dyall-Smith, M.L. (1991) *J. Bacteriol.* 173, 624-648

Iwabe, N., Kuma, K., Hasegawa, M., Osawa, S. & Miyata, T. (1989) *Proc. Natl. Acad. Sci. USA* 86, 9355-9359

James, K.D. (1990) Final Year Project Report No.461, Department of Biochemistry, University of Bath

Jiang, X.M., Neal, B., Santiago, F., Lee S.J., Romana, L.K. & Reeves, P.R. (1991) *Mol. Microbiol.* 5, 695-713

Kandler, O. & König, H. (1994) In *The Biochemistry of the Archaea (Archaeobacteria)*, 223-255. (Kates et al., eds.) Elsevier Science Publishers B.V.

Karpusas, M., Branchaud, B. & Remington, S.J. (1990) *Biochemistry* 29, 2213-2219

Karpusas, M., Holland, D. & Remington, S.J. (1991) *Biochemistry* 30, 6024-6031

Kates, M. (1994) In *The Biochemistry of the Archaea (Archaeobacteria)*, 261-295. (Kates et al., eds.) Elsevier Science Publishers B.V.

Kirchberger, J., Cadelis, F., Kopperschlager, G. & Vijayalakshmi, M.A., Klibanov, A.M. (1989) *Trends Biochem. Sci.* 14, 141-144

Koeplin, R., Wang, Hoette, B., Priefer, U.B. & Puhler, A. (1993) Unpublished.

Kornfeld, S. & Glaser, L. (1961) *J. Biol. Chem.* 236, 1791

Lake, J.A. (1988) *Nature* 331, 184-186

Lake, J.A. (1989) *Can. J. Microbiol.* 35, 109-118



Lam, W.L. & Doolittle, W.F. (1989) *Proc. Natl. Acad. Sci. USA* 86, 5478-5482

Lam, W.L., Cohen, A., Tsoulouhas, D. & Doolittle, W.F. (1990) *Proc. Natl. Acad. Sci. USA*. 87, 6614-6618

Lanyi, J.K. (1974) *Bacteriol. Rev.* 38 No.3, 272-290

Liao, D., Karpusas, M. & Remington S.J. (1991) *Biochemistry* 30, 6031-6036

Lill, U., Lefrank, S., Henschen, A. & Eggerer, H. (1992) *Eur. J. Biochem.* 208, 459-466

Lindquist, L., Kaiser, R., Reeves, P.R. & Lindberg, A.A. (1993) *Eur. J. Biochem.* 211, 763-770

Man, W., Li, Y., O'Connor, C.D. & Wilton, D.C. (1991) *Biochem. J.* 280, 521-526

Maniatis, T., Fritsch, E.F. & Sambrook, J. (1982) *Molecular Cloning, A Laboratory Manual*, Cold Spring Harbor Laboratory

Margulis, L. & Guerrero, R. (1991) *New Scientist* 23<sup>rd</sup> March, 46-50

Mayr, E. (1990) *Nature* 348, 491

Mayr, E. (1991) *Nature* 353, 122

McCabe, P.C., in *PCR Protocols: A Guide to Methods and Applications* (1990) Eds. Innis, M.A., Gelfand, D.H., Sninsky, J.J. & White, T.J.

Mevarech, M. & Werczberger, R. (1985) *J. Bacteriol.* 162, 461-462

Mitchell, C.G. & Weitzman, P.D.J. (1983) *FEBS Lett.* 151 No.2, 260-264

Muir, J.M., Hough, D.W. & Danson, M.J. (1994)a *System. Appl. Microbiol.* 16, 528-533

- Muir, J.M., Hough, D.W. & Danson, M.J. (1994)b Unpublished data.
- Mullakhanbhai, M.F. & Larsen, H. (1975) *Arch. Microbiol.* 104, 207-214
- Ner, S.S., Bhayana, V., Bell, A.W., Gile, I.G., Duckworth, H.W. & Bloxham, D.P. (1983) *Biochemistry* 22, 5243-5249
- Numata, O., Takemasa, T., Takagi, I., Hirono, M., Hirano, H., Chiba, J. & Watanabe, Y. (1991) *Biochem. Biophys. Res. Comm.* 174, 1028-1034
- Okazaki, R., Okazaki, T., Strominger, J.L. & Michelson, A.M. (1962) *J. Biol. Chem.* 237, 3014-3026
- Olsen, G.J. & Woese, C.R. (1989) *Can. J. Microbiol.* 35, 119-122
- Olsen, G.J. & Woese, C.R. (1993) *FASEB J.* 7, 113-123
- Parker, J.M.R., Gou, D. & Hodges, R.S. (1986) *Biochemistry* 258, 5425-5432
- Puehler, G., Lottspeich, F & Zillig, W. (1989) *Nucleic Acid Res.* 17, 4517-4534
- Rajakumar, K., Jost, H., Sasakawa, C., Okada, N., Yoshikawa, M. & Adler, B. (1994) Unpublished.
- Rao, M.J.K. & Argos, P. (1981) *Biochemistry* 20, 6536-6543
- Reiter, W.D., Hudepohl, U. & Zillig, W. (1990) *Proc. Natl. Acad. Sci. USA* 87, 9509-9513
- Remington, S.J. (1992) *Curr. Top. Cell. Regul.* 33, 209-229
- Remington, S.J., Wiegand, G. & Huber, R. (1982) *J. Mol. Biol.* 158, 111-152
- Richardson, J.S. & Richardson, D.C. (1988) *Science* 240 1648-1652

- Rodriguez-Valera, F. (1991) *Biochem. Soc. Symp.* 58, 135-147
- Rodriguez-Valera, F., Lillo, J.A.G., Antón, J. & Meseguer, I. (1989) *General and Applied Aspects of Halophilic Microorganisms*, 373-380 (F. Rodriguez-Valera, ed.), Plenum Press, New York.
- Rosenkrantz, M., Alam, T., Kim, K., Clark, B.J., Srere, P.A. & Guarente, L.P. (1986) *Mol. and Cell. Biol.* 6, 4509-4515
- Russell, R.J.M., Byrom, D., Danson, M.J.D., Hough, D.W. & Taylor, G.L. (1993) *J. Mol. Biol.* 232, 308-309
- Ryu, K. & Dordick, J.S. (1993) *J. Amer. Chem. Soc.* 205, 9 (Abstract)
- Schäfer, S., Barkowski, C. & Fuchs, G. (1986) *Arch. Microbiol.* 146, 301-308
- Schendel, F.J., August, P.R., Anderson, C.R., Hanson, R.S. & Flickinger, M.C. (1992) *Appl. and Environ. Microbiol.* 58, 335-345
- Schwartz, R.M. & Dayhoff, M.O. (1979) in *Atlas of Protein Sequence and Structure* (Dayhoff, M.O., ed.), National Biomedical Research Foundation, Washington D.C., 353-358
- Southern, E.M. (1975) *J. Mol. Biol.* 98, 503-517
- Srere, P.A., Brazil, H. & Gonen, L. (1963) *Acta Chem. Scand.* 17, S129-S134
- Sutherland, K.J., Henneke, C.M., Towner, P., Hough, D.W. & Danson, M.J. (1990) *Eur. J. Biochem.* 194, 839-844
- Tautz, D. & Renz, M. (1983) *Anal. Biochem.* 132, 14-19
- Vettakkorumakankav, N., Danson, M.J. Hough, D.W., Stevenson, K.J., Davison, M. & Young, J. (1992) *Biochem. Cell Biol.* 70, 70-75
- Wang, Z., Srere, P.A. & Evans, C.T. (1991) *Biochemistry* 30, 9281-9286

- Wang, L., Romana, L.K. & Reeves, P.R. (1992) *Genetics* 103, 429-443
- Weitzman, P.D.J. & Ridley, J. (1983) *Biochem. and Biophys. Res. Comm.* 112, 1021-1026
- Wheelis, M.L., Kandler, O. & Woese, C.R. (1992) *Proc. Natl. Acad. Sci. USA* 89, 2930-2934
- Woese, C.R. & Fox, G.E. (1977) *Proc. Natl. Acad. Sci. USA* 74 No.11, 5088-5090
- Woese, C.R., Kandler, O. & Wheelis, M.L. (1990) *Proc. Natl. Acad. Sci. USA* 87, 4576-4579
- Woese, C.R., Kandler, O. & Wheelis, M.L. (1991) *Nature* 351, 528
- Woese, C.R., Magrum, L.J & Fox, G.E. (1978) *J. Mol. Evol.* 11, 245-252
- Wood, D.O., Williamson, L.R., Winkler, H.H. & Krause, D.C. (1987) *J. Bacteriol.* 169, 3564-3572
- Zaccai, G & Cendrin, F (1989) *J. Mol. Biol.* 208, 491-500
- Zaccai, G & Eisenberg, H. (1990) *Trends Biochem. Sci.* 15, 333-337
- Zhang, L., Al-Hendy, A., Toivanen, P. & Skumik, M. (1993) *Mol. Microbiol.* 9, 309-321
- Zillig, W., Klenk, H., Palm, P., Leffers, H., Pühler, G., Gropp, F. & Garrett, R.A. (1989a) *Endocytobiosis & Cell Res.* 6, 1-25
- Zillig, W., Klenk, H., Palm, P., Pühler, G., Gropp, F., Garrett, R.A. & Leffers, H. (1989b) *Can. J. Microbiol.* 35, 73-80
- Zillig, W., Palm, P., Reiter, W.D., Gropp, F., Puhler, G. & Klenk, H. (1988) *Eur. J. Biochem.* 173, 473-482

Zusman, T., Rosenshine, I., Boehm, G., Jaenicke, R., Leskiw, B. & Mevarech, M. (1989) *J. Biol. Chem.* 264 No.32, 18878-18883